

Effects of hypoxia on coupled carbon and iron cycling differ between weekly and multiannual timescales in two freshwater reservoirs

Abigail Lewis¹, Madeline Schreiber¹, Barbara Niederlehner¹, Arpita Das¹, Nicholas Hammond¹, Mary Lofton¹, Heather Wander¹, and Cayelan Carey¹

¹Virginia Tech

November 24, 2022

Abstract

Freshwater lakes and reservoirs play a disproportionate role in the global carbon budget, sequestering more organic carbon (OC) than ocean sediments each year. However, it remains unknown how global declines in bottom-water oxygen concentrations may impact OC sequestration in freshwater sediments. In particular, associations between OC and iron (Fe) are hypothesized to play a critical role in stabilizing OC in sediment, and these complexes can be sensitive to changes in oxygen. Under low-oxygen (hypoxic) conditions, Fe-bound OC (Fe-OC) complexes may dissociate, decreasing OC sequestration. However, rates of OC respiration are also lower under hypoxic conditions, which could increase OC sequestration. To determine the net effects of hypoxia on OC and Fe cycling over multiple timescales, we paired whole-ecosystem experiments with sediment incubations in two eutrophic reservoirs. Our experiments demonstrated that short (2–4 week) periods of hypoxia can increase Fe and OC concentrations in the water column while decreasing OC and Fe-OC in sediment by 30%. However, exposure to seasonal hypoxia over multiple years was associated with a 57% increase in sediment OC and no change in Fe-OC. These results indicate that the large sediment Fe-OC pool (~30% of sediment OC) contains both oxygen-sensitive and oxygen-insensitive fractions, and over multiannual timescales, OC respiration rates play a greater role than Fe-OC protection in determining the effect of hypoxia on sediment OC content. Consequently, we anticipate that global declines in oxygen concentrations will alter OC and Fe cycling, with the direction and magnitude of effects depending upon the duration of hypoxia.

Abigail S. L. Lewis¹, Madeline E. Schreiber², B. R. Niederlehner¹, Arpita Das¹, Nicholas W. Hammond², Mary E. Lofton¹, Heather L. Wander¹, Cayelan C. Carey¹

¹Department of Biological Sciences, Virginia Tech, Blacksburg, Virginia, USA

²Department of Geosciences, Virginia Tech, Blacksburg, Virginia, USA

Corresponding author: Abigail S. L. Lewis (aslewis@vt.edu)

Key Points:

- Short-term (2–3 week) periods of hypoxia decreased iron-bound organic carbon and total organic carbon in reservoir sediments
- Multiannual periods of hypoxia increased total organic carbon in sediment, likely through decreased rates of respiration
- A substantial fraction of sediment organic carbon (~30%) was bound to iron in these two freshwater reservoirs

Abstract

Freshwater lakes and reservoirs play a disproportionate role in the global carbon budget, sequestering more organic carbon (OC) than ocean sediments each year. However, it remains unknown how global declines in

bottom-water oxygen concentrations may impact OC sequestration in freshwater sediments. In particular, associations between OC and iron (Fe) are hypothesized to play a critical role in stabilizing OC in sediment, and these complexes can be sensitive to changes in oxygen. Under low-oxygen (hypoxic) conditions, Fe-bound OC (Fe-OC) complexes may dissociate, decreasing OC sequestration. However, rates of OC respiration are also lower under hypoxic conditions, which could increase OC sequestration. To determine the net effects of hypoxia on OC and Fe cycling over multiple timescales, we paired whole-ecosystem experiments with sediment incubations in two eutrophic reservoirs. Our experiments demonstrated that short (2–4 week) periods of hypoxia can increase Fe and OC concentrations in the water column while decreasing OC and Fe-OC in sediment by 30%. However, exposure to seasonal hypoxia over multiple years was associated with a 57% increase in sediment OC and no change in Fe-OC. These results indicate that the large sediment Fe-OC pool (~30% of sediment OC) contains both oxygen-sensitive and oxygen-insensitive fractions, and over multiannual timescales, OC respiration rates play a greater role than Fe-OC protection in determining the effect of hypoxia on sediment OC content. Consequently, we anticipate that global declines in oxygen concentrations will alter OC and Fe cycling, with the direction and magnitude of effects depending upon the duration of hypoxia.

Plain Language Summary

Freshwater lakes and reservoirs (hereafter: lakes) play a remarkably important role in the global carbon cycle. Every year, more organic carbon (e.g., leaves, soil) is buried in lake sediments than in the sediments of all of the world’s oceans. However, these organic carbon inputs can also be decomposed, releasing greenhouse gases. The extent to which lakes bury carbon vs. release greenhouse gases may be changing, as oxygen concentrations are decreasing in the bottom waters of many lakes around the world. Here, we added oxygen to the bottom waters of a whole lake to test how changes in oxygen concentration affect carbon cycling. We found that over short timescales (weeks), low oxygen conditions decreased the amount of carbon in sediment by breaking apart chemical complexes with iron that can help retain carbon in sediment. However, over long timescales (years), low oxygen conditions appeared to *increase* carbon burial by decreasing the rate at which carbon inputs were decomposed. These results suggest that declining oxygen concentrations in lakes around the world may have important effects on global carbon cycling, with the direction and magnitude of the impact depending on the duration of low oxygen conditions.

1. Introduction

Freshwater lakes and reservoirs are increasingly recognized as hotspots in the global carbon cycle (Bastviken et al., 2011; Battin et al., 2009; Carey, Hanson, et al., 2022; Raymond et al., 2013; Tranvik et al., 2018). Due to high organic carbon (OC) loading from the surrounding watershed, more OC is buried in lakes and reservoirs than in ocean sediments each year (Dean & Gorham, 1998; Knoll et al., 2013; Mendonça et al., 2017; Pacheco et al., 2014). Much of this OC remains sequestered in the sediments, especially in reservoirs, which alone account for 25% of the global carbon sink from all terrestrial and freshwater sources (Le Quéré et al., 2015). However, OC inputs can also be respired to carbon dioxide and methane, making lakes and reservoirs a source of greenhouse gas emissions equivalent to 20% of the global emissions from fossil fuels (Deemer et al., 2016; DelSontro et al., 2018). To refine global carbon budgets and manage water resources in a changing world, it is important to understand what factors control the balance between OC sequestration and carbon emissions in these ecosystems.

Recent research suggests that associations between OC and iron (Fe) may play a critical role in OC sequestration across soils and marine environments (e.g., Hemingway et al., 2019; Kramer & Chadwick, 2018; Lalonde et al., 2012), and these associations are hypothesized to also be important in freshwater sediments (Björnerås et al., 2017; Peter et al., 2016; von Wachenfeldt et al., 2008; Weyhenmeyer et al., 2014). Fe can promote OC stability through multiple mechanisms, including occlusion of OC in aggregates, which can result in physical inaccessibility to microbial degradation and subsequent burial of OC in deeper soil or sediment horizons (Kleber et al., 2015 and references therein). Consequently, protection of OC through complexation with Fe may facilitate OC sequestration over decades to millennia (Kleber et al., 2015; Lalonde et al., 2012 and references therein)

Over shorter timescales (days to weeks), Fe-bound OC (Fe-OC) complexes are sensitive to the redox conditions of the surrounding environment (Figure 1). Fe-OC complexes form under oxic conditions (Riedel et al., 2013), as Fe(III) is more effective at complexing with organic matter than Fe(II) (Nierop et al., 2002). Under hypoxic (reducing) conditions, OC can be released from Fe-OC complexes through Fe(III) reduction and dissolution (e.g., Pan et al., 2016; Patzner et al., 2020; Skoog & Arias-Esquivel, 2009), which can either result directly from hypoxia or through resultant increases in pH that promote OC release (Kirk, 2004; Thompson et al., 2006). Given these conflicting patterns—i.e., that Fe-OC complexes can be preserved over decades to millennia and yet may be unstable under the reducing conditions which commonly occur on day to month timescales in aquatic sediments—it remains unclear how changing oxygen dynamics will affect coupled OC and Fe cycling in freshwater ecosystems.

Currently, the duration of bottom-water hypoxia (low oxygen conditions) is increasing in many lakes and reservoirs around the world (Bartosiewicz et al., 2019; Jane et al., 2021; Jenny et al., 2016; Williamson et al., 2015), which could have varying consequences for OC sequestration (Figure 1). In many dimictic lakes and reservoirs, bottom-water hypoxia is interrupted by oxic conditions during spring mixing and fall turnover, resulting in dynamic oxygen conditions on the week to month scale. Combined, these short-term patterns sum to determine the net role of lakes and reservoirs in the global carbon cycle over multiannual timescales. Periods of hypoxia have the potential to decrease OC sequestration through reductive dissolution of Fe(III) in Fe-OC complexes (Chen et al., 2020; Huang et al., 2021; Patzner et al., 2020). However, hypoxia also has the potential to increase OC sequestration by decreasing the rate of OC respiration (Carey et al., 2018; Carey, Hanson, et al., 2022; Hargrave, 1969; Peter et al., 2017; Sobek et al., 2009; Walker & Snodgrass, 1986), particularly if Fe-OC complexes are resistant to, or protected from, changes in oxygen concentrations in overlying water. Decreased OC respiration rates under hypoxic conditions is thought to occur primarily because respiration is less thermodynamically favorable in the absence of oxygen (e.g., Arndt et al., 2013; LaRowe & Van Cappellen, 2011). Because reductive dissolution of Fe(III) in Fe-OC complexes and decreased OC respiration under hypoxic conditions would have divergent effects on total OC sequestration, understanding the relative importance of these two processes across multiple timescales is critical for predicting the effect of hypoxia on OC sequestration in the bottom waters of lakes and reservoirs (Figure 1).

To date, few studies have explicitly examined Fe-OC in freshwater lakes and reservoirs, and those that have provide preliminary evidence that Fe-OC complexation may be lower in freshwater environments compared to better-characterized marine systems. Peter and Sobek (2018) analyzed Fe-OC in surficial sediment from five boreal lakes that spanned a gradient of oxygen conditions and found that less than 11% of sediment OC was bound to Fe, in comparison with ~20% across a range of primarily marine sediments (Lalonde et al., 2012). Further, Peter and Sobek (2018) found no association between Fe-OC content in sediment and oxygen in overlying water. However, it should be noted that the lakes in that study were particularly high in dissolved OC (DOC) concentrations (9–42 mg/L DOC), and may not be representative of all freshwater ecosystems. Bai et al. (2021) studied Fe-OC along a salinity gradient in a subtropical tidal wetland and similarly found that freshwater areas had lower levels of Fe-OC (18% of sediment OC in freshwater and 29% in saltwater), but these results were attributed primarily to wetland plant characteristics, which may not be relevant in the bottom waters of lakes and reservoirs.

Despite limited research on Fe-OC in freshwater sediments, there are multiple reasons to expect that Fe may play an important role in OC sequestration in some freshwater ecosystems. Concentrations of Fe and DOC are strongly correlated in many freshwaters (Björnerås et al., 2017; von Wachenfeldt et al., 2008; Weyhenmeyer et al., 2014), and aqueous Fe concentrations are strongly correlated with sediment OC accumulation in boreal lakes (Einola et al., 2011). Moreover, hypoxic release of DOC from lake sediments has been well-documented, and is often attributed to reductive dissolution of Fe (Brothers et al., 2014; Kim & Kim, 2020; Lau & del Giorgio, 2020; Peter et al., 2017). Still, few studies have examined whether reactions involving Fe-OC complexes are the driving force for observed correlations between dissolved Fe and OC (but see Peter et al. 2018). Furthermore, it remains unknown how the Fe-OC cycling occurring on sub-annual time scales may affect OC sequestration on the multi-annual timescales relevant for global carbon budgets.

Analyzing the complex effects of oxygen on coupled OC and Fe cycling requires multiple experimental approaches. Field surveys have been effective at identifying correlations between OC and Fe (Björnerås et al., 2017; von Wachenfeldt et al., 2008; Weyhenmeyer et al., 2014). However, these observational approaches have limited capacity for identifying causal relationships. Whole-ecosystem experiments may be highly effective at identifying real-world impacts of freshwater oxygen on Fe and OC dynamics, while allowing for important ecosystem-scale processes such as turbulence and external loading (Carpenter, 1996; Dzialowski et al., 2014; Schindler, 1998). However, high levels of variability on a whole-ecosystem scale may limit the detection of subtle changes in OC and Fe processing. Small-scale incubations may be particularly useful for identifying changes that result from hypoxia (i.e., increased DOC and Fe release from sediment, decreased levels of Fe-OC, changes in sediment OC). However, small-scale incubations are limited by fouling and changes in microbial communities, among other microcosm effects, and do not reflect the full suite of processes that interact to control OC and Fe cycling in lakes and reservoirs. Consequently, integrating multiple approaches can provide complementary information on Fe-OC dynamics across spatial and temporal scales and overcome the limitations of single-approach studies.

To analyze how hypoxia impacts OC and Fe cycling over multiple scales, this study paired whole-ecosystem oxygen manipulations with laboratory incubations. We had two objectives: (1) characterize Fe-OC levels in sediment of two iron-rich reservoirs, and (2) analyze how hypoxia affects coupled OC and Fe cycling over both short-term (2–4 week) and multiannual timescales. Through this work, we aimed to provide insight on how increasing prevalence and duration of hypoxia in lakes and reservoirs may affect the critical role of these ecosystems in the global carbon cycle.

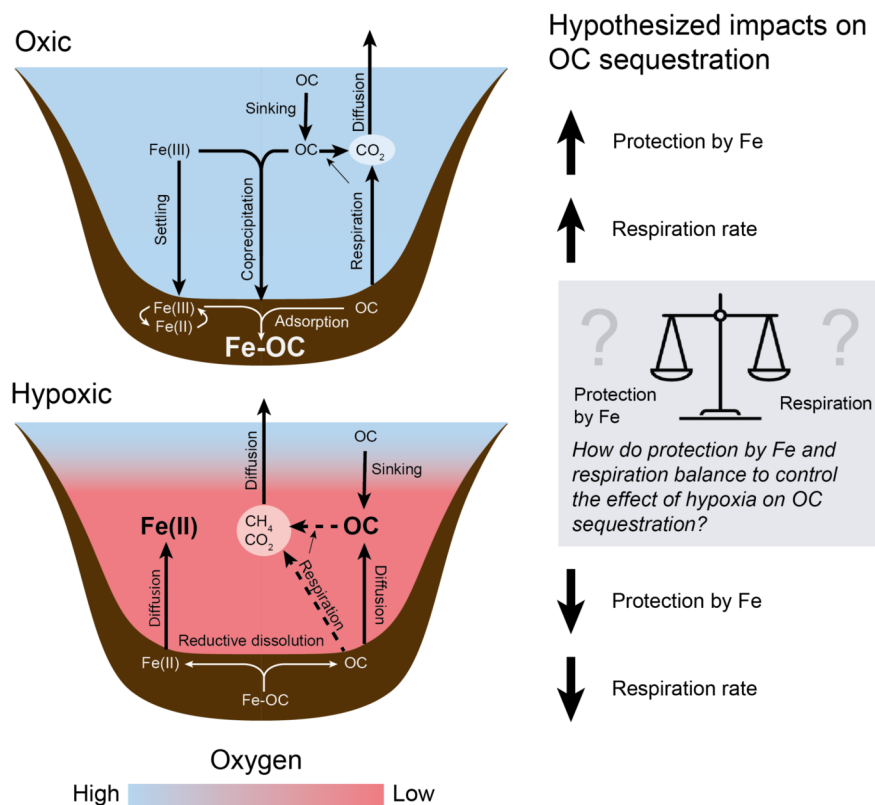


Figure 1: Conceptual diagram describing the hypothesized effects of changing oxygen conditions on coupled Fe-OC interactions in a lake or reservoir. Under oxic conditions (top), complexation of Fe and OC (both

through co-precipitation and adsorption) leads to increased concentrations of Fe-OC in sediments (increased Fe-OC protection), though oxic conditions may also lead to increased OC respiration rates. Under hypoxic conditions, reductive dissolution of Fe(III) in Fe-OC complexes increases dissolved concentrations of Fe(II) and OC in the water column while decreasing the amount of Fe-OC in sediment (decreasing Fe-OC protection), though hypoxia may also decrease OC respiration rates. The net effect of these processes on OC sequestration remains unknown, motivating this study. This figure is a simplification of complex interactions happening on a whole-ecosystem scale, and focuses on hypothesized dominant processes operating on the time scale of days to years.

2. Methods

2.1 Study Sites: Falling Creek and Beaverdam Reservoirs

Falling Creek Reservoir (FCR; 37.30°N, 79.84°W) and Beaverdam Reservoir (BVR; 37.31°N, 79.81°W) are small (FCR: 0.12 km², 9.3 m deep; BVR: 0.39 km², 11 m deep), eutrophic drinking water reservoirs located in southwestern Virginia, USA (Hounshell et al., 2021). Both reservoirs are located in forested catchments and both are dimictic, with summer stratified periods that typically last from May to October. BVR is located 3 km upstream of FCR and serves as the primary inflow source for FCR. Fe levels are high in in these reservoirs' catchments as a result of weathering and erosion of Fe-rich metamorphic rocks (Chapman et al., 2013; Woodward, 1932); the bedrock underlying both reservoirs is layered pyroxene granulite (Virginia Division of Mineral Resources, 2003). Both reservoirs have been owned and operated for drinking water provision by the Western Virginia Water Authority (WVWA) since their construction (FCR: 1898, BVR: 1872; Gerling et al., 2016; Hamre et al., 2018).

A suite of variables are routinely sampled in FCR and BVR as part of a long-term monitoring program; all data analyzed in this manuscript are available in the Environmental Data Initiative (EDI) repository with detailed metadata (Carey, Lewis, McClure, et al., 2022; Carey, Wander, Howard, et al., 2022; Carey, Wander, McClure, et al., 2022; Lewis et al., 2022; Lewis, Schreiber, et al., 2022; Schreiber et al., 2022)

2.2 Whole-ecosystem oxygenation experiments

In 2012, FCR was equipped with a side-stream supersaturation hypolimnetic oxygenation (HOx) system to improve water quality in the reservoir (Gerling et al., 2014). This type of HOx system functions by withdrawing water from the bottom of the reservoir, adding concentrated, pressurized oxygen gas to supersaturate the water with dissolved oxygen (DO), and then returning the oxygenated water at the same depth and temperature. Previous work in FCR has shown that the HOx system effectively increases DO concentrations throughout the hypolimnion without altering temperature or decreasing thermal stability (Gerling et al., 2014). From 2013–2019, the HOx system in FCR was operated at variable rates, maintaining an oxygenated hypolimnion for at least part of the summer (Carey, Thomas, et al., 2022). Conversely, oxygenation was reduced in 2020 and 2021, maintaining primarily hypoxic conditions throughout the summer stratified period. To assess the effects of multiannual changes in oxygen availability on OC and Fe-OC in sediment, we compared sediment core and sedimentation trap data from summer 2019 (which had a history of high-oxygen conditions during the preceding six years) to summer 2021 (which followed a summer of hypoxic conditions in 2020; Figure S2). Sediment data were not collected in 2020 due to the Covid-19 pandemic.

To assess how short-term changes in hypolimnetic DO concentrations impact Fe-OC on a whole-ecosystem scale, we operated the HOx in FCR on a variable schedule throughout the summer of 2019 (Carey, Thomas, et al., 2022). Oxygen was added in approximately two-week intervals at a rate of 25 kg O₂ day⁻¹ to the whole hypolimnion. Between oxygenation periods, we allowed the hypolimnion to become hypoxic over periods of at least two weeks without oxygenation. Because hypolimnetic volume varied throughout the summer (generally decreasing throughout the summer as the thermocline deepened), the mean concentration of oxygen added to the whole hypolimnion throughout an oxygenation period in 2019 ranged from 0.80 mg L⁻¹day⁻¹ to 0.90 mg L⁻¹day⁻¹.

BVR does not have a HOx system and experiences seasonal hypoxia from May through November (Hounshell

et al., 2021). Consequently, BVR serves as a reference ecosystem to analyze the effects of oxygenation in FCR.

2.2.1 Oxygen

We monitored DO concentrations throughout the full water column approximately two times per week in FCR and one time per week in BVR (Carey, Lewis, McClure, et al., 2022). High-resolution (~ 1 cm) depth profiles were taken using a conductivity, temperature, and depth profiler (CTD; Sea-Bird, Bellevue, Washington, USA) equipped with a DO sensor (SBE 43; Carey, Lewis, McClure, et al., 2022) from the reservoir’s surface to the sediments. We also measured dissolved oxygen using a YSI ProODO DO probe when the CTD was not available due to maintenance (YSI Inc. Yellow Springs, Ohio, USA; Carey, Wander, McClure, et al., 2022). YSI measurements were taken at discrete 1 m depth intervals. For a comparison of YSI and CTD measurements, see Carey et al. (2022).

2.2.2 Hypolimnetic Fe and DOC

We collected water samples for DOC and Fe analysis at the deepest site in each reservoir with a 4-L Van Dorn sampler (Wildlife Supply Company, Yulee, FL, USA). Samples were collected once per week at seven depths in FCR (0.1, 1.6, 3.8, 5.0, 6.2, 8.0, and 9.0 m), which corresponded to the reservoir’s extraction depths, and five depths in BVR (0.1, 3.0, 6.0, 9.0, and 11.0 m). In 2019, we conducted a limited amount of additional sampling in FCR on a second day each week, and these measurements included DOC from 0.1, 1.6, 5.0, and 9.0 m depths.

We analyzed DOC by filtering water samples through a 0.7- μ m glass fiber filter into an acid-washed bottle, which was rinsed with the filtered water three times before sample collection. The filtered samples were frozen for less than six months before analysis on an OC analyzer (Elementar Vario TOC cube, following APHA standard method 5310B; American Public Health Association, 2018b).

We collected both total and dissolved (filtered through 0.45- μ m filters) samples for Fe. Samples were preserved in the field using trace metal grade nitric acid and analyzed using ICP-MS (Thermo Electron X-Series, Waltham, MA, USA) following APHA Standard Method 3125-B (American Public Health Association, 2018a; Krueger et al., 2020; Munger et al., 2019; Schreiber et al., 2022).

2.2.3 Fe-OC in sediments

We analyzed the concentration of Fe-OC in surficial sediments from both FCR and BVR on multiple dates throughout the summer stratified periods of 2019 and 2021. In 2019, sediment cores in FCR were collected immediately before the HOx system was turned on or off, resulting in the most oxic or hypoxic conditions during that SSS activation or deactivation interval, respectively. Sediment cores at BVR were taken once in the middle of summer and once approximately two weeks before fall turnover in 2019. In 2021, sediment core samples were taken from both reservoirs on the same dates, approximately once per month. Additional sediment core samples were collected in March 2021, when both reservoirs were unstratified and had oxic hypolimnia.

On each sampling date, we collected four replicate hypolimnetic sediment cores using a K-B gravity sediment corer (Wildlife Supply Company, Yulee, FL, USA). Cores were collected in the deepest part of each reservoir, approximately 20 m from where water samples were taken. In 2019, each core was capped and kept on ice while transported back to the lab, where the top 1 centimeter of sediment from each core was immediately extruded, collected, and frozen in scintillation vials for future analysis. In 2021, cores were extruded in the field, and the samples were kept on ice while being transported back to the lab.

2.2.4 Sediment traps

To determine the amount of Fe-OC and total OC in samples of material settling from the water column (i.e., not estimate deposition rates), we deployed 19-L buckets approximately 1 m above the sediments at the deepest point of each reservoir (8 m at FCR and 10 m at BVR). These sediment traps were deployed from June–December 2021 and sampled every two weeks by slowly bringing the bucket to the surface, decanting

and discarding water from the bucket, collecting up to 5 L of the remaining water and particulate matter, and transporting this material back to the lab on ice. Upon arriving at the lab, we allowed the particulates to settle for approximately 5 minutes before decanting and discarding as much water as possible and filling four 50-mL centrifuge tubes with the remaining material. The samples were centrifuged for 10 minutes at 3100 rpm, then combined into one vial and frozen for later analysis. No sediment traps were deployed for Fe-OC analysis in 2019.

2.3 Microcosm incubations

To isolate the effects of oxygen from other interacting factors that affect Fe and OC on a whole-ecosystem scale, we conducted six-week microcosm incubations using hypolimnetic sediment and water from FCR. Incubations were conducted in 177-mL glass jars (Figure S1), after extensive pilot testing revealed that these jars were highly effective at maintaining hypoxic conditions when sealed and oxic conditions when uncapped. We started the experiment with 102 microcosms split evenly into oxic (uncapped) and hypoxic (capped) treatments. After two weeks (similar to the 2019 whole-ecosystem HOx manipulation), we switched the treatment of approximately half of the remaining microcosms, generating two additional oxygen regimes: hypoxic-to-oxic and oxic-to-hypoxic. Starting on week two, there were consequently a total of four oxygen regimes: hypoxic, oxic, hypoxic-to-oxic, and oxic-to-hypoxic.

To set up the experiment, we collected sediment and water from the deepest site in FCR on 30 June 2021, when the hypolimnion was hypoxic. Water was collected from 9 m depth using a Van Dorn sampler, and sediment was collected from the same location using an Ekman sampler. Samples were transported on ice back to the lab, then homogenized by stirring and shaking. We used a syringe to add the sediment slurry (20 mL) to each jar, then slowly added 150 mL of hypolimnetic water, making an effort to minimize sediment disturbance. We stored the microcosms in an unlit incubation chamber at 15 °C for the duration of the experiment, which corresponded to warm, end-of-summer conditions in the hypolimnion of FCR (Carey, Lewis, McClure, et al., 2022).

2.3.1 Microcosm sampling

Microcosms were sampled destructively for DO, total and dissolved Fe, total and dissolved OC, pH, sediment OC, and sediment Fe-OC. For the continuous oxic and hypoxic treatments, we sampled 3–6 replicates two times per week for four weeks (6 replicates: days 2, 6, 9, 13; 3 replicates: days 16, 20, 23). We added additional sampling for the hypoxic-to-oxic and oxic-to-hypoxic treatments: these treatments were sampled for the first three days after switching the oxygen regime (days 14, 15, 16), twice the following week (days 20, 23), and one more time a total of four weeks from when treatments were switched (day 34), with three replicates analyzed per sampling event. All microcosms under a hypoxic treatment were sampled in an anaerobic chamber which maintained mean ambient oxygen conditions <200 ppm (Coy Laboratory, Grass Lake, MI, USA) to reduce oxygen exposure during sampling.

To begin sampling a microcosm, DO was measured using a YSI DO probe. While measuring DO, we used the probe to gently swirl the water in the microcosm, homogenizing the water sample while minimizing sediment disturbance. Next, we used an acid-washed syringe to withdraw 30 mL of water for total OC (TOC), 13 mL for total Fe, 30 mL of water for DOC, and 13 mL for dissolved Fe analyses. DOC samples were filtered through a 0.7- μ m glass fiber filter, and dissolved Fe samples were filtered through 0.45- μ m filters. After taking samples for Fe and DOC, we withdrew as much water as possible without disturbing the sediment and measured pH from this sample in a separate container using an Ohaus Starter 300 pH probe (Parsippany, NJ, USA). Finally, we swirled the sediment with remaining water (approximately 1–5 mL) and poured this mixture into a 20 mL glass EPA vial, which we then froze for Fe-OC analysis. Hypoxic microcosms were stored in the anaerobic chamber for approximately two hours before analysis to ensure oxygen concentrations in the chamber were sufficiently low before opening the jars. Oxic microcosms were sampled immediately after removal from the incubator.

All microcosm samples were analyzed following standard methods. We stored TOC and DOC samples in bottles that had been acid-washed and rinsed three times with the sample water. All DOC and TOC

samples were frozen for <6 months prior to analysis on an OC analyzer (Elementar Vario TOC cube, following Standard Method 5310B; American Public Health Association, 2018b) Fe samples were preserved using trace metal grade nitric acid and analyzed using the ferrozine method (Gibbs, 1979). We also analyzed Fe samples from days 16 and 23 using inductively coupled plasma mass spectrometry (ICP-MS). All microcosm data are published with complete metadata in the Environmental Data Initiative repository (Lewis et al., 2022).

2.4 Fe-OC analysis

We analyzed the amount of Fe-OC in both the whole-ecosystem and microcosm sediment samples using the citrate bicarbonate dithionite (CBD) method. This method was first described for marine systems by Lalonde et al. (2012) and has since been adapted for freshwater lakes by Peter and Sobek (2018). It is important to note that our measurement of Fe-OC as the percentage of OC that is extractable using the CBD method is an operational definition (Fisher et al., 2021). We used this method to enable comparisons both between oxygen treatments and with other published work that used the same general approach (e.g., Lalonde et al., 2012; Peter & Sobek, 2018).

Following the CBD method, each sediment sample was freeze-dried and divided into three treatments: initial, reduction, and control. “Initial” samples received no treatment and were used to measure the OC content of the sediment. “Reduction” samples were treated with a metal-complexing agent (trisodium citrate) and reducing agent (sodium dithionite) in a buffered solution (sodium bicarbonate) to measure how much Fe and OC were released as a result of Fe reduction. Control samples were used to account for the release of Fe and OC in the reduction treatment that resulted from processes other than Fe reduction. They were treated with the same buffer (sodium bicarbonate) and sodium chloride in the same ionic strength as the trisodium citrate and sodium dithionite of the reduction treatment.

For both the control and reduction treatments, we measured 100 mg of homogenized, freeze-dried sediment into 15-mL polypropylene centrifuge tubes (Falcon Blue, Corning Inc., Corning, NY, USA). We then added 6 mL of either control or reduction buffer solution (0.11 M sodium bicarbonate) to each tube. The reduction buffer contained 0.27 M trisodium citrate, while the control buffer contained 1.6 M sodium chloride. After heating samples to 80°C in an oven, 0.1 g sodium dithionite was added to the reduction samples and 0.088 g sodium chloride was added to control samples, and samples were kept at 80°C for an additional 15 min. Samples were centrifuged for 10 min at 3100 RPM, and the supernatant was collected in a 50-mL centrifuge tube. This extraction process was repeated two more times for both treatments (Peter and Sobek, 2018). Finally, samples were rinsed three times using artificial lake water, which was prepared by diluting Artificial Hard Water from Marking and Dawson (1973) to 12.5% with Type I reagent grade water.

After extraction, all sediment samples (including those in the initial treatment) were dried and acid-fumigated for 48 hours to remove remaining citrate and bicarbonate (Harris et al., 2001). Samples were then run on a CN analyzer (Elementar VarioMax, Ronkonkoma, NY, USA) to determine the amount of OC per unit mass of sediment. We adjusted sediment mass to account for Fe loss during control and reduction treatments. The amount of OC removed with Fe reduction (CBD-extractable OC) was calculated as the difference between the OC content of the control and reduction samples and expressed as a percentage of the initial OC content of the sediment.

2.5 Data analysis

All analyses were performed in R (version 4.0.3; R core team 2020) using packages tidyverse (Wickham et al., 2019), lubridate (Grolemund & Wickham, 2011), ggpubr (Kassambara, 2020), egg (Auguie, 2019), rstatix (Kassambara, 2021), akima (Akima et al., 2022), colorRamps (Keitt, 2022), rLakeAnalyzer (Winslow et al., 2019), and tseries (Trapletti et al., 2022). All novel analysis code is archived as a Zenodo repository (Lewis, 2022).

2.5.1 Sediment Fe-OC characterization

We calculated summary statistics to describe iron-bound organic carbon and total organic carbon in surficial sediment (2019 and 2021) and settling particulate material (2021 only) across both reservoirs. We then

pooled data from both reservoirs to analyze the difference between settling material and surficial sediments using Welch’s t-tests. Because data were unavailable for settling material in 2019, the comparison of settling material to surficial sediment was limited to 2021 data only.

2.5.2 Whole-ecosystem experiments: short-term responses

We used Welch’s t-tests to assess whether sediment properties differed between the two-week periods of HOx activation compared to HOx deactivation during summer 2019 in FCR. Sediment time series did not exhibit significant temporal autocorrelation, justifying this approach (Lewis, Schreiber, et al., 2022).

To qualitatively assess whether oxygenation experiments led to differences in water column chemistry, we overlaid plots of DOC and Fe from the deepest sampling depth in each reservoir with dissolved oxygen at the same depths throughout the summer stratified period of 2019 .

2.5.3 Whole-ecosystem experiments: interannual differences

We assessed whether there were significant differences in sediment properties among the four reservoir-years—BVR in 2019 (hypoxic), BVR in 2021 (hypoxic), FCR in 2019 (oxic) and FCR in 2021 (hypoxic). First, we used Levene tests to assess homogeneity of variance among reservoir-years (Table S1). While Fe-OC (both per unit sediment and as a percentage of sediment OC) met the ANOVA assumption of homogeneous variance, total sediment OC did not. Consequently, we used one-way ANOVAs and Tukey post hoc tests for Fe-OC metrics, but used Welch one-way ANOVAs and Games-Howell post-hoc tests, both of which account for unequal variances, for sediment OC (Tables S2 and S3).

2.5.4 Microcosm incubations

We used one-way ANOVAs and Tukey post-hoc tests to assess whether sediment properties differed between microcosm treatments, after testing for homogeneity of variance using Levene tests (Table S4). For this analysis, we used data from days 20 and 23 (pooled together because replicates were sampled destructively), as these were the final days when data were available for all treatments.

Speciation-solubility calculations were conducted for day 23 of the microcosm experiments using the Spece8 module of Geochemists’ Workbench (GWB; Aquatic Solutions LLC, Champaign, IL, USA) and the wateqf thermodynamic database (Ball & Nordstrom, 1991). The goal of the calculations was to assess the predicted speciation of Fe in the presence of OC under the environmental conditions of each microcosm treatment (following Oyewumi & Schreiber, 2017). Environmental conditions considered in this analysis included pH, DO, temperature, DOC, major cations (Ca, Na, K), Fe, and major anions (Cl, SO₄; bicarbonate was not measured so we calculated that via charge balance). We assumed that DOC consisted primarily of humic acid for the calculations.

3. Results

3.1 Fe-OC levels in surficial hypolimnetic sediment are high and greater than in settling particulate matter

A substantial proportion of sediment OC was associated with Fe in both FCR and BVR. In FCR (averaged across 2019 and 2021), one gram of surficial sediment contained a mean of 481 μmol Fe-OC (± 138 , 1 SD), 31 \pm 8% of the total sediment OC pool (n=30). BVR had slightly lower Fe-OC than FCR on average, and one gram of surficial sediment contained a mean of 418 \pm 121 μmol Fe-OC, 24 \pm 7% of the total sediment OC pool (n=20). Total OC comprised 9 \pm 3% of sediment mass in FCR and 10 \pm 1% of sediment mass in BVR.

Levels of Fe-OC, both as a fraction of sediment mass and as a fraction of total sediment OC, were significantly higher in sediment core samples than in settling material collected in hypolimnetic traps (Figure 2). In 2021, averaged across both reservoirs, one gram of the reservoir surficial sediments contained a mean of 443 \pm 133 μmol of Fe-OC (n=28), 69% higher than settling material collected in the traps, which contained a mean of 262 \pm 143 μmol Fe-OC (n=17; $t_{32}=-4.24$, $p<0.001$; Figure 2a). A mean of 24 \pm 6% of the total sediment OC pool was bound to Fe in sediments (n=28), while only 9 \pm 4% of sediment OC was bound to Fe in settling

material ($n=17$; $t_{43}=-10.44$, $p<0.001$; Figure 2c). Total OC was 60% higher in settling material ($\mu=16.5\pm3.3$) than in surficial sediments ($\mu=10.3\pm1.6$; $t_{20}=7.33$, $p<0.001$; Figure 2b).

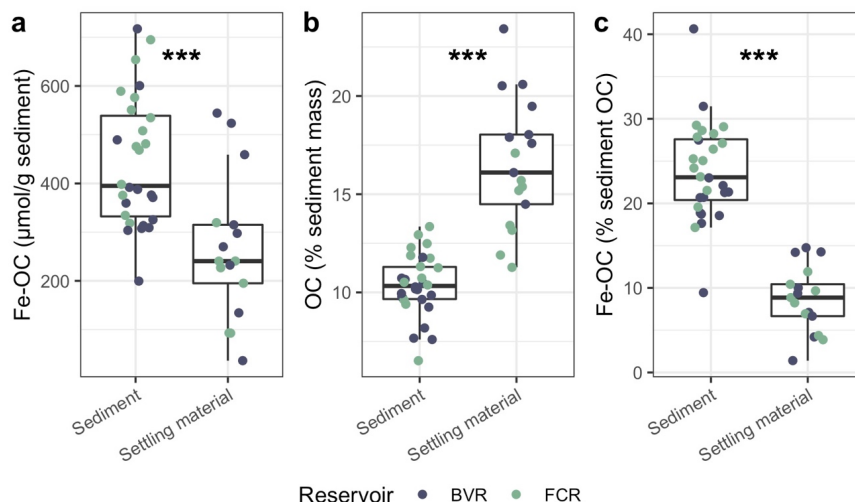


Figure 2: Iron-bound organic carbon (Fe-OC; a), total sediment organic carbon (b), and Fe-OC as a percentage of sediment OC (c) all differed significantly between surficial sediment and settling particulate matter. Asterisks indicate statistical significance of the difference between surficial sediment and sediment traps: *** indicates $p < 0.001$ (Welch's ANOVA). Note that only 2021 data are presented because settling particulate material was not collected in 2019.

3.2 Short-term hypoxia decreases sediment OC and Fe-OC on a whole-ecosystem scale

Intermittent activation of the HOx in FCR in 2019 was associated with substantial changes in sediment characteristics. The amount of Fe-OC per g sediment was 30% lower during hypoxic ($\mu=394\pm173$, $n=9$) compared to oxic ($\mu=560\pm70$, $n=7$) periods in 2019 ($t_{11}=-2.6$, $p=0.02$; Figure 3b). Likewise, the total amount of OC (as a percentage of sediment mass) decreased by 30% during hypoxic ($\mu=6.0\pm1.55$, $n=11$) compared to oxic periods ($\mu=8.5\pm0.8$, $n=7$; $t_{15}=-4.6$, $p<0.001$; Figure 3b). Fe-OC as a percentage of total sediment OC did not significantly change with variation in oxygen during these experiments (oxic: $\mu=36.7\pm3.8$, $n=7$; hypoxic: $\mu=35.7\pm7.9$, $n=9$; $t_{12}=-0.3$, $p=0.747$; Figure 3c).

In the hypolimnion of FCR, total Fe concentrations tended to increase as oxygen decreased and decrease as oxygen increased (Figure 4b). Consequently, Fe concentrations were generally lower in FCR compared to the unoxygenated reference reservoir (BVR) in 2019. Trends in DOC were more variable, though DOC concentrations were typically highest when oxygen concentrations were low in FCR (Figure 4).

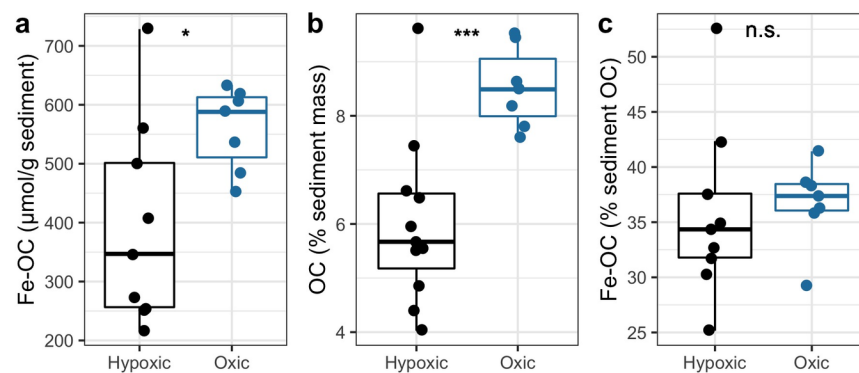


Figure 3: Iron-bound organic carbon (Fe-OC; a) and total organic carbon (b) in sediment were significantly higher under oxic compared to hypoxic conditions in Falling Creek Reservoir (FCR) during the summer stratified period of 2019. Fe-OC as a percentage of sediment OC did not differ significantly between hypoxic and oxic conditions. Here, oxic and hypoxic conditions are classified based upon mean oxygen levels during the two weeks preceding sampling (Figure S3). Statistical significance of differences between oxic and hypoxic periods is indicated using asterisks: * indicates $p < 0.05$, *** indicates $p < 0.001$.

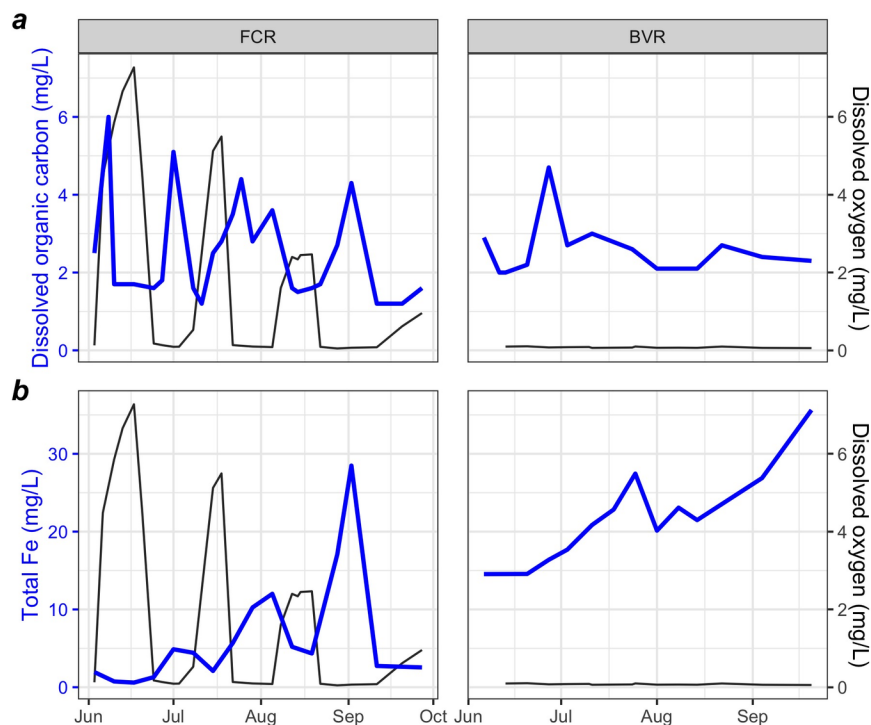


Figure 4: Increased dissolved oxygen concentrations were associated with decreased dissolved organic carbon (a) and total iron (Fe; b) in the hypolimnia of Falling Creek Reservoir (FCR; left) and Beaverdam Reservoir (BVR; right) during the summer stratified period of 2019.

3.3 Multiannual hypoxia is associated with increased sediment OC in FCR and BVR

Activation of the oxygenation system increased summer hypolimnetic DO concentrations in FCR from 2014 through 2019, and lower oxygen addition rates allowed for primarily hypoxic conditions in 2020 and 2021 (Figure S2). BVR exhibited summer hypolimnetic hypoxia throughout the duration of the study (Figure S2).

In FCR, the amount of OC in sediment increased by 57% as DO concentrations decreased from 2019 to 2021 (Figure 5b; Table S1, S2). Consequently, total OC was lower in FCR than BVR in 2019, but not in 2021 (Figure 5b; Table S1, S2). However, the amount of Fe-OC per gram of sediment did not change (Figure 5a; Table S1). As a result, the percentage of sediment OC that was bound to Fe decreased from 2019 to 2021 in FCR (Figure 5c; Table S1, S3). None of these three sediment characteristics differed between 2019 and 2021 in BVR (Figure 5d-f; Table S1, S2, S3).

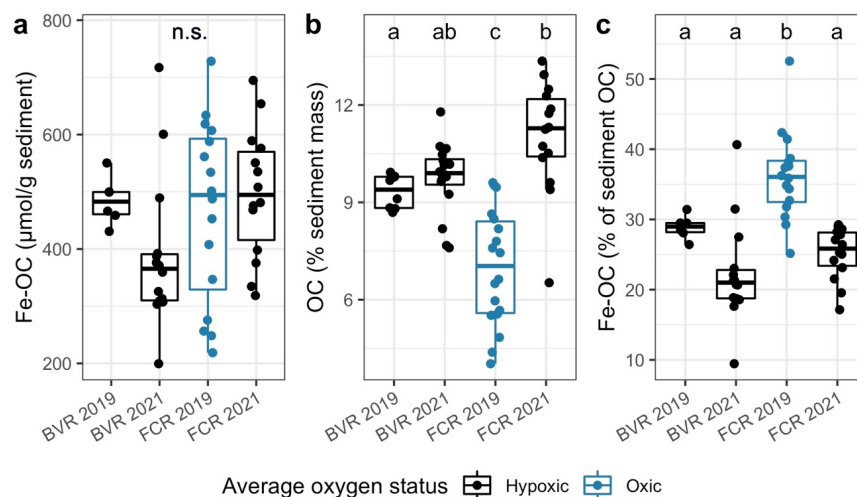


Figure 5: Sediment organic carbon metrics differed significantly in association with oxygen on a multiannual scale. Metrics assessed include iron-bound organic carbon (Fe-OC) (a), total sediment organic carbon (OC; b), and Fe-OC as a percentage of OC (c) in Falling Creek Reservoir (FCR) and Beaverdam Reservoir (BVR). Blue color indicates the reservoir-year with the highest mean oxygen (2019 in FCR) and letters delineate groups that are significantly different ($p < 0.05$; Table S1, S2, S3).

3.4 Experimental microcosm incubations reveal rapid effects of hypoxia on Fe and OC

Experimental microcosm incubations successfully established four distinct oxygen regimes. DO concentrations increased rapidly when hypoxic microcosms were unsealed and decreased rapidly when microcosms were sealed (Figure 6). At the transition from hypoxic-to-oxic conditions, DO concentrations increased to approximately the same level as the continuous oxygen treatment (~ 7 mg/L) within one day. At the transition from oxic-to-hypoxic conditions, DO concentrations decreased below 1 mg/L within one day and declined to 0 mg/L by the end of the experiment.

Changes in oxygen conditions were associated with clear but asynchronous changes in aqueous OC and Fe. As microcosms switched from oxic-to-hypoxic conditions, TOC, DOC and total Fe decreased near synchronously, while dissolved Fe decreased below detection within one day of oxygen exposure. At the transition from hypoxic-to-oxic conditions, DOC and TOC rapidly increased to the same level as microcosms that had experienced continuous hypoxia (~ 10 mg/L; Figure 6). However, concentrations of both dissolved and total Fe only began to increase after three weeks of hypoxia (Figure 6). Measured DOC and TOC were strongly and linearly correlated, with DOC representing a mean of $96 \pm 14\%$ of TOC (Figure S4); thus, we focus our discussion on DOC hereafter, but the same trends apply to TOC.

At the end of the experiment, sediment OC differed significantly among treatments (one-way ANOVA: $F_{3,20}=9.09$, $p<0.001$). Sediment OC was significantly higher in microcosms that started under oxic conditions (oxic: $\mu=4.6\pm0.3$, oxic-to-hypoxic: $\mu=4.5\pm0.3$) than microcosms that started under hypoxic conditions (hypoxic: $\mu=4.0\pm0.0$, hypoxic-to-oxic: $\mu=4.1\pm0.2$; Figure 7). Fe-OC did not differ significantly between treatments as a proportion of sediment mass ($F_{3,20}=0.51$, $p=0.683$) or as a proportion of sediment OC ($F_{3,20}=2.40$, $p=0.098$).

Speciation calculations (Table S5) based upon ICP-MS results (Figure S5) suggest that oxygen conditions had primary control over Fe speciation, with a lesser impact on Fe-OC. The experiments that were maintained under hypoxic conditions had dominant Fe species of Fe(II), FeHCO_3^+ , FeCO_3 , and FeSO_4 (all of these species contained Fe in its reduced state, Fe(II)). For all of the microcosms that were exposed to oxygen at any time (hypoxic-to-oxic, oxic-to-hypoxic, oxic), the dominant Fe species were Fe(OH)_3 , Fe(OH)_2^+ , Fe(OH)_4^- , FeOH_2^+ and FeHumate^+ (all of these species contained Fe in the oxidized state, Fe(III)). pH remained circumneutral across all treatments (Figure S6). These results indicate that 1) exposure to oxic conditions at any time in the experiment shifted the dominant oxidation state to Fe(III); 2) under oxic conditions, and to a lesser extent, hypoxic conditions, Fe complexed with DOC.

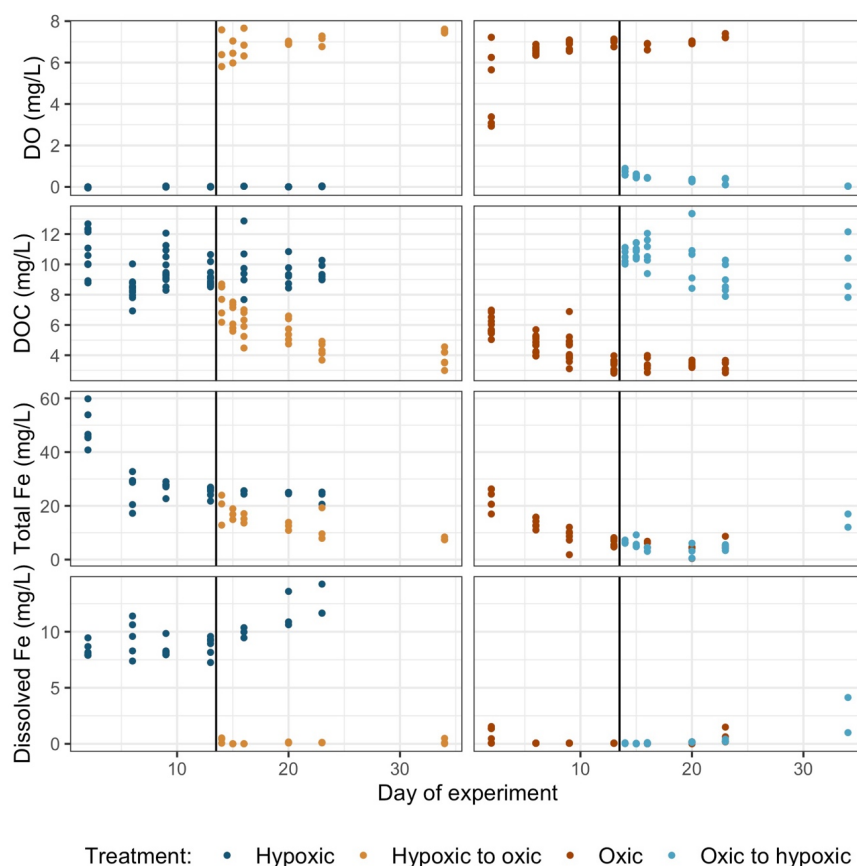


Figure 6: Varied oxygen regimes led to differences in water chemistry among experimental microcosm treatments. Metrics assessed include dissolved oxygen (DO), dissolved organic carbon (DOC), total iron (Fe), and dissolved Fe concentrations in microcosms that were sampled destructively over the course of 34 days. Vertical lines indicate when oxygen conditions were switched, creating the oxic-to-hypoxic and hypoxic-to-oxic treatments.

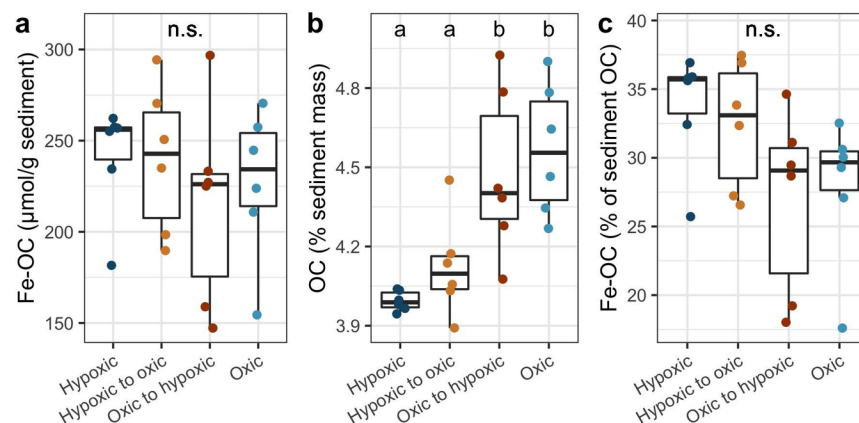


Figure 7: Experimental oxygen microcosm treatments altered some, but not all, sediment properties. Metrics assessed include moles of iron-bound organic carbon (Fe-OC) per unit sediment mass (a), total sediment organic carbon (b), and Fe-OC as a percentage of sediment OC (c). Letters delineate treatments that are significantly different ($p < 0.05$): no treatments were significantly different for Fe-OC metrics (a, c). Days 20 and 23 were chosen for statistical comparisons as the last days in the experiment when data were available from all treatments.

4. Discussion

Our results suggest that oxygen affects coupled OC and Fe cycling differently over short-term (several weeks) compared to long-term (multiannual) timescales (Figure 8). Short periods of hypoxia decreased total OC and Fe-OC in sediment and increased concentrations of DOC and Fe in overlying water, indicating that a portion of the sediment Fe-OC pool is sensitive to changes in oxygen. However, over longer timescales, low oxygen conditions in FCR from 2019–2021 were associated with a 57% increase in sediment OC, indicating that the effects of hypoxia on Fe-OC (i.e., dissociation of Fe-OC complexes) may be outweighed by decreases in respiration rates under hypoxic conditions. Notably, Fe-OC comprised nearly one-third of surficial sediment OC in both FCR and BVR—regardless of oxygen status—which is substantially more than previously reported for freshwater lakes (Peter & Sobek, 2018). Below, we discuss short-term (section 4.1) and multiannual (section 4.2) results in the context of previous work, analyze net processing rates across the sediment-water interface (section 4.3), and discuss why Fe-OC levels may be higher in these reservoirs than other freshwater systems (section 4.4).

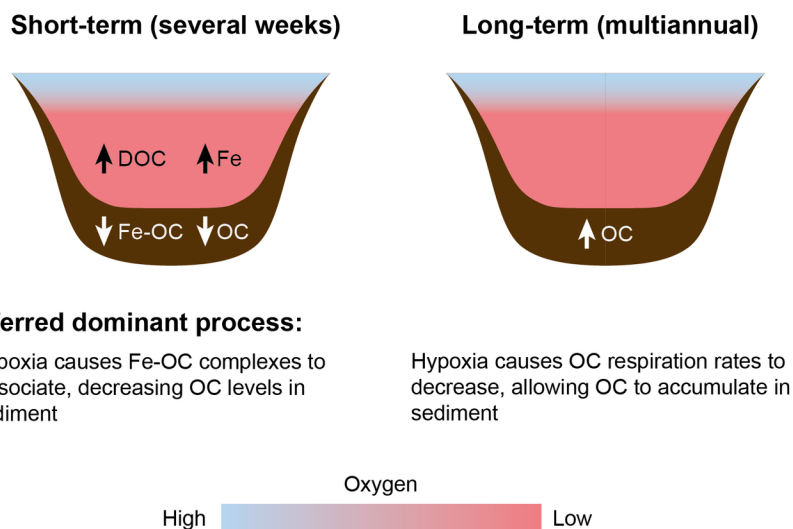


Figure 8: Experimental results suggest that the dominant process through which hypoxia affects sediment organic carbon differs between weekly and multiannual timescales. Left: in microcosm incubations, short-term (weeks) periods of hypoxia led to increased DOC and aqueous Fe, while decreasing sediment OC. On a whole-ecosystem scale, hypolimnetic Fe was closely correlated with oxygen concentrations, and short periods of hypoxia decreased both Fe-OC and OC in sediment. Consequently, Fe-OC protection appears to be a more dominant control on sediment OC sequestration than respiration on short timescales. Right: two years of summer hypoxia in FCR led to increased OC in sediment on a whole-ecosystem scale, suggesting that respiration may be a more dominant control on OC sequestration than protection by Fe on this timescale.

4.1 Short-term periods of hypoxia lead to release of Fe-protected OC and decrease total sediment OC

Both whole-ecosystem and microcosm experiments suggest that short-term periods (i.e., weeks) of hypoxia can dramatically alter coupled OC and Fe cycling. Whole-ecosystem experiments revealed changes in hypolimnetic DOC and Fe, sediment OC, and sediment Fe-OC associated with water-column oxygenation (Figures 3, 4, 8), while microcosm incubations showed clear differences in aqueous Fe, and DOC and sediment OC among treatments (Figures 6, 7). The magnitude of these effects was substantial: on a whole-ecosystem scale, two weeks of hypoxic conditions decreased both sediment Fe-OC and total sediment OC by a mean of 30%. Declining Fe-OC and total OC in sediment, as well as concomitant increases in Fe and OC in overlying water, are consistent with the expectation that hypoxia causes reductive dissolution of Fe(III) in Fe-OC complexes, releasing soluble Fe and DOC on day to week scales (e.g., Carey et al., 2018; Pan et al., 2016; Patzner et al., 2020; Peter et al., 2016; Skoog & Arias-Esquivel, 2009; Figures 1, 8).

Our results contribute to an accumulating body of evidence that short-term fluctuations in oxygen concentrations may have important effects on OC storage in soils and sediment. Previous research has shown that recently-formed Fe-OC associations may be particularly prone to hypoxic release, and reduction of Fe(III) in Fe-OC compounds can increase OC respiration rates during hypoxic conditions (Chen et al., 2020). As a result of these and other processes, periodic fluctuations in oxygen conditions may sustain or stimulate respiration rates relative to both constant oxic and constant hypoxic conditions (Bastviken et al., 2004; Huang et al., 2021). Here, we found substantial decreases in sediment OC and Fe-OC following two weeks of hypoxia, with restored OC and Fe-OC after two weeks of oxic conditions (Figure 3, S3), suggesting that at least a fraction of the sediment Fe-OC pool is sensitive to short-term changes in oxygen concentrations in overlying water on a whole-ecosystem scale.

While sediment Fe-OC responded to oxygenation on a whole-ecosystem scale, Fe-OC did not vary significantly

among oxygen treatments in experimental incubations. We expect that this difference derives at least in part from the sediments we analyzed: whole-ecosystem samples were composed of the top 1 cm of sediment from sediment cores, while sediment for the experimental incubations was sampled using an Ekman grab, and therefore included deeper layers of sediment. In soil, deeper horizons are thought to have more stable Fe-OC aggregates (Rumpel & Kögel-Knabner, 2011). Our results suggest that the same pattern may be true in sediments, resulting in burial of stable Fe-OC compounds in deeper sediments over time.

Formation and dissociation of Fe-OC complexes are two of many ways in which Fe and OC are impacted by hypoxia; both Fe and OC can also respond independently to changes in DO concentrations. Fe is oxidized from Fe(II) (soluble) to Fe(III) minerals (insoluble) both biotically and abiotically under oxic conditions (Kappler et al., 2021). Increased microbial biomass may be partially responsible for the increase in sediment OC under oxic conditions in experimental microcosms, as we observed the formation of orange (likely Fe-oxidizing) biofilms on top of the sediment layer in oxic microcosms (Figure S1). Fe reduction is also often associated with an increase in pH, which may increase the solubility of OC (Tavakkoli et al., 2015). However, pH did not differ consistently between microcosm treatments in this study and remained circumneutral on a whole-ecosystem scale (Figure S6 and S7). While these alternative mechanisms likely play a role in Fe and OC release, the decrease in Fe-OC and total OC following inactivation of the oxygenation system in FCR suggests that, at least for some surficial sediments, short (~2 week) periods of hypoxia can cause Fe-OC complexes to dissociate and decrease sediment OC burial on a whole-ecosystem scale.

4.2 Over multiannual timescales, OC respiration rates play a greater role than Fe-OC in determining the net effect of hypoxia on sediment OC content

Over multiannual timescales (2019–2021), exposure to seasonal hypoxia increased the amount of OC in sediments from FCR by 57% without changing the amount of Fe-OC (Figure 5). This clearly contrasts with short-term experimental results, which showed decreased OC content following short periods of hypoxia (section 4.3). While many factors could affect OC and Fe-OC over multiannual timescales, the fact that no comparable effects were seen in the unoxygenated reference reservoir (BVR) suggests that these changes may be attributed to changes in DO concentrations in overlying water. Over two years of summer hypoxia, OC levels in sediment from FCR increased to the extent that they were no longer significantly different from the hypoxic reference reservoir (Figure 5), suggesting that legacy effects of oxygen conditions on total sediment OC may diminish after a two-year interval.

Increases in sediment OC content with increased hypoxic duration are consistent with a reduction in sediment OC respiration rates under hypoxic conditions (Carey et al., 2018; Hargrave, 1969; Walker & Snodgrass, 1986). OC respiration rates decrease under hypoxic conditions because OC must be broken down using alternative electron acceptors, which produce a lower energy yield (Bastviken et al., 2003, 2004). Previous work conducted in BVR found that CH₄ was the dominant terminal electron acceptor in the hypolimnion during hypoxic summer conditions, and CH₄ has one of the lowest energy yields of alternate electron acceptors (McClure et al., 2021). Consequently, as less OC is respired in hypoxic hypolimnetic water and sediments, OC can accumulate more quickly in surficial sediments. Our results suggest that over multiannual timescales, this process (decreased respiration under hypoxic conditions) outweighs the counteracting decrease in Fe protection of OC that we observed during short periods of hypoxia.

Sediment Fe-OC content (per g sediment mass) did not significantly change after two years of hypoxic conditions in FCR (Figure 5), indicating that at least a fraction of these compounds are able to withstand fluctuations in environmental redox conditions. Long-term stability of Fe-OC complexes can be promoted by the formation of strong chemical bonds between OC and mineral surfaces, and these bonds continue to form over time (Kaiser et al., 2007). Likewise, weathering of Fe increases the porosity of mineral surfaces and allows for OC protection within pore spaces (Kaiser & Guggenberger, 2003; Kleber et al., 2005). Decreased accessibility to microbial decomposition (e.g., through burial) may further increase the ability of Fe-OC compounds to persist over time (Kaiser & Guggenberger, 2003; Kleber et al., 2015). In FCR, the history of oxic conditions (2013–2019) may have contributed to the formation of particularly stable Fe-OC complexes in sediment, which were then able to withstand two summers of hypoxia.

Importantly, much of the OC that accumulates under hypoxic conditions does not end up being bound to Fe. This result may be due to Fe oxidation state, as sorptive associations between DOC and Fe in sediment are much less likely to form if Fe is in a reduced state (Fe(II); Nierop et al., 2002). Because total OC increased following hypoxia and Fe-OC did not change, Fe-OC as a percentage of sediment OC was significantly lower after two years of hypoxia than before this hypoxic period. Declines in the percentage of OC that is bound to Fe may have important implications for ecosystem-scale carbon cycling, as OC that is associated with Fe is comparatively more protected from respiration (e.g., Chen et al., 2018, 2020; Hemingway et al., 2019; Kleber et al., 2005). Increased stocks of OC that are not associated with Fe may increase rates of methane production and OC release from the sediment to the water column (e.g., Hounshell et al., 2021), and could increase aerobic respiration rates under subsequent oxic periods (e.g., Chen et al., 2020; Huang et al., 2021).

4.3 Substantial OC and Fe cycling occurs at the sediment-water interface

Notably, the OC content of the top 1 cm of sediment was significantly lower than that of settling particulate material in both FCR and BVR, and nearly three times as much of this OC was bound to Fe in sediments compared to settling material (Figure 2). These results imply a substantial level of OC and Fe processing at the sediment-water interface, and they reinforce previous research in suggesting that the sediment-water interface is a hotspot for biogeochemical cycling freshwater lakes and reservoirs (e.g., Dadi et al., 2017; Hanson et al., 2015; Krueger et al., 2020).

From a mass-balance perspective, the difference in Fe-OC between settling material and surficial sediments suggests that Fe-OC complexes are either formed or preferentially preserved (compared to OC that is not associated with Fe) in sediments. Preferential preservation of Fe-OC is well-supported, as complexation with Fe has been shown to decrease OC turnover rates across multiple ecosystems (Eusterhues et al., 2014; Kaiser & Guggenberger, 2003; Kalbitz et al., 2005; Kleber et al., 2005; Lalonde et al., 2012; Mikutta & Kaiser, 2011). However, the difference in Fe-OC between settling material and surficial sediments likely also results in large part from Fe-OC associations formed in sediment (e.g., through adsorption of organic matter onto existing Fe minerals and Fe-OC complexes), as Fe(III) levels are much higher in sediments (e.g., Davison et al., 1991) and the composition of OC in sediments may be more preferable for complexation with Fe. While we did not measure OC quality in this study, we anticipate that settling material may have higher autochthonous OC levels and be more rapidly respired, while sediment OC may be enriched in allochthonous aromatic OC, which preferentially associates with Fe (Kramer et al., 2012; Riedel et al., 2013; Shields et al., 2016). Documenting changes in Fe-OC throughout the process of sediment diagenesis enhances our understanding of OC sequestration, as few if any previous studies have quantified the difference between Fe-OC inputs and stocks in aquatic sediments.

4.4 High Fe-OC levels reflect site-specific characteristics

On average, nearly one-third of surficial sediment OC was bound to Fe (dithionite-extractable) across two years in FCR and BVR (Figure 5). This percentage is far greater than that documented by Peter et al. (2018), where Fe-OC comprised [?]11% of total sediment OC across five boreal lakes. Furthermore, the levels of Fe-OC recorded here are higher than the mean of 21.5+8.6% reported for a broad range of marine sediments (Lalonde et al. 2012). With few other studies analyzing Fe-OC in freshwater lakes and reservoirs to date, our analysis provides new evidence that Fe-OC may play an important role in carbon sequestration in some freshwaters.

Differences in the percentage of organic matter that is bound to Fe may result from differences in overlying DO concentrations, as described throughout this study, as well as a number of other factors. For example, increasing ratios of Fe:OC and increasing absolute concentrations of Fe and OC can all increase the amount of Fe-OC coprecipitation (Chen et al., 2016; Kleber et al., 2015 and references therein). Likewise, differing Fe forms, OC quality, and pH may also impact the formation and stability of Fe-OC complexes (Curti et al., 2021; Kaiser et al., 2007; Kaiser & Guggenberger, 2003; Kleber et al., 2015); these differences may derive from contrasting geology, catchment vegetation, and trophic status, among many other factors. However, none of these factors fully explain differences in Fe-OC content between sites studied to date (e.g., Lalonde

et al., 2012; Peter & Sobek, 2018).

Despite having higher Fe-OC levels (as a percentage of total sediment OC) than most aquatic sediments studied to date, other sediment characteristics in FCR and BVR are within the range of those measured in other locations. FCR and BVR have much lower sediment OC content than the boreal lakes analyzed by Peter and Sobek (2018; 14–38% of sediment mass), but higher sediment OC than the primarily marine sediments analyzed by Lalonde et al. (2012; 0–7% of sediment mass). Fe concentrations are high in sediment from FCR and BVR, with a mean of 53,466 mg/kg dry weight (Krueger et al., 2020). However, Peter and Sobek (2018) observed low Fe-OC as a percentage of sediment OC ($\mu=6.7\%$) in one extremely high-Fe lake (Övre Skärsjön; 226,172 mg/kg reducible Fe in sediment). Likewise, pH in FCR and BVR is circumneutral (Figure S7), well within the range of 5.4–7.6 reported by Peter and Sobek (2018), and both Peter and Sobek (2018) and Lalonde et al. (2012) included a range of oxic and hypoxic sediments in their analyses. These observations from a range of aquatic sediments suggest that site-specific characteristics associated with catchment geology, water residence time, OC and Fe input rates, OC quality, and Fe mineral forms play an important role in determining the percentage of sediment OC that is bound to Fe. Understanding the controls on Fe-OC in freshwater sediment will require Fe-OC characterization at a greater number and diversity of lakes and reservoirs. Such research will be essential to understanding how freshwater OC sequestration may be affected by global changes in Fe concentrations (Weyhenmeyer et al., 2014), water temperatures (Dokulil et al., 2021; O'Reilly et al., 2015), and pH (Garmo et al., 2014; Gavin et al., 2018; Stoddard et al., 1999), among other factors.

5. Conclusions

Results from this study help reconcile previous Fe-OC research and shed light on how declining oxygen concentrations may impact the role of lakes and reservoirs in the global carbon cycle. Research across terrestrial soils and marine sediments has provided contradictory evidence that Fe-OC complexes are (1) readily dissociated under hypoxic conditions and (2) capable of promoting sediment OC burial into deeper (hypoxic) layers over the course of decades to millennia. Here, we find that the timescale of analysis plays a critical role in understanding the net effect of hypoxia on sediment OC and Fe-OC. Specifically, a portion of the Fe-OC pool in surficial sediment is highly responsive to hypoxia in overlying water on a weekly timescale, resulting in decreased sediment OC. However, over longer timescales, the decrease in OC that results from dissociation of Fe-OC complexes is outweighed by the increase in sediment OC that results from slower respiration rates under hypoxia. At both timescales, our results reinforce that Fe may serve as an important control over OC cycling and sediment preservation of OC in some freshwater ecosystems. As the duration of hypoxia increases in lakes and reservoirs (Jane et al., 2021; Jenny et al., 2016), our results suggest that OC dynamics will respond non-linearly. While short periods of hypoxia may decrease OC burial, increasing prevalence and duration of hypoxia over multiannual timescales has the potential to increase OC burial in freshwater sediment, intensifying the role of freshwaters as sinks in the global carbon cycle.

Acknowledgements

We are grateful for ongoing partnerships with the Western Virginia Water Authority that facilitated this research. Additionally, we thank the Virginia Tech Reservoir Group for helping to collect these data, particularly Adrienne Breef-Pilz for organizing the 2021 field season and helping to collect sediment cores in 2021, James Maze and Dexter Howard for helping to collect sediment cores in 2019, Ryan McClure for leading CTD data collection before 2019, and Alex Hounshell for organizing the 2019 field season. We thank Chip Frazier and Jeb Barrett for providing access to laboratory equipment and Jeff Parks in the VT ICP-MS lab for analyzing Fe samples. This work is supported by the Institute for Critical Science and Applied Technology at Virginia Tech and the U.S. National Science Foundation (NSF) foundation grants DGE-1651272, DEB-1753639, SCC-1737424, DBI-1933016, and DBI-1933102.

Author Contributions

ASL conceptualized this study with CCC and MES. ASL performed chemical Fe-OC extractions, analyzed data, developed figures, and wrote this manuscript with MES, MEL, and CCC. BRN led analytical chemistry

methods development and performed DOC analyses. NWH and MES oversaw whole-ecosystem Fe sampling, analysis, and data collation. AD helped to design and run the microcosm experiment and process sediment samples. HLW collated and processed DOC and YSI data and reviewed code for this manuscript. CCC oversaw whole-ecosystem experiments. All authors edited and approved the final manuscript.

Open Research

All data used in this study are available in the Environmental Data Initiative (Carey et al., 2021; Carey, Lewis, Gantzer, et al., 2022; Carey, Lewis, McClure, et al., 2022; Carey, Wander, McClure, et al., 2022; Lewis et al., 2022; Lewis, Schreiber, et al., 2022; Schreiber et al., 2022). Code to reproduce results in this manuscript is available in a Zenodo repository (Lewis, 2022).

References

- Akima, H., Gebhardt, A., Petzold, T., Maechler, M., & code), bilinear. (2022). akima: Interpolation of Irregularly and Regularly Spaced Data (Version 0.6-3.4). Retrieved from <https://CRAN.R-project.org/package=akima>
- American Public Health Association. (2018a). 3125 metals by inductively coupled plasma-mass spectrometry. In *Standard Methods For the Examination of Water and Wastewater*. American Public Health Association. <https://doi.org/10.2105/smww.2882.048>
- American Public Health Association. (2018b). 5310 total organic carbon (toc). In *Standard Methods For the Examination of Water and Wastewater*. American Public Health Association. <https://doi.org/10.2105/SMWW.2882.104>
- Arndt, S., Jørgensen, B. B., LaRowe, D. E., Middelburg, J. J., Pancost, R. D., & Regnier, P. (2013). Quantifying the degradation of organic matter in marine sediments: A review and synthesis. *Earth-Science Reviews*, 123, 53–86. <https://doi.org/10.1016/j.earscirev.2013.02.008>
- Auguie, B. (2019). egg: Extensions for “ggplot2”: Custom Geom, Custom Themes, Plot Alignment, Labelled Panels, Symmetric Scales, and Fixed Panel Size (Version 0.4.5). Retrieved from <https://CRAN.R-project.org/package=egg>
- Bai, J., Luo, M., Yang, Y., Xiao, S., Zhai, Z., & Huang, J. (2021). Iron-bound carbon increases along a freshwater-oligohaline gradient in a subtropical tidal wetland. *Soil Biology and Biochemistry*, 154, 108128. <https://doi.org/10.1016/j.soilbio.2020.108128>
- Ball, J. W., & Nordstrom, D. K. (1991). *User’s manual for WATEQ4F, with revised thermodynamic data base and text cases for calculating speciation of major, trace, and redox elements in natural waters* (USGS Numbered Series No. 91–183). *User’s manual for WATEQ4F, with revised thermodynamic data base and text cases for calculating speciation of major, trace, and redox elements in natural waters* (Vol. 91–183). U.S. Geological Survey. <https://doi.org/10.3133/ofr91183>
- Bartosiewicz, M., Przytulska, A., Lapierre, J.-F., Laurion, I., Lehmann, M. F., & Maranger, R. (2019). Hot tops, cold bottoms: Synergistic climate warming and shielding effects increase carbon burial in lakes. *Limnology and Oceanography Letters*, 4 (5), 132–144. <https://doi.org/10.1002/lol2.10117>
- Bastviken, D., Olsson, M., & Tranvik, L. (2003). Simultaneous measurements of organic carbon mineralization and bacterial production in oxic and anoxic lake sediments. *Microbial Ecology*, 46 (1), 73–82. <https://doi.org/10.1007/s00248-002-1061-9>
- Bastviken, D., Persson, L., Odham, G., & Tranvik, L. (2004). Degradation of dissolved organic matter in oxic and anoxic lake water. *Limnology and Oceanography*, 49 (1), 109–116.

<https://doi.org/10.4319/lo.2004.49.1.0109>

Bastviken, D., Tranvik, L. J., Downing, J. A., Crill, P. M., & Enrich-Prast, A. (2011). Freshwater methane emissions offset the continental carbon sink. *Science*, 331 (6013), 50–50. <https://doi.org/10.1126/science.1196808>

Battin, T. J., Luyssaert, S., Kaplan, L. A., Aufdenkampe, A. K., Richter, A., & Tranvik, L. J. (2009). The boundless carbon cycle. *Nature Geoscience*, 2 (9), 598–600. <https://doi.org/10.1038/ngeo618>

Björneras, C., Weyhenmeyer, G. A., Evans, C. D., Gessner, M. O., Grossart, H.-P., Kangur, K., et al. (2017). Widespread increases in iron concentration in European and North American freshwaters. *Global Biogeochemical Cycles*, 31 (10), 1488–1500. <https://doi.org/10.1002/2017GB005749>

Brothers, S., Kohler, J., Attermeyer, K., Grossart, H. P., Mehner, T., Meyer, N., et al. (2014). A feedback loop links brownification and anoxia in a temperate, shallow lake. *Limnology and Oceanography*, 59 (4), 1388–1398. <https://doi.org/10.4319/lo.2014.59.4.1388>

Carey, C. C., Doubek, J. P., McClure, R. P., & Hanson, P. C. (2018). Oxygen dynamics control the burial of organic carbon in a eutrophic reservoir. *Limnology and Oceanography Letters*, 3 (3), 293–301. <https://doi.org/10.1002/lol2.10057>

Carey, C. C., Wander, H. L., Woelmer, W. M., Lofton, M. E., Breef-Pilz, A., Doubek, J. P., et al. (2021). Water chemistry time series for Beaverdam Reservoir, Carvins Cove Reservoir, Falling Creek Reservoir, Gatewood Reservoir, and Spring Hollow Reservoir in southwestern Virginia, USA 2013-2020 [Data set]. Environmental Data Initiative. <https://doi.org/10.6073/PASTA/6343E979A970E8A2590B4A450E851DD2>

Carey, C. C., Hanson, P. C., Thomas, R. Q., Gerling, A. B., Hounshell, A. G., Lewis, A. S. L., et al. (2022). Anoxia decreases the magnitude of the carbon, nitrogen, and phosphorus sink in freshwaters. *Global Change Biology*, 28 (16), 4861–4881. <https://doi.org/10.1111/gcb.16228>

Carey, C. C., Lewis, A. S. L., Gantzer, P. A., Bierlein, K. A., & WVWA. (2022). Bathymetry for Falling Creek Reservoir and Beaverdam Reservoir, Virginia, USA [Data set]. Environmental Data Initiative. Retrieved from <https://portal.s.edirepository.org/nis/mapbrowse?packageid=edi.939.2>

Carey, C. C., Thomas, R. Q., & Hanson, P. C. (2022). General Lake Model-Aquatic EcoDynamics model parameter set for Falling Creek Reservoir, Vinton, Virginia, USA 2013-2019 [Data set]. Environmental Data Initiative. <https://doi.org/10.6073/PASTA/9F7D037D9A133076A0A0D123941C6396>

Carey, C. C., Wander, H. L., McClure, R. P., Lofton, M. E., Hamre, K. D., Doubek, J. P., et al. (2022). Secchi depth data and discrete depth profiles of photosynthetically active radiation, temperature, dissolved oxygen, and pH for Beaverdam Reservoir, Carvins Cove Reservoir, Falling Creek Reservoir, Gatewood Reservoir, and Spring Hollow Reservoir in southwestern Virginia, USA 2013-2021 [Data set]. Environmental Data Initiative. <https://doi.org/10.6073/PASTA/887D8AB8C57FB8FDF3582507F3223CD6>

Carey, C. C., Lewis, A. S. L., McClure, R. P., Gerling, A. B., Breef-Pilz, A., & Das, A. (2022). Time series of high-frequency profiles of depth, temperature, dissolved oxygen, conductivity, specific conductance, chlorophyll a, turbidity, pH, oxidation-reduction potential, photosynthetic active radiation, and descent rate for Beaverdam Reservoir, Carvins Cove Reservoir, Falling Creek Reservoir, Gatewood Reservoir, and Spring Hollow Reservoir in Southwestern Virginia, USA 2013-2021 [Data set]. Environmental Data Initiative. <https://doi.org/10.6073/PASTA/C4C45B5B10B4CB4CD4B5E613C3EFFBD0>

Carey, C. C., Wander, H. L., Howard, D. W., Niederlehner, B. R., Woelmer, W. M., Lofton, M. E., et al. (2022). Water chemistry time series for Beaverdam Reservoir, Carvins Cove Reservoir, Falling Creek Reservoir, Gatewood Reservoir, and Spring Hollow Reservoir in southwestern Virginia, USA 2013-2021 [Data set]. Environmental Data Initiative. <https://doi.org/10.6073/PASTA/7BD797155CDBB5F1ACDF0547C6BA9023>

Carpenter, S. R. (1996). Microcosm experiments have limited relevance for community and ecosystem ecology. *Ecology* , 77 (3), 677–680. <https://doi.org/10.2307/2265490>

Chapman, M. J., Cravotta III, C. A., Szabo, Z., & Lindsey, B. D. (2013). Naturally occurring contaminants in the Piedmont and Blue Ridge crystalline-rock aquifers and Piedmont Early Mesozoic basin siliciclastic-rock aquifers, eastern United States, 1994–2008. Retrieved June 25, 2022, from <https://pubs.er.usgs.gov/publication/sir20135072>

Chen, C., Meile, C., Wilmoth, J., Barcellos, D., & Thompson, A. (2018). Influence of pO₂ on Iron Redox Cycling and Anaerobic Organic Carbon Mineralization in a Humid Tropical Forest Soil. *Environmental Science & Technology* , 52 (14), 7709–7719. <https://doi.org/10.1021/acs.est.8b01368>

Chen, C., Hall, S. J., Coward, E., & Thompson, A. (2020). Iron-mediated organic matter decomposition in humid soils can counteract protection. *Nature Communications* , 11 (1), 2255. <https://doi.org/10.1038/s41467-020-16071-5>

Chen, K.-Y., Chen, T.-Y., Chan, Y.-T., Cheng, C.-Y., Tzou, Y.-M., Liu, Y.-T., & Teah, H.-Y. (2016). Stabilization of Natural Organic Matter by Short-Range-Order Iron Hydroxides. *Environmental Science & Technology* , 50 (23), 12612–12620. <https://doi.org/10.1021/acs.est.6b02793>

Curti, L., Moore, O. W., Babakhani, P., Xiao, K.-Q., Woulds, C., Bray, A. W., et al. (2021). Carboxyl-richness controls organic carbon preservation during coprecipitation with iron (oxyhydr)oxides in the natural environment. *Communications Earth & Environment* , 2 (1), 1–13. <https://doi.org/10.1038/s43247-021-00301-9>

Dadi, T., Wendt-Potthoff, K., & Koschorreck, M. (2017). Sediment resuspension effects on dissolved organic carbon fluxes and microbial metabolic potentials in reservoirs. *Aquatic Sciences* , 79 (3), 749–764. <https://doi.org/10.1007/s00027-017-0533-4>

Davison, W., Grime, G. W., Morgan, J. a. W., & Clarke, K. (1991). Distribution of dissolved iron in sediment pore waters at submillimetre resolution. *Nature* , 352 (6333), 323–325. <https://doi.org/10.1038/352323a0>

Dean, W. E., & Gorham, E. (1998). Magnitude and significance of carbon burial in lakes, reservoirs, and peatlands, 4.

Deemer, B. R., Harrison, J. A., Li, S., Beaulieu, J. J., DelSontro, T., Barros, N., et al. (2016). Greenhouse gas emissions from reservoir water surfaces: A new global synthesis. *BioScience* , 66 (11), 949–964. <https://doi.org/10.1093/biosci/biw117>

DelSontro, T., Beaulieu, J. J., & Downing, J. A. (2018). Greenhouse gas emissions from lakes and impoundments: Upscaling in the face of global change. *Limnology and Oceanography Letters* , 3 (3), 64–75. <https://doi.org/10.1002/lol2.10073>

Dokulil, M. T., de Eyto, E., Maberly, S. C., May, L., Weyhenmeyer, G. A., & Woolway, R. I. (2021). Increasing maximum lake surface temperature under climate change. *Climatic Change* , 165 (3), 56. <https://doi.org/10.1007/s10584-021-03085-1>

Dzialowski, A. R., Rzepecki, M., Kostrzevska-Szlakowska, I., Kalinowska, K., Palash, A., & Lennon, J. T. (2014). Are the abiotic and biotic characteristics of aquatic mesocosms representative of in situ conditions? *Journal of Limnology* , 73 (3). <https://doi.org/10.4081/jlimnol.2014.721>

Einola, E., Rantakari, M., Kankaala, P., Kortelainen, P., Ojala, A., Pajunen, H., et al. (2011). Carbon pools and fluxes in a chain of five boreal lakes: A dry and wet year comparison. *Journal of Geophysical Research: Biogeosciences* , 116 (G3). <https://doi.org/10.1029/2010JG001636>

Eusterhues, K., Neidhardt, J., Hadrich, A., Kusel, K., & Totsche, K. U. (2014). Biodegradation of ferrihydrite-associated organic matter. *Biogeochemistry* , 119 (1–3), 45–50. <https://doi.org/10.1007/s10533-013-9943-0>

- Fisher, B. J., Faust, J. C., Moore, O. W., Peacock, C. L., & Marz, C. (2021). Technical Note: Uncovering the influence of methodological variations on the extractability of iron bound organic carbon, 20.
- Garmo, O. A., Skjelkvale, B. L., de Wit, H. A., Colombo, L., Curtis, C., Folster, J., et al. (2014). Trends in surface water chemistry in acidified areas in Europe and North America from 1990 to 2008. *Water, Air, & Soil Pollution* , 225 (3), 1880. <https://doi.org/10.1007/s11270-014-1880-6>
- Gavin, A. L., Nelson, S. J., Klemmer, A. J., Fernandez, I. J., Strock, K. E., & McDowell, W. H. (2018). Acidification and climate linkages to increased dissolved organic carbon in high-elevation lakes. *Water Resources Research* , 54 (8), 5376–5393. <https://doi.org/10.1029/2017WR020963>
- Gerling, A. B., Browne, R. G., Gantzer, P. A., Mobley, M. H., Little, J. C., & Carey, C. C. (2014). First report of the successful operation of a side stream supersaturation hypolimnetic oxygenation system in a eutrophic, shallow reservoir. *Water Research* , 67 , 129–143. <https://doi.org/10.1016/j.watres.2014.09.002>
- Gerling, A. B., Munger, Z. W., Doubek, J. P., Hamre, K. D., Gantzer, P. A., Little, J. C., & Carey, C. C. (2016). Whole-catchment manipulations of internal and external loading reveal the sensitivity of a century-old reservoir to hypoxia. *Ecosystems* , 19 (3), 555–571. <https://doi.org/10.1007/s10021-015-9951-0>
- Gibbs, M. M. (1979). A simple method for the rapid determination of iron in natural waters. *Water Research* , 13 (3), 295–297. [https://doi.org/10.1016/0043-1354\(79\)90209-4](https://doi.org/10.1016/0043-1354(79)90209-4)
- Grolemund, G., & Wickham, H. (2011). Dates and Times Made Easy with lubridate. *Journal of Statistical Software* , 40 , 1–25. <https://doi.org/10.18637/jss.v040.i03>
- Hamre, K. D., Lofton, M. E., McClure, R. P., Munger, Z. W., Doubek, J. P., Gerling, A. B., et al. (2018). In situ fluorometry reveals a persistent, perennial hypolimnetic cyanobacterial bloom in a seasonally anoxic reservoir. *Freshwater Science* , 37 (3), 483–495. <https://doi.org/10.1086/699327>
- Hanson, P. C., Pace, M. L., Carpenter, S. R., Cole, J. J., & Stanley, E. H. (2015). Integrating landscape carbon cycling: research needs for resolving organic carbon budgets of lakes. *Ecosystems* , 18 (3), 363–375. <https://doi.org/10.1007/s10021-014-9826-9>
- Hargrave, B. T. (1969). Similarity of oxygen uptake by benthic communities. *Limnology and Oceanography* , 14 (5), 801–805. <https://doi.org/10.4319/lo.1969.14.5.0801>
- Harris, D., Horwath, W. R., & Kessel, C. van. (2001). Acid fumigation of soils to remove carbonates prior to total organic carbon or CARBON-13 isotopic analysis. *Soil Science Society of America Journal* , 65 (6), 1853–1856. <https://doi.org/10.2136/sssaj2001.1853>
- Hemingway, J. D., Rothman, D. H., Grant, K. E., Rosengard, S. Z., Eglinton, T. I., Derry, L. A., & Galy, V. V. (2019). Mineral protection regulates long-term global preservation of natural organic carbon. *Nature* , 570 (7760), 228–231. <https://doi.org/10.1038/s41586-019-1280-6>
- Hounshell, A. G., McClure, R. P., Lofton, M. E., & Carey, C. C. (2021). Whole-ecosystem oxygenation experiments reveal substantially greater hypolimnetic methane concentrations in reservoirs during anoxia. *Limnology and Oceanography Letters* , 6 (1), 33–42.
- Huang, W., Wang, K., Ye, C., Hockaday, W. C., Wang, G., & Hall, S. J. (2021). High carbon losses from oxygen-limited soils challenge biogeochemical theory and model assumptions. *Global Change Biology* , 27 (23), 6166–6180. <https://doi.org/10.1111/gcb.15867>
- Jane, S., Hansen, G., Kraemer, B., Leavitt, P., Mincer, J., North, R., et al. (2021). Widespread deoxygenation of temperate lakes. *Nature* , 594 . <https://doi.org/10.1038/s41586-021-03550-y>
- Jenny, J.-P., Francus, P., Normandeau, A., Lapointe, F., Perga, M.-E., Ojala, A., et al. (2016). Global spread of hypoxia in freshwater ecosystems during the last three centuries is caused by rising local human pressure. *Global Change Biology* , 22 (4), 1481–1489. <https://doi.org/10.1111/gcb.13193>

- Kaiser, K., & Guggenberger, G. (2003). Mineral surfaces and soil organic matter. *European Journal of Soil Science* , 54 (2), 219–236. <https://doi.org/10.1046/j.1365-2389.2003.00544.x>
- Kaiser, K., Mikutta, R., & Guggenberger, G. (2007). Increased stability of organic matter sorbed to ferrihydrite and goethite on aging. *Soil Science Society of America Journal* , 71 (3), 711–719. <https://doi.org/10.2136/sssaj2006.0189>
- Kalbitz, K., Schwesig, D., Rethemeyer, J., & Matzner, E. (2005). Stabilization of dissolved organic matter by sorption to the mineral soil. *Soil Biology and Biochemistry* , 37 (7), 1319–1331. <https://doi.org/10.1016/j.soilbio.2004.11.028>
- Kappler, A., Bryce, C., Mansor, M., Lueder, U., Byrne, J. M., & Swanner, E. D. (2021). An evolving view on biogeochemical cycling of iron. *Nature Reviews Microbiology* , 1–15. <https://doi.org/10.1038/s41579-020-00502-7>
- Kassambara, A. (2020). ggpubr: “ggplot2” Based Publication Ready Plots (Version 0.4.0). Retrieved from <https://CRAN.R-project.org/package=ggpubr>
- Kassambara, A. (2021). rstatix: Pipe-Friendly Framework for Basic Statistical Tests (Version 0.7.0). Retrieved from <https://CRAN.R-project.org/package=rstatix>
- Keitt, T. (2022). colorRamps: Builds Color Tables (Version 2.3.1). Retrieved from <https://CRAN.R-project.org/package=colorRamps>
- Kim, J., & Kim, T.-H. (2020). Distribution of Humic Fluorescent Dissolved Organic Matter in Lake Shihwa: the Role of the Redox Condition. *Estuaries and Coasts* , 43 (3), 578–588. <https://doi.org/10.1007/s12237-018-00491-0>
- Kirk, G. (2004). Reduction and Oxidation. In G. Kirk (Ed.), *The Biogeochemistry of Submerged Soils* (pp. 93–134). John Wiley & Sons, Ltd. <https://doi.org/10.1002/047086303X.ch4>
- Kleber, M., Mikutta, R., Torn, M. S., & Jahn, R. (2005). Poorly crystalline mineral phases protect organic matter in acid subsoil horizons. *European Journal of Soil Science* , 56 (6), 717–725. <https://doi.org/10.1111/j.1365-2389.2005.00706.x>
- Kleber, M., Eusterhues, K., Keiluweit, M., Mikutta, C., Mikutta, R., & Nico, P. S. (2015). Chapter One - Mineral–Organic Associations: Formation, Properties, and Relevance in Soil Environments. In D. L. Sparks (Ed.), *Advances in Agronomy* (Vol. 130, pp. 1–140). Academic Press. <https://doi.org/10.1016/bs.agron.2014.10.005>
- Knoll, L. B., Vanni, M. J., Renwick, W. H., Dittman, E. K., & Gephart, J. A. (2013). Temperate reservoirs are large carbon sinks and small CO₂ sources: Results from high-resolution carbon budgets. *Global Biogeochemical Cycles* , 27 (1), 52–64. <https://doi.org/10.1002/gbc.20020>
- Kramer, M. G., & Chadwick, O. A. (2018). Climate-driven thresholds in reactive mineral retention of soil carbon at the global scale. *Nature Climate Change* , 8 (12), 1104–1108. <https://doi.org/10.1038/s41558-018-0341-4>
- Kramer, M. G., Sanderman, J., Chadwick, O. A., Chorover, J., & Vitousek, P. M. (2012). Long-term carbon storage through retention of dissolved aromatic acids by reactive particles in soil. *Global Change Biology* , 18 (8), 2594–2605. <https://doi.org/10.1111/j.1365-2486.2012.02681.x>
- Krueger, K. M., Vavrus, C. E., Lofton, M. E., McClure, R. P., Gantzer, P., Carey, C. C., & Schreiber, M. E. (2020). Iron and manganese fluxes across the sediment-water interface in a drinking water reservoir. *Water Research* , 182 , 116003. <https://doi.org/10.1016/j.watres.2020.116003>
- Lalonde, K., Mucci, A., Ouellet, A., & Gelinas, Y. (2012). Preservation of organic matter in sediments promoted by iron. *Nature* , 483 (7388), 198–200. <https://doi.org/10.1038/nature10855>

- LaRowe, D. E., & Van Cappellen, P. (2011). Degradation of natural organic matter: A thermodynamic analysis. *Geochimica et Cosmochimica Acta* , 75 (8), 2030–2042. <https://doi.org/10.1016/j.gca.2011.01.020>
- Lau, M. P., & del Giorgio, P. (2020). Reactivity, fate and functional roles of dissolved organic matter in anoxic inland waters. *Biology Letters* , 16 (2), 20190694. <https://doi.org/10.1098/rsbl.2019.0694>
- Le Quere, C., Moriarty, R., Andrew, R. M., Peters, G. P., Ciais, P., Friedlingstein, P., et al. (2015). Global carbon budget 2014. *Earth System Science Data* , 7 (1), 47–85. <https://doi.org/10.5194/essd-7-47-2015>
- Lewis, A. S. L. (2022). Effects of hypoxia on coupled carbon and iron cycling in two freshwater reservoirs v1.0.0. Zenodo. Retrieved from <https://doi.org/10.5281/zenodo.6845416>
- Lewis, A. S. L., Niederlehner, B. R., Das, A., Wander, H. L., Schreiber, M. E., & Carey, C. C. (2022). Experimental microcosm incubations assessing the effect of hypoxia on aqueous iron and organic carbon, pH, sediment organic carbon, and sediment iron-bound organic carbon. Environmental Data Initiative. Retrieved from <https://portal-s.edirepository.org/nis/mapbrowse?packageid=edi.880.3>
- Lewis, A. S. L., Schreiber, M. E., Niederlehner, B. R., Das, A., & Carey, C. C. (2022). Total organic carbon, total nitrogen, and iron-bound organic carbon in surficial sediment and settling particulate material from Falling Creek and Beaverdam Reservoirs in 2019 and 2021. Environmental Data Initiative. Retrieved from <https://portal-s.edirepository.org/nis/mapbrowse?packageid=edi.881.4>
- Marking, L. L., & Dawson, V. K. (1973). *Toxicity of quinaldine sulfate to fish* (Report No. 48) (pp. 0–8). La Crosse, WI. Retrieved from <http://pubs.er.usgs.gov/publication/2001015>
- McClure, R. P., Schreiber, M. E., Lofton, M. E., Chen, S., Krueger, K. M., & Carey, C. C. (2021). Ecosystem-Scale Oxygen Manipulations Alter Terminal Electron Acceptor Pathways in a Eutrophic Reservoir. *Ecosystems* , 24 (6), 1281–1298. <https://doi.org/10.1007/s10021-020-00582-9>
- Mendonça, R., Muller, R. A., Clow, D., Verpoorter, C., Raymond, P., Tranvik, L. J., & Sobek, S. (2017). Organic carbon burial in global lakes and reservoirs. *Nature Communications* , 8 (1), 1694. <https://doi.org/10.1038/s41467-017-01789-6>
- Mikutta, R., & Kaiser, K. (2011). Organic matter bound to mineral surfaces: Resistance to chemical and biological oxidation. *Soil Biology and Biochemistry* , 43 (8), 1738–1741. <https://doi.org/10.1016/j.soilbio.2011.04.012>
- Munger, Z. W., Carey, C. C., Gerling, A. B., Doubek, J. P., Hamre, K. D., McClure, R. P., & Schreiber, M. E. (2019). Oxygenation and hydrologic controls on iron and manganese mass budgets in a drinking-water reservoir. *Lake and Reservoir Management* , 35 (3), 277–291. <https://doi.org/10.1080/10402381.2018.1545811>
- Nierop, K. G. J., Jansen, B., & Verstraten, J. M. (2002). Dissolved organic matter, aluminium and iron interactions: precipitation induced by metal/carbon ratio, pH and competition. *The Science of the Total Environment* , 300 (1–3), 201–211. [https://doi.org/10.1016/S0048-9697\(02\)00254-1](https://doi.org/10.1016/S0048-9697(02)00254-1)
- O'Reilly, C. M., Sharma, S., Gray, D. K., Hampton, S. E., Read, J. S., Rowley, R. J., et al. (2015). Rapid and highly variable warming of lake surface waters around the globe. *Geophysical Research Letters* , 42 (24), 10,773–10,781. <https://doi.org/10.1002/2015GL066235>
- Oyewumi, O., & Schreiber, M. E. (2017). Using column experiments to examine transport of As and other trace elements released from poultry litter: Implications for trace element mobility in agricultural watersheds. *Environmental Pollution* , 227 , 223–233. <https://doi.org/10.1016/j.envpol.2017.04.063>
- Pacheco, F. S., Roland, F., & Downing, J. A. (2014). Eutrophication reverses whole-lake carbon budgets. *Inland Waters* , 4 (1), 41–48. <https://doi.org/10.5268/IW-4.1.614>
- Pan, W., Kan, J., Inamdar, S., Chen, C., & Sparks, D. (2016). Dissimilatory microbial iron reduction release DOC (dissolved organic carbon) from carbon-ferrihydrite association. *Soil Biology and Biochemistry* , 103 , 232–240. <https://doi.org/10.1016/j.soilbio.2016.08.026>

- Patzner, M. S., Mueller, C. W., Malusova, M., Baur, M., Nikeleit, V., Scholten, T., et al. (2020). Iron mineral dissolution releases iron and associated organic carbon during permafrost thaw. *Nature Communications* , 11 (1), 6329. <https://doi.org/10.1038/s41467-020-20102-6>
- Peter, S., & Sobek, S. (2018). High variability in iron-bound organic carbon among five boreal lake sediments. *Biogeochemistry* , 139 (1), 19–29. <https://doi.org/10.1007/s10533-018-0456-8>
- Peter, S., Isidorova, A., & Sobek, S. (2016). Enhanced carbon loss from anoxic lake sediment through diffusion of dissolved organic carbon. *Journal of Geophysical Research: Biogeosciences* , 121 (7), 1959–1977. <https://doi.org/10.1002/2016JG003425>
- Peter, S., Agstam, O., & Sobek, S. (2017). Widespread release of dissolved organic carbon from anoxic boreal lake sediments. *Inland Waters* , 7 (2), 151–163. <https://doi.org/10.1080/20442041.2017.1300226>
- Raymond, P. A., Hartmann, J., Lauerwald, R., Sobek, S., McDonald, C., Hoover, M., et al. (2013). Global carbon dioxide emissions from inland waters. *Nature* , 503 (7476), 355–359. <https://doi.org/10.1038/nature12760>
- Riedel, T., Zak, D., Biester, H., & Dittmar, T. (2013). Iron traps terrestrially derived dissolved organic matter at redox interfaces. *Proceedings of the National Academy of Sciences* , 110 (25), 10101–10105. <https://doi.org/10.1073/pnas.1221487110>
- Rumpel, C., & Kogel-Knabner, I. (2011). Deep soil organic matter—a key but poorly understood component of terrestrial C cycle. *Plant and Soil* , 338 (1), 143–158. <https://doi.org/10.1007/s11104-010-0391-5>
- Schindler, D. W. (1998). Whole-ecosystem experiments: replication versus realism: the need for ecosystem-scale experiments. *Ecosystems* , 1 (4), 323–334. <https://doi.org/10.1007/s100219900026>
- Schreiber, M. E., Hammond, N. W., Krueger, K. M., Munger, Z. W., Ming, C. L., Breef-Pilz, A., & Carey, C. C. (2022). Time series of total and soluble iron and manganese concentrations from Falling Creek Reservoir and Beaverdam Reservoir in southwestern Virginia, USA from 2014 through 2021 [Data set]. Environmental Data Initiative. <https://doi.org/10.6073/PASTA/7CDF3D7A234963B265F09B7D6D08F357>
- Shields, M. R., Bianchi, T. S., Gelinas, Y., Allison, M. A., & Twilley, R. R. (2016). Enhanced terrestrial carbon preservation promoted by reactive iron in deltaic sediments. *Geophysical Research Letters* , 43 (3), 1149–1157. <https://doi.org/10.1002/2015GL067388>
- Skoog, A. C., & Arias-Esquivel, V. A. (2009). The effect of induced anoxia and reoxygenation on benthic fluxes of organic carbon, phosphate, iron, and manganese. *Science of The Total Environment* , 407 (23), 6085–6092. <https://doi.org/10.1016/j.scitotenv.2009.08.030>
- Sobek, S., Durisch-Kaiser, E., Zurbrugg, R., Wongfun, N., Wessels, M., Pasche, N., & Wehrli, B. (2009). Organic carbon burial efficiency in lake sediments controlled by oxygen exposure time and sediment source. *Limnology and Oceanography* , 54 (6), 2243–2254. <https://doi.org/10.4319/lo.2009.54.6.2243>
- Stoddard, J. L., Jeffries, D. S., Lukewille, A., Clair, T. A., Dillon, P. J., Driscoll, C. T., et al. (1999). Regional trends in aquatic recovery from acidification in North America and Europe. *Nature* , 401 (6753), 575–578. <https://doi.org/10.1038/44114>
- Tavakkoli, E., Rengasamy, P., Smith, E., & McDonald, G. K. (2015). The effect of cation–anion interactions on soil pH and solubility of organic carbon. *European Journal of Soil Science* , 66 (6), 1054–1062. <https://doi.org/10.1111/ejss.12294>
- Thompson, A., Chadwick, O. A., Rancourt, D. G., & Chorover, J. (2006). Iron-oxide crystallinity increases during soil redox oscillations. *Geochimica et Cosmochimica Acta* , 70 (7), 1710–1727. <https://doi.org/10.1016/j.gca.2005.12.005>
- Tranvik, L. J., Cole, J. J., & Prairie, Y. T. (2018). The study of carbon in inland waters—from isolated ecosystems to players in the global carbon cycle. *Limnology and Oceanography Letters* , 3 (3), 41–48.

<https://doi.org/10.1002/lol2.10068>

Trapletti, A., Hornik, K., & code), B. L. (BDS test. (2022). tseries: Time Series Analysis and Computational Finance (Version 0.10-51). Retrieved from <https://CRAN.R-project.org/package=tseries>

Virginia Division of Mineral Resources. (2003). Digital representation of the 1993 geologic map of Virginia.

von Wachenfeldt, E., Sobek, S., Bastviken, D., & Tranvik, L. J. (2008). Linking allochthonous dissolved organic matter and boreal lake sediment carbon sequestration: The role of light-mediated flocculation. *Limnology and Oceanography* , 53 (6), 2416–2426. <https://doi.org/10.4319/lo.2008.53.6.2416>

Walker, R. R., & Snodgrass, W. J. (1986). Model for sediment oxygen demand in lakes. *Journal of Environmental Engineering* , 112 (1), 25–43. [https://doi.org/10.1061/\(ASCE\)0733-9372\(1986\)112:1\(25\)](https://doi.org/10.1061/(ASCE)0733-9372(1986)112:1(25))

Weyhenmeyer, G. A., Prairie, Y. T., & Tranvik, L. J. (2014). Browning of boreal freshwaters coupled to carbon-iron interactions along the aquatic continuum. *PloS One* , 9 (2), e88104. <https://doi.org/10.1371/journal.pone.0088104>

Wickham, H., Averick, M., Bryan, J., Chang, W., McGowan, L. D., Francois, R., et al. (2019). Welcome to the Tidyverse. *Journal of Open Source Software* , 4 (43), 1686. <https://doi.org/10.21105/joss.01686>

Williamson, C. E., Overholt, E. P., Pilla, R. M., Leach, T. H., Brentrup, J. A., Knoll, L. B., et al. (2015). Ecological consequences of long-term browning in lakes. *Scientific Reports* , 5 (1), 1–10. <https://doi.org/10.1038/srep18666>

Winslow, L., Read, J., Woolway, R., Brentrup, J., Leach, T., Zwart, J., et al. (2019). rLakeAnalyzer: Lake Physics Tools (Version 1.11.4.1). Retrieved from <https://CRAN.R-project.org/package=rLakeAnalyzer>

Woodward, H. P. (1932). *Geology and Mineral Resources of the Roanoke Area, Virginia* .

Hosted file

supplemental info - final.docx available at <https://authorea.com/users/550878/articles/604492-effects-of-hypoxia-on-coupled-carbon-and-iron-cycling-differ-between-weekly-and-multiannual-timescales-in-two-freshwater-reservoirs>

Abigail S. L. Lewis¹, Madeline E. Schreiber², B. R. Niederlehner¹,
Arpita Das¹, Nicholas W. Hammond², Mary E. Lofton¹, Heather L.
Wander¹, Cayelan C. Carey¹

¹Department of Biological Sciences, Virginia Tech, Blacksburg, Virginia, USA

²Department of Geosciences, Virginia Tech, Blacksburg, Virginia, USA

Corresponding author: Abigail S. L. Lewis (aslewis@vt.edu)

Key Points:

- Short-term (2–3 week) periods of hypoxia decreased iron-bound organic carbon and total organic carbon in reservoir sediments
- Multiannual periods of hypoxia increased total organic carbon in sediment, likely through decreased rates of respiration
- A substantial fraction of sediment organic carbon (~30%) was bound to iron in these two freshwater reservoirs

Abstract

Freshwater lakes and reservoirs play a disproportionate role in the global carbon budget, sequestering more organic carbon (OC) than ocean sediments each year. However, it remains unknown how global declines in bottom-water oxygen concentrations may impact OC sequestration in freshwater sediments. In particular, associations between OC and iron (Fe) are hypothesized to play a critical role in stabilizing OC in sediment, and these complexes can be sensitive to changes in oxygen. Under low-oxygen (hypoxic) conditions, Fe-bound OC (Fe-OC) complexes may dissociate, decreasing OC sequestration. However, rates of OC respiration are also lower under hypoxic conditions, which could increase OC sequestration. To determine the net effects of hypoxia on OC and Fe cycling over multiple timescales, we paired whole-ecosystem experiments with sediment incubations in two eutrophic reservoirs. Our experiments demonstrated that short (2–4 week) periods of hypoxia can increase Fe and OC concentrations in the water column while decreasing OC and Fe-OC in sediment by 30%. However, exposure to seasonal hypoxia over multiple years was associated with a 57% increase in sediment OC and no change in Fe-OC. These results indicate that the large sediment Fe-OC pool (~30% of sediment OC) contains both oxygen-sensitive and oxygen-insensitive fractions, and over multiannual timescales, OC respiration rates play a greater role than Fe-OC protection in determining the effect of hypoxia on sediment OC content. Consequently, we anticipate that global declines in oxygen concentrations will alter OC and Fe cycling, with the direction and magnitude of effects depending upon the duration of hypoxia.

Plain Language Summary

Freshwater lakes and reservoirs (hereafter: lakes) play a remarkably important role in the global carbon cycle. Every year, more organic carbon (e.g., leaves, soil) is buried in lake sediments than in the sediments of all of the world's oceans.

However, these organic carbon inputs can also be decomposed, releasing greenhouse gases. The extent to which lakes bury carbon vs. release greenhouse gases may be changing, as oxygen concentrations are decreasing in the bottom waters of many lakes around the world. Here, we added oxygen to the bottom waters of a whole lake to test how changes in oxygen concentration affect carbon cycling. We found that over short timescales (weeks), low oxygen conditions decreased the amount of carbon in sediment by breaking apart chemical complexes with iron that can help retain carbon in sediment. However, over long timescales (years), low oxygen conditions appeared to *increase* carbon burial by decreasing the rate at which carbon inputs were decomposed. These results suggest that declining oxygen concentrations in lakes around the world may have important effects on global carbon cycling, with the direction and magnitude of the impact depending on the duration of low oxygen conditions.

1. Introduction

Freshwater lakes and reservoirs are increasingly recognized as hotspots in the global carbon cycle (Bastviken et al., 2011; Battin et al., 2009; Carey, Hanson, et al., 2022; Raymond et al., 2013; Tranvik et al., 2018). Due to high organic carbon (OC) loading from the surrounding watershed, more OC is buried in lakes and reservoirs than in ocean sediments each year (Dean & Gorham, 1998; Knoll et al., 2013; Mendonça et al., 2017; Pacheco et al., 2014). Much of this OC remains sequestered in the sediments, especially in reservoirs, which alone account for 25% of the global carbon sink from all terrestrial and freshwater sources (Le Quéré et al., 2015). However, OC inputs can also be respired to carbon dioxide and methane, making lakes and reservoirs a source of greenhouse gas emissions equivalent to 20% of the global emissions from fossil fuels (Deemer et al., 2016; DelSontro et al., 2018). To refine global carbon budgets and manage water resources in a changing world, it is important to understand what factors control the balance between OC sequestration and carbon emissions in these ecosystems.

Recent research suggests that associations between OC and iron (Fe) may play a critical role in OC sequestration across soils and marine environments (e.g., Hemingway et al., 2019; Kramer & Chadwick, 2018; Lalonde et al., 2012), and these associations are hypothesized to also be important in freshwater sediments (Björnerås et al., 2017; Peter et al., 2016; von Wachenfeldt et al., 2008; Weyhenmeyer et al., 2014). Fe can promote OC stability through multiple mechanisms, including occlusion of OC in aggregates, which can result in physical inaccessibility to microbial degradation and subsequent burial of OC in deeper soil or sediment horizons (Kleber et al., 2015 and references therein). Consequently, protection of OC through complexation with Fe may facilitate OC sequestration over decades to millennia (Kleber et al., 2015; Lalonde et al., 2012 and references therein)

Over shorter timescales (days to weeks), Fe-bound OC (Fe-OC) complexes are sensitive to the redox conditions of the surrounding environment (Figure 1). Fe-OC complexes form under oxic conditions (Riedel et al., 2013), as Fe(III) is more

effective at complexing with organic matter than Fe(II) (Nierop et al., 2002). Under hypoxic (reducing) conditions, OC can be released from Fe-OC complexes through Fe(III) reduction and dissolution (e.g., Pan et al., 2016; Patzner et al., 2020; Skoog & Arias-Esquivel, 2009), which can either result directly from hypoxia or through resultant increases in pH that promote OC release (Kirk, 2004; Thompson et al., 2006). Given these conflicting patterns—i.e., that Fe-OC complexes can be preserved over decades to millennia and yet may be unstable under the reducing conditions which commonly occur on day to month timescales in aquatic sediments—it remains unclear how changing oxygen dynamics will affect coupled OC and Fe cycling in freshwater ecosystems.

Currently, the duration of bottom-water hypoxia (low oxygen conditions) is increasing in many lakes and reservoirs around the world (Bartosiewicz et al., 2019; Jane et al., 2021; Jenny et al., 2016; Williamson et al., 2015), which could have varying consequences for OC sequestration (Figure 1). In many dimictic lakes and reservoirs, bottom-water hypoxia is interrupted by oxic conditions during spring mixing and fall turnover, resulting in dynamic oxygen conditions on the week to month scale. Combined, these short-term patterns sum to determine the net role of lakes and reservoirs in the global carbon cycle over multiannual timescales. Periods of hypoxia have the potential to decrease OC sequestration through reductive dissolution of Fe(III) in Fe-OC complexes (Chen et al., 2020; Huang et al., 2021; Patzner et al., 2020). However, hypoxia also has the potential to increase OC sequestration by decreasing the rate of OC respiration (Carey et al., 2018; Carey, Hanson, et al., 2022; Hargrave, 1969; Peter et al., 2017; Sobek et al., 2009; Walker & Snodgrass, 1986), particularly if Fe-OC complexes are resistant to, or protected from, changes in oxygen concentrations in overlying water. Decreased OC respiration rates under hypoxic conditions is thought to occur primarily because respiration is less thermodynamically favorable in the absence of oxygen (e.g., Arndt et al., 2013; LaRowe & Van Cappellen, 2011). Because reductive dissolution of Fe(III) in Fe-OC complexes and decreased OC respiration under hypoxic conditions would have divergent effects on total OC sequestration, understanding the relative importance of these two processes across multiple timescales is critical for predicting the effect of hypoxia on OC sequestration in the bottom waters of lakes and reservoirs (Figure 1).

To date, few studies have explicitly examined Fe-OC in freshwater lakes and reservoirs, and those that have provide preliminary evidence that Fe-OC complexation may be lower in freshwater environments compared to better-characterized marine systems. Peter and Sobek (2018) analyzed Fe-OC in surficial sediment from five boreal lakes that spanned a gradient of oxygen conditions and found that less than 11% of sediment OC was bound to Fe, in comparison with ~20% across a range of primarily marine sediments (Lalonde et al., 2012). Further, Peter and Sobek (2018) found no association between Fe-OC content in sediment and oxygen in overlying water. However, it should be noted that the lakes in that study were particularly high in dissolved OC (DOC) concentrations (9–42 mg/L DOC), and may not be representative of all freshwater ecosystems. Bai et al. (2021) studied Fe-OC along a salinity

gradient in a subtropical tidal wetland and similarly found that freshwater areas had lower levels of Fe-OC (18% of sediment OC in freshwater and 29% in saltwater), but these results were attributed primarily to wetland plant characteristics, which may not be relevant in the bottom waters of lakes and reservoirs.

Despite limited research on Fe-OC in freshwater sediments, there are multiple reasons to expect that Fe may play an important role in OC sequestration in some freshwater ecosystems. Concentrations of Fe and DOC are strongly correlated in many freshwaters (Björnerås et al., 2017; von Wachenfeldt et al., 2008; Weyhenmeyer et al., 2014), and aqueous Fe concentrations are strongly correlated with sediment OC accumulation in boreal lakes (Einola et al., 2011). Moreover, hypoxic release of DOC from lake sediments has been well-documented, and is often attributed to reductive dissolution of Fe (Brothers et al., 2014; Kim & Kim, 2020; Lau & del Giorgio, 2020; Peter et al., 2017). Still, few studies have examined whether reactions involving Fe-OC complexes are the driving force for observed correlations between dissolved Fe and OC (but see Peter et al. 2018). Furthermore, it remains unknown how the Fe-OC cycling occurring on sub-annual time scales may affect OC sequestration on the multi-annual timescales relevant for global carbon budgets.

Analyzing the complex effects of oxygen on coupled OC and Fe cycling requires multiple experimental approaches. Field surveys have been effective at identifying correlations between OC and Fe (Björnerås et al., 2017; von Wachenfeldt et al., 2008; Weyhenmeyer et al., 2014). However, these observational approaches have limited capacity for identifying causal relationships. Whole-ecosystem experiments may be highly effective at identifying real-world impacts of freshwater oxygen on Fe and OC dynamics, while allowing for important ecosystem-scale processes such as turbulence and external loading (Carpenter, 1996; Dzialowski et al., 2014; Schindler, 1998). However, high levels of variability on a whole-ecosystem scale may limit the detection of subtle changes in OC and Fe processing. Small-scale incubations may be particularly useful for identifying changes that result from hypoxia (i.e., increased DOC and Fe release from sediment, decreased levels of Fe-OC, changes in sediment OC). However, small-scale incubations are limited by fouling and changes in microbial communities, among other microcosm effects, and do not reflect the full suite of processes that interact to control OC and Fe cycling in lakes and reservoirs. Consequently, integrating multiple approaches can provide complementary information on Fe-OC dynamics across spatial and temporal scales and overcome the limitations of single-approach studies.

To analyze how hypoxia impacts OC and Fe cycling over multiple scales, this study paired whole-ecosystem oxygen manipulations with laboratory incubations. We had two objectives: (1) characterize Fe-OC levels in sediment of two iron-rich reservoirs, and (2) analyze how hypoxia affects coupled OC and Fe cycling over both short-term (2–4 week) and multiannual timescales. Through this work, we aimed to provide insight on how increasing prevalence and duration of

hypoxia in lakes and reservoirs may affect the critical role of these ecosystems in the global carbon cycle.

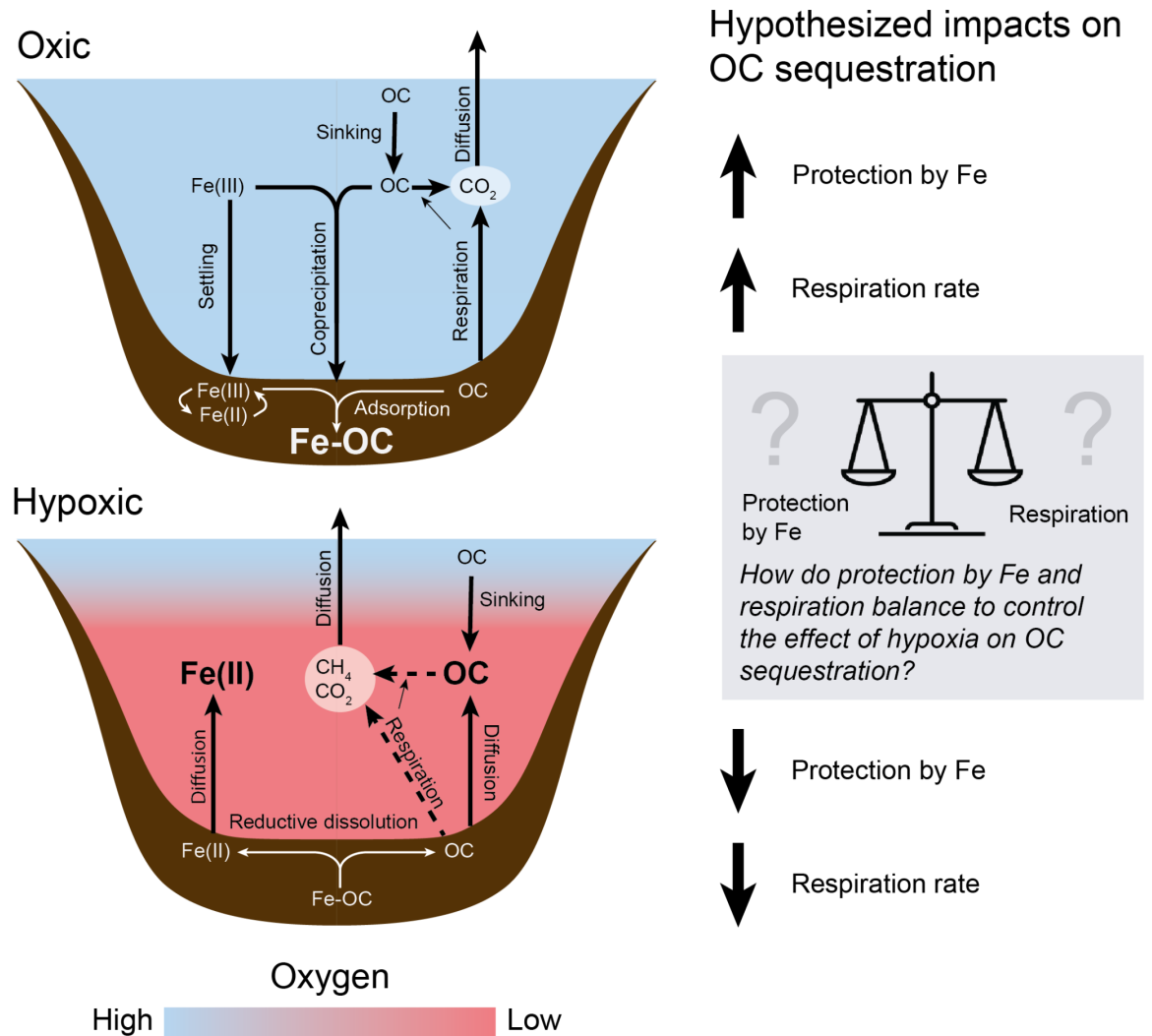


Figure 1: Conceptual diagram describing the hypothesized effects of changing oxygen conditions on coupled Fe-OC interactions in a lake or reservoir. Under oxic conditions (top), complexation of Fe and OC (both through co-precipitation and adsorption) leads to increased concentrations of Fe-OC in sediments (increased Fe-OC protection), though oxic conditions may also lead to increased OC respiration rates. Under hypoxic conditions, reductive dissolution of Fe(III) in Fe-OC complexes increases dissolved concentrations of Fe(II) and OC in the water column while decreasing the amount of Fe-OC in sediment (decreasing Fe-

OC protection), though hypoxia may also decrease OC respiration rates. The net effect of these processes on OC sequestration remains unknown, motivating this study. This figure is a simplification of complex interactions happening on a whole-ecosystem scale, and focuses on hypothesized dominant processes operating on the time scale of days to years.

2. Methods

2.1 Study Sites: Falling Creek and Beaverdam Reservoirs

Falling Creek Reservoir (FCR; 37.30°N, 79.84°W) and Beaverdam Reservoir (BVR; 37.31°N, 79.81°W) are small (FCR: 0.12 km², 9.3 m deep; BVR: 0.39 km², 11 m deep), eutrophic drinking water reservoirs located in southwestern Virginia, USA (Hounshell et al., 2021). Both reservoirs are located in forested catchments and both are dimictic, with summer stratified periods that typically last from May to October. BVR is located 3 km upstream of FCR and serves as the primary inflow source for FCR. Fe levels are high in these reservoirs' catchments as a result of weathering and erosion of Fe-rich metamorphic rocks (Chapman et al., 2013; Woodward, 1932); the bedrock underlying both reservoirs is layered pyroxene granulite (Virginia Division of Mineral Resources, 2003). Both reservoirs have been owned and operated for drinking water provision by the Western Virginia Water Authority (WVWA) since their construction (FCR: 1898, BVR: 1872; Gerling et al., 2016; Hamre et al., 2018).

A suite of variables are routinely sampled in FCR and BVR as part of a long-term monitoring program; all data analyzed in this manuscript are available in the Environmental Data Initiative (EDI) repository with detailed metadata (Carey, Lewis, McClure, et al., 2022; Carey, Wander, Howard, et al., 2022; Carey, Wander, McClure, et al., 2022; Lewis et al., 2022; Lewis, Schreiber, et al., 2022; Schreiber et al., 2022)

2.2 Whole-ecosystem oxygenation experiments

In 2012, FCR was equipped with a side-stream supersaturation hypolimnetic oxygenation (HOx) system to improve water quality in the reservoir (Gerling et al., 2014). This type of HOx system functions by withdrawing water from the bottom of the reservoir, adding concentrated, pressurized oxygen gas to supersaturate the water with dissolved oxygen (DO), and then returning the oxygenated water at the same depth and temperature. Previous work in FCR has shown that the HOx system effectively increases DO concentrations throughout the hypolimnion without altering temperature or decreasing thermal stability (Gerling et al., 2014). From 2013–2019, the HOx system in FCR was operated at variable rates, maintaining an oxygenated hypolimnion for at least part of the summer (Carey, Thomas, et al., 2022). Conversely, oxygenation was reduced in 2020 and 2021, maintaining primarily hypoxic conditions throughout the summer stratified period. To assess the effects of multiannual changes in oxygen availability on OC and Fe-OC in sediment, we compared sediment core and sedimentation trap data from summer 2019 (which had a history of high-oxygen conditions during the preceding six years) to summer 2021 (which followed a

summer of hypoxic conditions in 2020; Figure S2). Sediment data were not collected in 2020 due to the Covid-19 pandemic.

To assess how short-term changes in hypolimnetic DO concentrations impact Fe-OC on a whole-ecosystem scale, we operated the HOx in FCR on a variable schedule throughout the summer of 2019 (Carey, Thomas, et al., 2022). Oxygen was added in approximately two-week intervals at a rate of 25 kg O₂ day⁻¹ to the whole hypolimnion. Between oxygenation periods, we allowed the hypolimnion to become hypoxic over periods of at least two weeks without oxygenation. Because hypolimnetic volume varied throughout the summer (generally decreasing throughout the summer as the thermocline deepened), the mean concentration of oxygen added to the whole hypolimnion throughout an oxygenation period in 2019 ranged from 0.80 mg L⁻¹ day⁻¹ to 0.90 mg L⁻¹ day⁻¹.

BVR does not have a HOx system and experiences seasonal hypoxia from May through November (Hounshell et al., 2021). Consequently, BVR serves as a reference ecosystem to analyze the effects of oxygenation in FCR.

2.2.1 Oxygen

We monitored DO concentrations throughout the full water column approximately two times per week in FCR and one time per week in BVR (Carey, Lewis, McClure, et al., 2022). High-resolution (~1 cm) depth profiles were taken using a conductivity, temperature, and depth profiler (CTD; Sea-Bird, Bellevue, Washington, USA) equipped with a DO sensor (SBE 43; Carey, Lewis, McClure, et al., 2022) from the reservoir’s surface to the sediments. We also measured dissolved oxygen using a YSI ProODO DO probe when the CTD was not available due to maintenance (YSI Inc. Yellow Springs, Ohio, USA; Carey, Wander, McClure, et al., 2022). YSI measurements were taken at discrete 1 m depth intervals. For a comparison of YSI and CTD measurements, see Carey et al. (2022).

2.2.2 Hypolimnetic Fe and DOC

We collected water samples for DOC and Fe analysis at the deepest site in each reservoir with a 4-L Van Dorn sampler (Wildlife Supply Company, Yulee, FL, USA). Samples were collected once per week at seven depths in FCR (0.1, 1.6, 3.8, 5.0, 6.2, 8.0, and 9.0 m), which corresponded to the reservoir’s extraction depths, and five depths in BVR (0.1, 3.0, 6.0, 9.0, and 11.0 m). In 2019, we conducted a limited amount of additional sampling in FCR on a second day each week, and these measurements included DOC from 0.1, 1.6, 5.0, and 9.0 m depths.

We analyzed DOC by filtering water samples through a 0.7-μm glass fiber filter into an acid-washed bottle, which was rinsed with the filtered water three times before sample collection. The filtered samples were frozen for less than six months before analysis on an OC analyzer (Elementar Vario TOC cube, following APHA standard method 5310B; American Public Health Association, 2018b).

We collected both total and dissolved (filtered through 0.45- μ m filters) samples for Fe. Samples were preserved in the field using trace metal grade nitric acid and analyzed using ICP-MS (Thermo Electron X-Series, Waltham, MA, USA) following APHA Standard Method 3125-B (American Public Health Association, 2018a; Krueger et al., 2020; Munger et al., 2019; Schreiber et al., 2022).

2.2.3 Fe-OC in sediments

We analyzed the concentration of Fe-OC in surficial sediments from both FCR and BVR on multiple dates throughout the summer stratified periods of 2019 and 2021. In 2019, sediment cores in FCR were collected immediately before the HOx system was turned on or off, resulting in the most oxic or hypoxic conditions during that SSS activation or deactivation interval, respectively. Sediment cores at BVR were taken once in the middle of summer and once approximately two weeks before fall turnover in 2019. In 2021, sediment core samples were taken from both reservoirs on the same dates, approximately once per month. Additional sediment core samples were collected in March 2021, when both reservoirs were unstratified and had oxic hypolimnia.

On each sampling date, we collected four replicate hypolimnetic sediment cores using a K-B gravity sediment corer (Wildlife Supply Company, Yulee, FL, USA). Cores were collected in the deepest part of each reservoir, approximately 20 m from where water samples were taken. In 2019, each core was capped and kept on ice while transported back to the lab, where the top 1 centimeter of sediment from each core was immediately extruded, collected, and frozen in scintillation vials for future analysis. In 2021, cores were extruded in the field, and the samples were kept on ice while being transported back to the lab.

2.2.4 Sediment traps

To determine the amount of Fe-OC and total OC in samples of material settling from the water column (i.e., not estimate deposition rates), we deployed 19-L buckets approximately 1 m above the sediments at the deepest point of each reservoir (8 m at FCR and 10 m at BVR). These sediment traps were deployed from June–December 2021 and sampled every two weeks by slowly bringing the bucket to the surface, decanting and discarding water from the bucket, collecting up to 5 L of the remaining water and particulate matter, and transporting this material back to the lab on ice. Upon arriving at the lab, we allowed the particulates to settle for approximately 5 minutes before decanting and discarding as much water as possible and filling four 50-mL centrifuge tubes with the remaining material. The samples were centrifuged for 10 minutes at 3100 rpm, then combined into one vial and frozen for later analysis. No sediment traps were deployed for Fe-OC analysis in 2019.

2.3 Microcosm incubations

To isolate the effects of oxygen from other interacting factors that affect Fe and OC on a whole-ecosystem scale, we conducted six-week microcosm incubations using hypolimnetic sediment and water from FCR. Incubations were conducted

in 177-mL glass jars (Figure S1), after extensive pilot testing revealed that these jars were highly effective at maintaining hypoxic conditions when sealed and oxic conditions when uncapped. We started the experiment with 102 microcosms split evenly into oxic (uncapped) and hypoxic (capped) treatments. After two weeks (similar to the 2019 whole-ecosystem HOx manipulation), we switched the treatment of approximately half of the remaining microcosms, generating two additional oxygen regimes: hypoxic-to-oxic and oxic-to-hypoxic. Starting on week two, there were consequently a total of four oxygen regimes: hypoxic, oxic, hypoxic-to-oxic, and oxic-to-hypoxic.

To set up the experiment, we collected sediment and water from the deepest site in FCR on 30 June 2021, when the hypolimnion was hypoxic. Water was collected from 9 m depth using a Van Dorn sampler, and sediment was collected from the same location using an Ekman sampler. Samples were transported on ice back to the lab, then homogenized by stirring and shaking. We used a syringe to add the sediment slurry (20 mL) to each jar, then slowly added 150 mL of hypolimnetic water, making an effort to minimize sediment disturbance. We stored the microcosms in an unlit incubation chamber at 15 °C for the duration of the experiment, which corresponded to warm, end-of-summer conditions in the hypolimnion of FCR (Carey, Lewis, McClure, et al., 2022).

2.3.1 Microcosm sampling

Microcosms were sampled destructively for DO, total and dissolved Fe, total and dissolved OC, pH, sediment OC, and sediment Fe-OC. For the continuous oxic and hypoxic treatments, we sampled 3–6 replicates two times per week for four weeks (6 replicates: days 2, 6, 9, 13; 3 replicates: days 16, 20, 23). We added additional sampling for the hypoxic-to-oxic and oxic-to-hypoxic treatments: these treatments were sampled for the first three days after switching the oxygen regime (days 14, 15, 16), twice the following week (days 20, 23), and one more time a total of four weeks from when treatments were switched (day 34), with three replicates analyzed per sampling event. All microcosms under a hypoxic treatment were sampled in an anaerobic chamber which maintained mean ambient oxygen conditions <200 ppm (Coy Laboratory, Grass Lake, MI, USA) to reduce oxygen exposure during sampling.

To begin sampling a microcosm, DO was measured using a YSI DO probe. While measuring DO, we used the probe to gently swirl the water in the microcosm, homogenizing the water sample while minimizing sediment disturbance. Next, we used an acid-washed syringe to withdraw 30 mL of water for total OC (TOC), 13 mL for total Fe, 30 mL of water for DOC, and 13 mL for dissolved Fe analyses. DOC samples were filtered through a 0.7- μ m glass fiber filter, and dissolved Fe samples were filtered through 0.45- μ m filters. After taking samples for Fe and DOC, we withdrew as much water as possible without disturbing the sediment and measured pH from this sample in a separate container using an Ohaus Starter 300 pH probe (Parsippany, NJ, USA). Finally, we swirled the sediment with remaining water (approximately 1–5 mL) and poured this mixture into a 20 mL glass EPA vial, which we then froze for Fe-OC analysis. Hypoxic

microcosms were stored in the anaerobic chamber for approximately two hours before analysis to ensure oxygen concentrations in the chamber were sufficiently low before opening the jars. Oxic microcosms were sampled immediately after removal from the incubator.

All microcosm samples were analyzed following standard methods. We stored TOC and DOC samples in bottles that had been acid-washed and rinsed three times with the sample water. All DOC and TOC samples were frozen for <6 months prior to analysis on an OC analyzer (Elementar Vario TOC cube, following Standard Method 5310B; American Public Health Association, 2018b). Fe samples were preserved using trace metal grade nitric acid and analyzed using the ferrozine method (Gibbs, 1979). We also analyzed Fe samples from days 16 and 23 using inductively coupled plasma mass spectrometry (ICP-MS). All microcosm data are published with complete metadata in the Environmental Data Initiative repository (Lewis et al., 2022).

2.4 Fe-OC analysis

We analyzed the amount of Fe-OC in both the whole-ecosystem and microcosm sediment samples using the citrate bicarbonate dithionite (CBD) method. This method was first described for marine systems by Lalonde et al. (2012) and has since been adapted for freshwater lakes by Peter and Sobek (2018). It is important to note that our measurement of Fe-OC as the percentage of OC that is extractable using the CBD method is an operational definition (Fisher et al., 2021). We used this method to enable comparisons both between oxygen treatments and with other published work that used the same general approach (e.g., Lalonde et al., 2012; Peter & Sobek, 2018).

Following the CBD method, each sediment sample was freeze-dried and divided into three treatments: initial, reduction, and control. “Initial” samples received no treatment and were used to measure the OC content of the sediment. “Reduction” samples were treated with a metal-complexing agent (trisodium citrate) and reducing agent (sodium dithionite) in a buffered solution (sodium bicarbonate) to measure how much Fe and OC were released as a result of Fe reduction. Control samples were used to account for the release of Fe and OC in the reduction treatment that resulted from processes other than Fe reduction. They were treated with the same buffer (sodium bicarbonate) and sodium chloride in the same ionic strength as the trisodium citrate and sodium dithionite of the reduction treatment.

For both the control and reduction treatments, we measured 100 mg of homogenized, freeze-dried sediment into 15-mL polypropylene centrifuge tubes (Falcon Blue, Corning Inc., Corning, NY, USA). We then added 6 mL of either control or reduction buffer solution (0.11 M sodium bicarbonate) to each tube. The reduction buffer contained 0.27 M trisodium citrate, while the control buffer contained 1.6 M sodium chloride. After heating samples to 80°C in an oven, 0.1 g sodium dithionite was added to the reduction samples and 0.088 g sodium chloride was added to control samples, and samples were kept at 80°C for an

additional 15 min. Samples were centrifuged for 10 min at 3100 RPM, and the supernatant was collected in a 50-mL centrifuge tube. This extraction process was repeated two more times for both treatments (Peter and Sobek, 2018). Finally, samples were rinsed three times using artificial lake water, which was prepared by diluting Artificial Hard Water from Marking and Dawson (1973) to 12.5% with Type I reagent grade water.

After extraction, all sediment samples (including those in the initial treatment) were dried and acid-fumigated for 48 hours to remove remaining citrate and bicarbonate (Harris et al., 2001). Samples were then run on a CN analyzer (Elementar VarioMax, Ronkonkoma, NY, USA) to determine the amount of OC per unit mass of sediment. We adjusted sediment mass to account for Fe loss during control and reduction treatments. The amount of OC removed with Fe reduction (CBD-extractable OC) was calculated as the difference between the OC content of the control and reduction samples and expressed as a percentage of the initial OC content of the sediment.

2.5 Data analysis

All analyses were performed in R (version 4.0.3; R core team 2020) using packages tidyverse (Wickham et al., 2019), lubridate (Grolemund & Wickham, 2011), ggpubr (Kassambara, 2020), egg (Auguie, 2019), rstatix (Kassambara, 2021), akima (Akima et al., 2022), colorRamps (Keitt, 2022), rLakeAnalyzer (Winslow et al., 2019), and tseries (Trapletti et al., 2022). All novel analysis code is archived as a Zenodo repository (Lewis, 2022).

2.5.1 Sediment Fe-OC characterization

We calculated summary statistics to describe iron-bound organic carbon and total organic carbon in surficial sediment (2019 and 2021) and settling particulate material (2021 only) across both reservoirs. We then pooled data from both reservoirs to analyze the difference between settling material and surficial sediments using Welch’s t-tests. Because data were unavailable for settling material in 2019, the comparison of settling material to surficial sediment was limited to 2021 data only.

2.5.2 Whole-ecosystem experiments: short-term responses

We used Welch’s t-tests to assess whether sediment properties differed between the two-week periods of HOx activation compared to HOx deactivation during summer 2019 in FCR. Sediment time series did not exhibit significant temporal autocorrelation, justifying this approach (Lewis, Schreiber, et al., 2022).

To qualitatively assess whether oxygenation experiments led to differences in water column chemistry, we overlaid plots of DOC and Fe from the deepest sampling depth in each reservoir with dissolved oxygen at the same depths throughout the summer stratified period of 2019 .

2.5.3 Whole-ecosystem experiments: interannual differences

We assessed whether there were significant differences in sediment properties among the four reservoir-years—BVR in 2019 (hypoxic), BVR in 2021 (hypoxic), FCR in 2019 (oxic) and FCR in 2021 (hypoxic). First, we used Levene tests to assess homogeneity of variance among reservoir-years (Table S1). While Fe-OC (both per unit sediment and as a percentage of sediment OC) met the ANOVA assumption of homogeneous variance, total sediment OC did not. Consequently, we used one-way ANOVAs and Tukey post hoc tests for Fe-OC metrics, but used Welch one-way ANOVAs and Games-Howell post-hoc tests, both of which account for unequal variances, for sediment OC (Tables S2 and S3).

2.5.4 *Microcosm incubations*

We used one-way ANOVAs and Tukey post-hoc tests to assess whether sediment properties differed between microcosm treatments, after testing for homogeneity of variance using Levene tests (Table S4). For this analysis, we used data from days 20 and 23 (pooled together because replicates were sampled destructively), as these were the final days when data were available for all treatments.

Speciation-solubility calculations were conducted for day 23 of the microcosm experiments using the Spece8 module of Geochemists’ Workbench (GWB; Aquatic Solutions LLC, Champaign, IL, USA) and the wateqf thermodynamic database (Ball & Nordstrom, 1991). The goal of the calculations was to assess the predicted speciation of Fe in the presence of OC under the environmental conditions of each microcosm treatment (following Oyewumi & Schreiber, 2017). Environmental conditions considered in this analysis included pH, DO, temperature, DOC, major cations (Ca, Na, K), Fe, and major anions (Cl, SO₄; bicarbonate was not measured so we calculated that via charge balance). We assumed that DOC consisted primarily of humic acid for the calculations.

3. Results

3.1 Fe-OC levels in surficial hypolimnetic sediment are high and greater than in settling particulate matter

A substantial proportion of sediment OC was associated with Fe in both FCR and BVR. In FCR (averaged across 2019 and 2021), one gram of surficial sediment contained a mean of 481 μmol Fe-OC (± 138 , 1 SD), $31 \pm 8\%$ of the total sediment OC pool ($n=30$). BVR had slightly lower Fe-OC than FCR on average, and one gram of surficial sediment contained a mean of 418 ± 121 μmol Fe-OC, $24 \pm 7\%$ of the total sediment OC pool ($n=20$). Total OC comprised $9 \pm 3\%$ of sediment mass in FCR and $10 \pm 1\%$ of sediment mass in BVR.

Levels of Fe-OC, both as a fraction of sediment mass and as a fraction of total sediment OC, were significantly higher in sediment core samples than in settling material collected in hypolimnetic traps (Figure 2). In 2021, averaged across both reservoirs, one gram of the reservoir surficial sediments contained a mean of 443 ± 133 μmol of Fe-OC ($n=28$), 69% higher than settling material collected in the traps, which contained a mean of 262 ± 143 μmol Fe-OC ($n=17$; $t_{32}=-4.24$, $p<0.001$; Figure 2a). A mean of $24 \pm 6\%$ of the total sediment OC pool was

bound to Fe in sediments ($n=28$), while only $9\pm4\%$ of sediment OC was bound to Fe in settling material ($n=17$; $t_{43}=-10.44$, $p<0.001$; Figure 2c). Total OC was 60% higher in settling material ($\mu=16.5\pm3.3$) than in surficial sediments ($\mu=10.3\pm1.6$; $t_{20}=7.33$, $p<0.001$; Figure 2b).

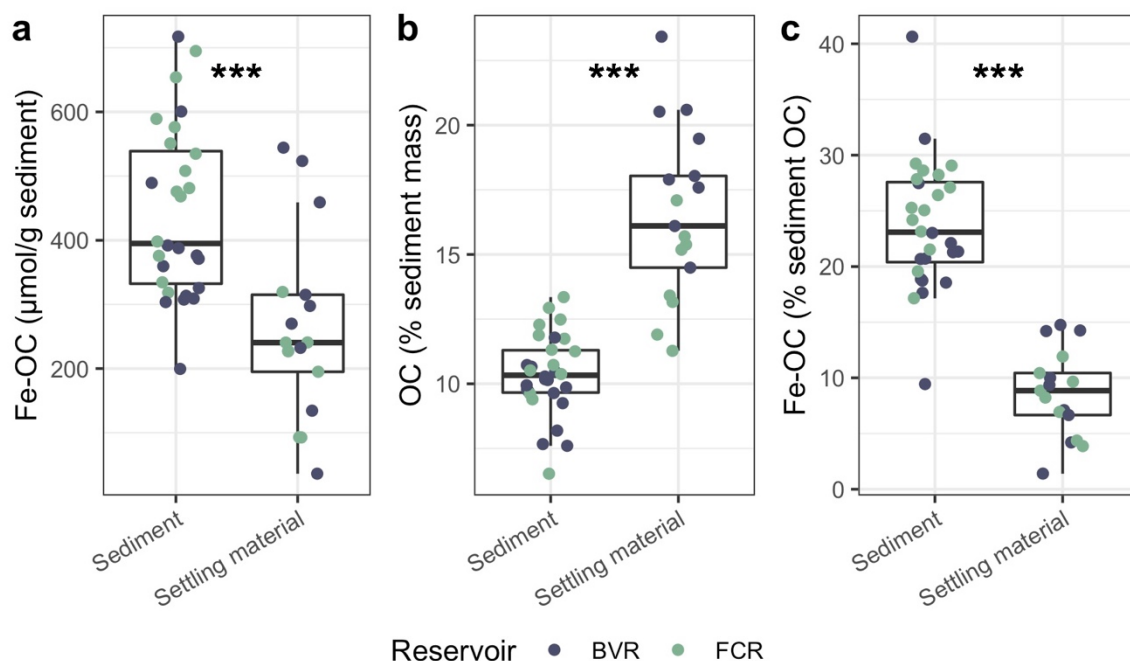


Figure 2: Iron-bound organic carbon (Fe-OC; a), total sediment organic carbon (b), and Fe-OC as a percentage of sediment OC (c) all differed significantly between surficial sediment and settling particulate matter. Asterisks indicate statistical significance of the difference between surficial sediment and sediment traps: *** indicates $p < 0.001$ (Welch's ANOVA). Note that only 2021 data are presented because settling particulate material was not collected in 2019.

3.2 Short-term hypoxia decreases sediment OC and Fe-OC on a whole-ecosystem scale

Intermittent activation of the HOx in FCR in 2019 was associated with substantial changes in sediment characteristics. The amount of Fe-OC per g sediment was 30% lower during hypoxic ($\mu=394\pm173$, $n=9$) compared to oxic ($\mu=560\pm70$, $n=7$) periods in 2019 ($t_{11}=-2.6$, $p=0.02$; Figure 3b). Likewise, the total amount of OC (as a percentage of sediment mass) decreased by 30% during hypoxic ($\mu=6.0\pm1.55$, $n=11$) compared to oxic periods ($\mu=8.5\pm0.8$, $n=7$; $t_{15}=-4.6$, $p<0.001$; Figure 3b). Fe-OC as a percentage of total sediment OC did not significantly change with variation in oxygen during these experiments (oxic: $\mu=36.7\pm3.8$, $n=7$; hypoxic: $\mu=35.7\pm7.9$, $n=9$; $t_{12}=-0.3$, $p=0.747$; Figure 3c).

In the hypolimnion of FCR, total Fe concentrations tended to increase as oxy-

gen decreased and decrease as oxygen increased (Figure 4b). Consequently, Fe concentrations were generally lower in FCR compared to the unoxygenated reference reservoir (BVR) in 2019. Trends in DOC were more variable, though DOC concentrations were typically highest when oxygen concentrations were low in FCR (Figure 4).

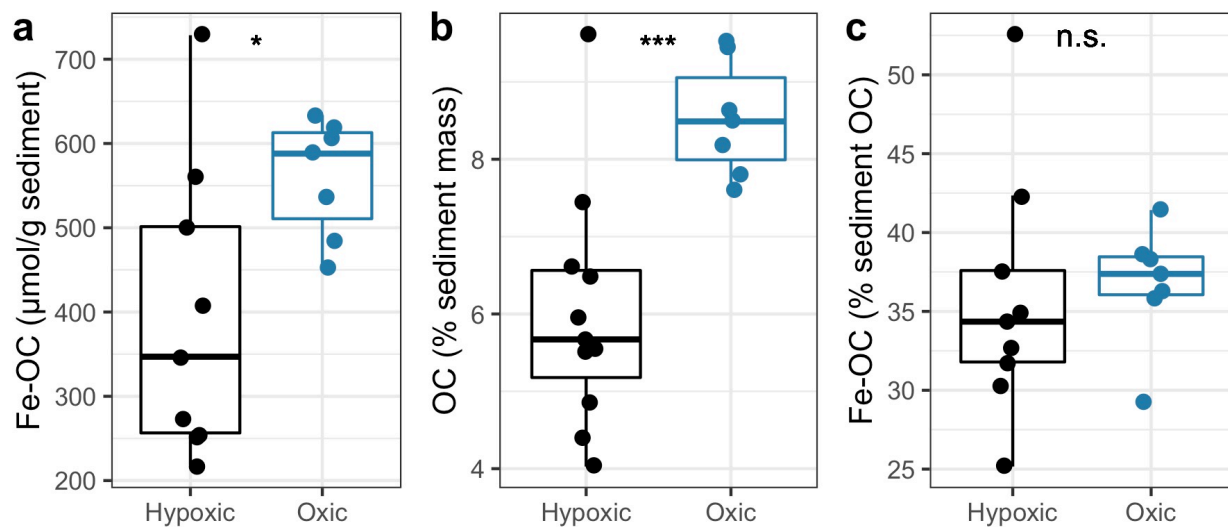


Figure 3: Iron-bound organic carbon (Fe-OC; a) and total organic carbon (b) in sediment were significantly higher under oxic compared to hypoxic conditions in Falling Creek Reservoir (FCR) during the summer stratified period of 2019. Fe-OC as a percentage of sediment OC did not differ significantly between hypoxic and oxic conditions. Here, oxic and hypoxic conditions are classified based upon mean oxygen levels during the two weeks preceding sampling (Figure S3). Statistical significance of differences between oxic and hypoxic periods is indicated using asterisks: * indicates $p < 0.05$, *** indicates $p < 0.001$.

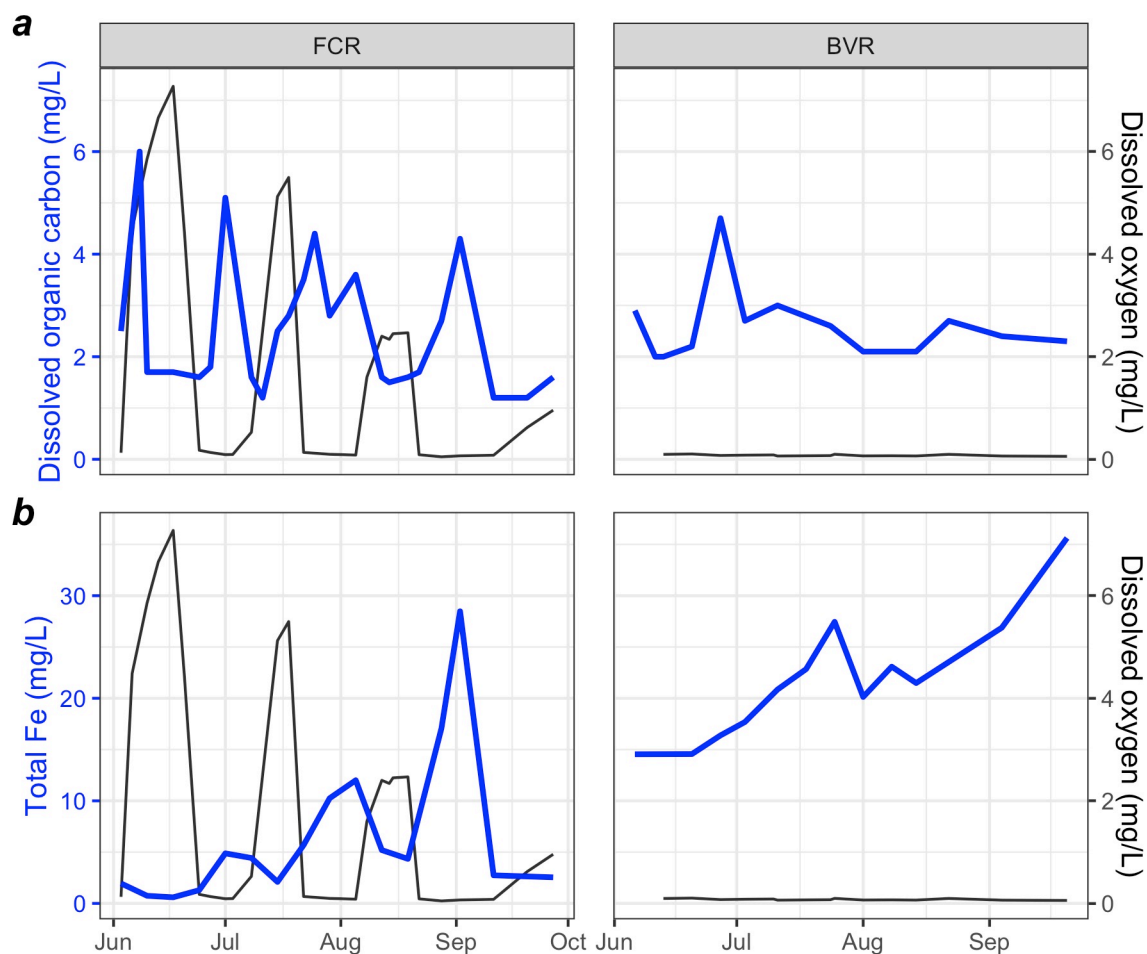


Figure 4: Increased dissolved oxygen concentrations were associated with decreased dissolved organic carbon (a) and total iron (Fe; b) in the hypolimnia of Falling Creek Reservoir (FCR; left) and Beaverdam Reservoir (BVR; right) during the summer stratified period of 2019.

3.3 Multiannual hypoxia is associated with increased sediment OC in FCR and BVR

Activation of the oxygenation system increased summer hypolimnetic DO concentrations in FCR from 2014 through 2019, and lower oxygen addition rates allowed for primarily hypoxic conditions in 2020 and 2021 (Figure S2). BVR exhibited summer hypolimnetic hypoxia throughout the duration of the study (Figure S2).

In FCR, the amount of OC in sediment increased by 57% as DO concentrations decreased from 2019 to 2021 (Figure 5b; Table S1, S2). Consequently, total OC

was lower in FCR than BVR in 2019, but not in 2021 (Figure 5b; Table S1, S2). However, the amount of Fe-OC per gram of sediment did not change (Figure 5a; Table S1). As a result, the percentage of sediment OC that was bound to Fe decreased from 2019 to 2021 in FCR (Figure 5c; Table S1, S3). None of these three sediment characteristics differed between 2019 and 2021 in BVR (Figure 5d–f; Table S1, S2, S3).

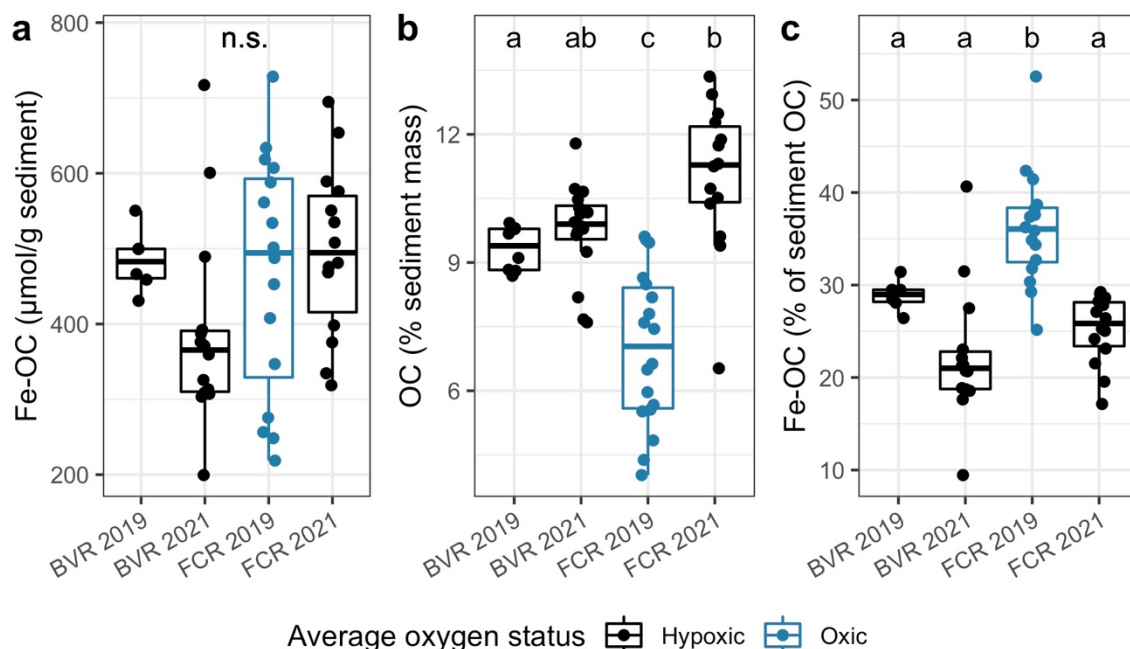


Figure 5: Sediment organic carbon metrics differed significantly in association with oxygen on a multiannual scale. Metrics assessed include iron-bound organic carbon (Fe-OC) (a), total sediment organic carbon (OC; b), and Fe-OC as a percentage of OC (c) in Falling Creek Reservoir (FCR) and Beaverdam Reservoir (BVR). Blue color indicates the reservoir-year with the highest mean oxygen (2019 in FCR) and letters delineate groups that are significantly different ($p < 0.05$; Table S1, S2, S3).

3.4 Experimental microcosm incubations reveal rapid effects of hypoxia on Fe and OC

Experimental microcosm incubations successfully established four distinct oxygen regimes. DO concentrations increased rapidly when hypoxic microcosms were unsealed and decreased rapidly when microcosms were sealed (Figure 6). At the transition from hypoxic-to-oxic conditions, DO concentrations increased to approximately the same level as the continuous oxygen treatment (~ 7 mg/L) within one day. At the transition from oxic-to-hypoxic conditions, DO concentrations decreased below 1 mg/L within one day and declined to 0 mg/L by the

end of the experiment.

Changes in oxygen conditions were associated with clear but asynchronous changes in aqueous OC and Fe. As microcosms switched from oxic-to-hypoxic conditions, TOC, DOC and total Fe decreased near synchronously, while dissolved Fe decreased below detection within one day of oxygen exposure. At the transition from hypoxic-to-oxic conditions, DOC and TOC rapidly increased to the same level as microcosms that had experienced continuous hypoxia (~ 10 mg/L; Figure 6). However, concentrations of both dissolved and total Fe only began to increase after three weeks of hypoxia (Figure 6). Measured DOC and TOC were strongly and linearly correlated, with DOC representing a mean of $96 \pm 14\%$ of TOC (Figure S4); thus, we focus our discussion on DOC hereafter, but the same trends apply to TOC.

At the end of the experiment, sediment OC differed significantly among treatments (one-way ANOVA: $F_{3,20}=9.09$, $p<0.001$). Sediment OC was significantly higher in microcosms that started under oxic conditions (oxic: $\mu=4.6 \pm 0.3$, oxic-to-hypoxic: $\mu=4.5 \pm 0.3$) than microcosms that started under hypoxic conditions (hypoxic: $\mu=4.0 \pm 0.0$, hypoxic-to-oxic: $\mu=4.1 \pm 0.2$; Figure 7). Fe-OC did not differ significantly between treatments as a proportion of sediment mass ($F_{3,20}=0.51$, $p=0.683$) or as a proportion of sediment OC ($F_{3,20}=2.40$, $p=0.098$).

Speciation calculations (Table S5) based upon ICP-MS results (Figure S5) suggest that oxygen conditions had primary control over Fe speciation, with a lesser impact on Fe-OC. The experiments that were maintained under hypoxic conditions had dominant Fe species of Fe(II) , FeHCO_3^+ , FeCO_3 , and FeSO_4 (all of these species contained Fe in its reduced state, Fe(II)). For all of the microcosms that were exposed to oxygen at any time (hypoxic-to-oxic, oxic-to-hypoxic, oxic), the dominant Fe species were Fe(OH)_3 , Fe(OH)_2^+ , Fe(OH)_4^- , FeOH_2^+ and FeHumate^+ (all of these species contained Fe in the oxidized state, Fe(III)). pH remained circumneutral across all treatments (Figure S6). These results indicate that 1) exposure to oxic conditions at any time in the experiment shifted the dominant oxidation state to Fe(III) ; 2) under oxic conditions, and to a lesser extent, hypoxic conditions, Fe complexed with DOC.

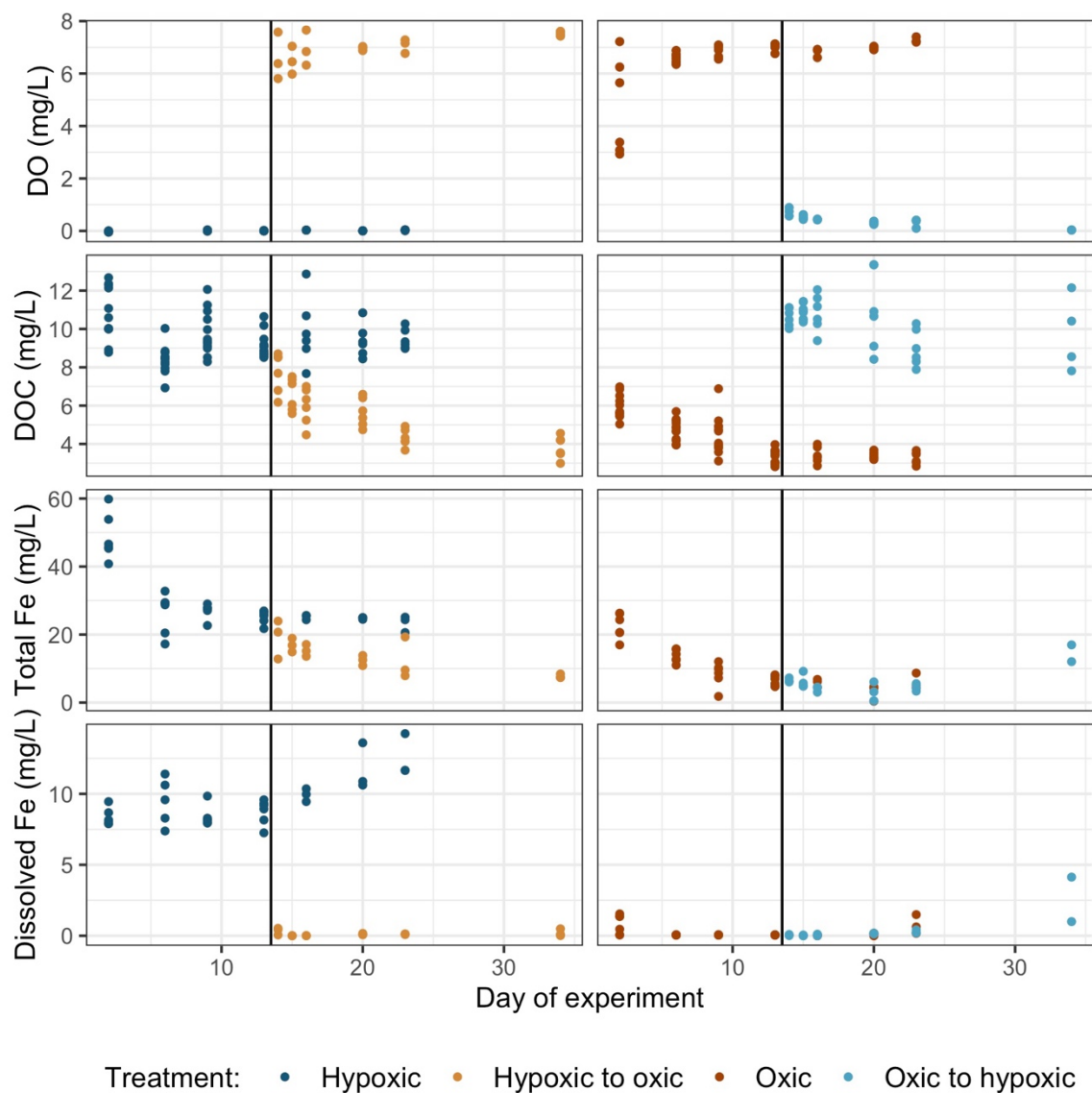


Figure 6: Varied oxygen regimes led to differences in water chemistry among experimental microcosm treatments. Metrics assessed include dissolved oxygen (DO), dissolved organic carbon (DOC), total iron (Fe), and dissolved Fe concentrations in microcosms that were sampled destructively over the course of 34 days. Vertical lines indicate when oxygen conditions were switched, creating the oxic-to-hypoxic and hypoxic-to-oxic treatments.

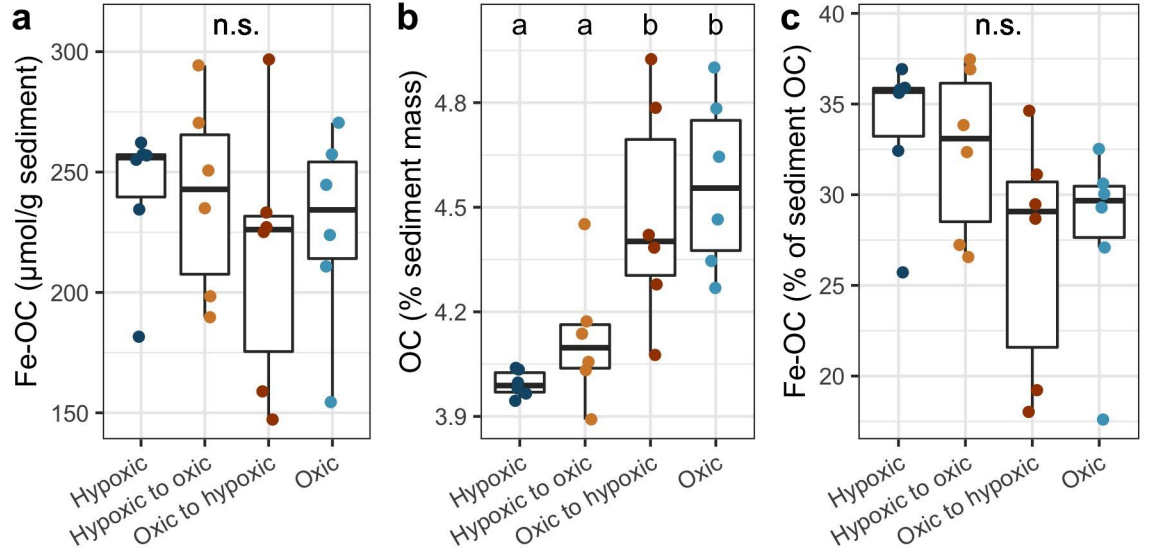


Figure 7: Experimental oxygen microcosm treatments altered some, but not all, sediment properties. Metrics assessed include moles of iron-bound organic carbon (Fe-OC) per unit sediment mass (a), total sediment organic carbon (b), and Fe-OC as a percentage of sediment OC (c). Letters delineate treatments that are significantly different ($p < 0.05$): no treatments were significantly different for Fe-OC metrics (a, c). Days 20 and 23 were chosen for statistical comparisons as the last days in the experiment when data were available from all treatments.

4. Discussion

Our results suggest that oxygen affects coupled OC and Fe cycling differently over short-term (several weeks) compared to long-term (multiannual) timescales (Figure 8). Short periods of hypoxia decreased total OC and Fe-OC in sediment and increased concentrations of DOC and Fe in overlying water, indicating that a portion of the sediment Fe-OC pool is sensitive to changes in oxygen. However, over longer timescales, low oxygen conditions in FCR from 2019–2021 were associated with a 57% increase in sediment OC, indicating that the effects of hypoxia on Fe-OC (i.e., dissociation of Fe-OC complexes) may be outweighed by decreases in respiration rates under hypoxic conditions. Notably, Fe-OC comprised nearly one-third of surficial sediment OC in both FCR and BVR—regardless of oxygen status—which is substantially more than previously reported for freshwater lakes (Peter & Sobek, 2018). Below, we discuss short-term (section 4.1) and multiannual (section 4.2) results in the context of previous work, analyze net processing rates across the sediment-water interface (section 4.3), and discuss why Fe-OC levels may be higher in these reservoirs than other freshwater systems (section 4.4).

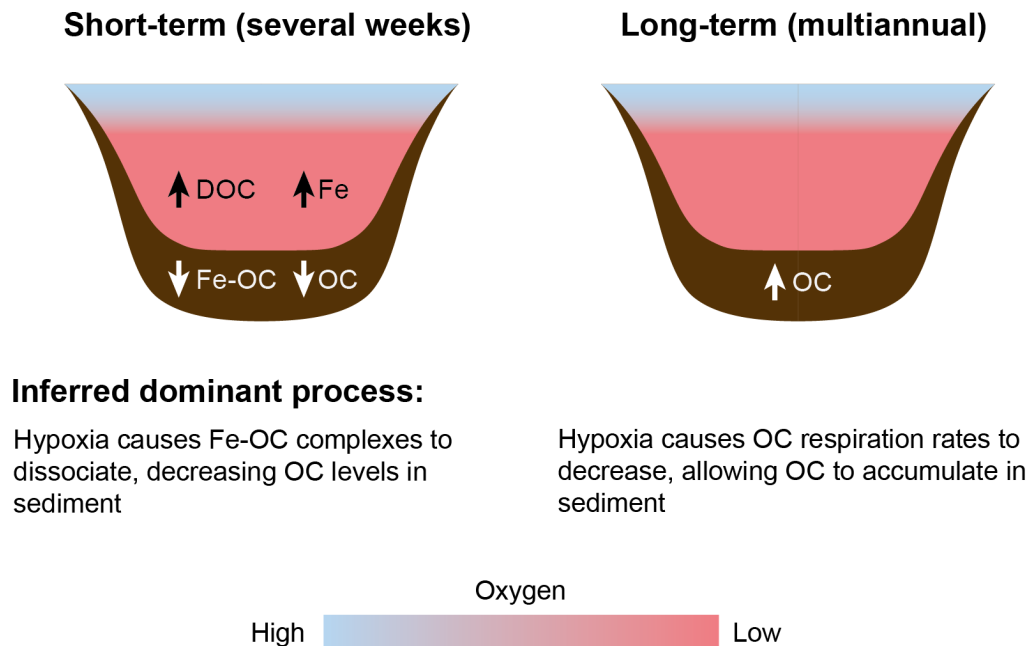


Figure 8: Experimental results suggest that the dominant process through which hypoxia affects sediment organic carbon differs between weekly and multiannual timescales. Left: in microcosm incubations, short-term (weeks) periods of hypoxia led to increased DOC and aqueous Fe, while decreasing sediment OC. On a whole-ecosystem scale, hypolimnetic Fe was closely correlated with oxygen concentrations, and short periods of hypoxia decreased both Fe-OC and OC in sediment. Consequently, Fe-OC protection appears to be a more dominant control on sediment OC sequestration than respiration on short timescales. Right: two years of summer hypoxia in FCR led to increased OC in sediment on a whole-ecosystem scale, suggesting that respiration may be a more dominant control on OC sequestration than protection by Fe on this timescale.

4.1 Short-term periods of hypoxia lead to release of Fe-protected OC and decrease total sediment OC

Both whole-ecosystem and microcosm experiments suggest that short-term periods (i.e., weeks) of hypoxia can dramatically alter coupled OC and Fe cycling. Whole-ecosystem experiments revealed changes in hypolimnetic DOC and Fe, sediment OC, and sediment Fe-OC associated with water-column oxygenation (Figures 3, 4, 8), while microcosm incubations showed clear differences in aqueous Fe, and DOC and sediment OC among treatments (Figures 6, 7). The magnitude of these effects was substantial: on a whole-ecosystem scale, two weeks of hypoxic conditions decreased both sediment Fe-OC and total sediment OC by a mean of 30%. Declining Fe-OC and total OC in sediment, as well

as concomitant increases in Fe and OC in overlying water, are consistent with the expectation that hypoxia causes reductive dissolution of Fe(III) in Fe-OC complexes, releasing soluble Fe and DOC on day to week scales (e.g., Carey et al., 2018; Pan et al., 2016; Patzner et al., 2020; Peter et al., 2016; Skoog & Arias-Esquivel, 2009; Figures 1, 8).

Our results contribute to an accumulating body of evidence that short-term fluctuations in oxygen concentrations may have important effects on OC storage in soils and sediment. Previous research has shown that recently-formed Fe-OC associations may be particularly prone to hypoxic release, and reduction of Fe(III) in Fe-OC compounds can increase OC respiration rates during hypoxic conditions (Chen et al., 2020). As a result of these and other processes, periodic fluctuations in oxygen conditions may sustain or stimulate respiration rates relative to both constant oxic and constant hypoxic conditions (Bastviken et al., 2004; Huang et al., 2021). Here, we found substantial decreases in sediment OC and Fe-OC following two weeks of hypoxia, with restored OC and Fe-OC after two weeks of oxic conditions (Figure 3, S3), suggesting that at least a fraction of the sediment Fe-OC pool is sensitive to short-term changes in oxygen concentrations in overlying water on a whole-ecosystem scale.

While sediment Fe-OC responded to oxygenation on a whole-ecosystem scale, Fe-OC did not vary significantly among oxygen treatments in experimental incubations. We expect that this difference derives at least in part from the sediments we analyzed: whole-ecosystem samples were composed of the top 1 cm of sediment from sediment cores, while sediment for the experimental incubations was sampled using an Ekman grab, and therefore included deeper layers of sediment. In soil, deeper horizons are thought to have more stable Fe-OC aggregates (Rumpel & Kögel-Knabner, 2011). Our results suggest that the same pattern may be true in sediments, resulting in burial of stable Fe-OC compounds in deeper sediments over time.

Formation and dissociation of Fe-OC complexes are two of many ways in which Fe and OC are impacted by hypoxia; both Fe and OC can also respond independently to changes in DO concentrations. Fe is oxidized from Fe(II) (soluble) to Fe(III) minerals (insoluble) both biotically and abiotically under oxic conditions (Kappler et al., 2021). Increased microbial biomass may be partially responsible for the increase in sediment OC under oxic conditions in experimental microcosms, as we observed the formation of orange (likely Fe-oxidizing) biofilms on top of the sediment layer in oxic microcosms (Figure S1). Fe reduction is also often associated with an increase in pH, which may increase the solubility of OC (Tavakkoli et al., 2015). However, pH did not differ consistently between microcosm treatments in this study and remained circumneutral on a whole-ecosystem scale (Figure S6 and S7). While these alternative mechanisms likely play a role in Fe and OC release, the decrease in Fe-OC and total OC following inactivation of the oxygenation system in FCR suggests that, at least for some surficial sediments, short (~2 week) periods of hypoxia can cause Fe-OC complexes to dissociate and decrease sediment OC burial on a whole-ecosystem

scale.

4.2 Over multiannual timescales, OC respiration rates play a greater role than Fe-OC in determining the net effect of hypoxia on sediment OC content

Over multiannual timescales (2019–2021), exposure to seasonal hypoxia increased the amount of OC in sediments from FCR by 57% without changing the amount of Fe-OC (Figure 5). This clearly contrasts with short-term experimental results, which showed decreased OC content following short periods of hypoxia (section 4.3). While many factors could affect OC and Fe-OC over multiannual timescales, the fact that no comparable effects were seen in the unoxygenated reference reservoir (BVR) suggests that these changes may be attributed to changes in DO concentrations in overlying water. Over two years of summer hypoxia, OC levels in sediment from FCR increased to the extent that they were no longer significantly different from the hypoxic reference reservoir (Figure 5), suggesting that legacy effects of oxygen conditions on total sediment OC may diminish after a two-year interval.

Increases in sediment OC content with increased hypoxic duration are consistent with a reduction in sediment OC respiration rates under hypoxic conditions (Carey et al., 2018; Hargrave, 1969; Walker & Snodgrass, 1986). OC respiration rates decrease under hypoxic conditions because OC must be broken down using alternative electron acceptors, which produce a lower energy yield (Bastviken et al., 2003, 2004). Previous work conducted in BVR found that CH_4 was the dominant terminal electron acceptor in the hypolimnion during hypoxic summer conditions, and CH_4 has one of the lowest energy yields of alternate electron acceptors (McClure et al., 2021). Consequently, as less OC is respired in hypoxic hypolimnetic water and sediments, OC can accumulate more quickly in surficial sediments. Our results suggest that over multiannual timescales, this process (decreased respiration under hypoxic conditions) outweighs the counter-acting decrease in Fe protection of OC that we observed during short periods of hypoxia.

Sediment Fe-OC content (per g sediment mass) did not significantly change after two years of hypoxic conditions in FCR (Figure 5), indicating that at least a fraction of these compounds are able to withstand fluctuations in environmental redox conditions. Long-term stability of Fe-OC complexes can be promoted by the formation of strong chemical bonds between OC and mineral surfaces, and these bonds continue to form over time (Kaiser et al., 2007). Likewise, weathering of Fe increases the porosity of mineral surfaces and allows for OC protection within pore spaces (Kaiser & Guggenberger, 2003; Kleber et al., 2005). Decreased accessibility to microbial decomposition (e.g., through burial) may further increase the ability of Fe-OC compounds to persist over time (Kaiser & Guggenberger, 2003; Kleber et al., 2015). In FCR, the history of oxic conditions (2013–2019) may have contributed to the formation of particularly stable Fe-OC complexes in sediment, which were then able to withstand two summers of hypoxia.

Importantly, much of the OC that accumulates under hypoxic conditions does not end up being bound to Fe. This result may be due to Fe oxidation state, as sorptive associations between DOC and Fe in sediment are much less likely to form if Fe is in a reduced state (Fe(II); Nierop et al., 2002). Because total OC increased following hypoxia and Fe-OC did not change, Fe-OC as a percentage of sediment OC was significantly lower after two years of hypoxia than before this hypoxic period. Declines in the percentage of OC that is bound to Fe may have important implications for ecosystem-scale carbon cycling, as OC that is associated with Fe is comparatively more protected from respiration (e.g., Chen et al., 2018, 2020; Hemingway et al., 2019; Kleber et al., 2005). Increased stocks of OC that are not associated with Fe may increase rates of methane production and OC release from the sediment to the water column (e.g., Hounshell et al., 2021), and could increase aerobic respiration rates under subsequent oxic periods (e.g., Chen et al., 2020; Huang et al., 2021).

4.3 Substantial OC and Fe cycling occurs at the sediment-water interface

Notably, the OC content of the top 1 cm of sediment was significantly lower than that of settling particulate material in both FCR and BVR, and nearly three times as much of this OC was bound to Fe in sediments compared to settling material (Figure 2). These results imply a substantial level of OC and Fe processing at the sediment-water interface, and they reinforce previous research in suggesting that the sediment-water interface is a hotspot for biogeochemical cycling freshwater lakes and reservoirs (e.g., Dadi et al., 2017; Hanson et al., 2015; Krueger et al., 2020).

From a mass-balance perspective, the difference in Fe-OC between settling material and surficial sediments suggests that Fe-OC complexes are either formed or preferentially preserved (compared to OC that is not associated with Fe) in sediments. Preferential preservation of Fe-OC is well-supported, as complexation with Fe has been shown to decrease OC turnover rates across multiple ecosystems (Eusterhues et al., 2014; Kaiser & Guggenberger, 2003; Kalbitz et al., 2005; Kleber et al., 2005; Lalonde et al., 2012; Mikutta & Kaiser, 2011). However, the difference in Fe-OC between settling material and surficial sediments likely also results in large part from Fe-OC associations formed in sediment (e.g., through adsorption of organic matter onto existing Fe minerals and Fe-OC complexes), as Fe(III) levels are much higher in sediments (e.g., Davison et al., 1991) and the composition of OC in sediments may be more preferable for complexation with Fe. While we did not measure OC quality in this study, we anticipate that settling material may have higher autochthonous OC levels and be more rapidly respired, while sediment OC may be enriched in allochthonous aromatic OC, which preferentially associates with Fe (Kramer et al., 2012; Riedel et al., 2013; Shields et al., 2016). Documenting changes in Fe-OC throughout the process of sediment diagenesis enhances our understanding of OC sequestration, as few if any previous studies have quantified the difference between Fe-OC inputs and stocks in aquatic sediments.

4.4 High Fe-OC levels reflect site-specific characteristics

On average, nearly one-third of surficial sediment OC was bound to Fe (dithionite-extractable) across two years in FCR and BVR (Figure 5). This percentage is far greater than that documented by Peter et al. (2018), where Fe-OC comprised 11% of total sediment OC across five boreal lakes. Furthermore, the levels of Fe-OC recorded here are higher than the mean of $21.5 \pm 8.6\%$ reported for a broad range of marine sediments (Lalonde et al. 2012). With few other studies analyzing Fe-OC in freshwater lakes and reservoirs to date, our analysis provides new evidence that Fe-OC may play an important role in carbon sequestration in some freshwaters.

Differences in the percentage of organic matter that is bound to Fe may result from differences in overlying DO concentrations, as described throughout this study, as well as a number of other factors. For example, increasing ratios of Fe:OC and increasing absolute concentrations of Fe and OC can all increase the amount of Fe-OC coprecipitation (Chen et al., 2016; Kleber et al., 2015 and references therein). Likewise, differing Fe forms, OC quality, and pH may also impact the formation and stability of Fe-OC complexes (Curti et al., 2021; Kaiser et al., 2007; Kaiser & Guggenberger, 2003; Kleber et al., 2015); these differences may derive from contrasting geology, catchment vegetation, and trophic status, among many other factors. However, none of these factors fully explain differences in Fe-OC content between sites studied to date (e.g., Lalonde et al., 2012; Peter & Sobek, 2018).

Despite having higher Fe-OC levels (as a percentage of total sediment OC) than most aquatic sediments studied to date, other sediment characteristics in FCR and BVR are within the range of those measured in other locations. FCR and BVR have much lower sediment OC content than the boreal lakes analyzed by Peter and Sobek (2018; 14–38% of sediment mass), but higher sediment OC than the primarily marine sediments analyzed by Lalonde et al. (2012; 0–7% of sediment mass). Fe concentrations are high in sediment from FCR and BVR, with a mean of 53,466 mg/kg dry weight (Krueger et al., 2020). However, Peter and Sobek (2018) observed low Fe-OC as a percentage of sediment OC ($\mu=6.7\%$) in one extremely high-Fe lake (Övre Skärsjön; 226,172 mg/kg reducible Fe in sediment). Likewise, pH in FCR and BVR is circumneutral (Figure S7), well within the range of 5.4–7.6 reported by Peter and Sobek (2018), and both Peter and Sobek (2018) and Lalonde et al. (2012) included a range of oxic and hypoxic sediments in their analyses. These observations from a range of aquatic sediments suggest that site-specific characteristics associated with catchment geology, water residence time, OC and Fe input rates, OC quality, and Fe mineral forms play an important role in determining the percentage of sediment OC that is bound to Fe. Understanding the controls on Fe-OC in freshwater sediment will require Fe-OC characterization at a greater number and diversity of lakes and reservoirs. Such research will be essential to understanding how freshwater OC sequestration may be affected by global changes in Fe concentrations (Weyhenmeyer et al., 2014), water temperatures (Dokulil et al., 2021; O'Reilly et al., 2015), and pH (Garmo et al., 2014; Gavin et al., 2018; Stoddard et al., 1999), among other factors.

5. Conclusions

Results from this study help reconcile previous Fe-OC research and shed light on how declining oxygen concentrations may impact the role of lakes and reservoirs in the global carbon cycle. Research across terrestrial soils and marine sediments has provided contradictory evidence that Fe-OC complexes are (1) readily dissociated under hypoxic conditions and (2) capable of promoting sediment OC burial into deeper (hypoxic) layers over the course of decades to millennia. Here, we find that the timescale of analysis plays a critical role in understanding the net effect of hypoxia on sediment OC and Fe-OC. Specifically, a portion of the Fe-OC pool in surficial sediment is highly responsive to hypoxia in overlying water on a weekly timescale, resulting in decreased sediment OC. However, over longer timescales, the decrease in OC that results from dissociation of Fe-OC complexes is outweighed by the increase in sediment OC that results from slower respiration rates under hypoxia. At both timescales, our results reinforce that Fe may serve as an important control over OC cycling and sediment preservation of OC in some freshwater ecosystems. As the duration of hypoxia increases in lakes and reservoirs (Jane et al., 2021; Jenny et al., 2016), our results suggest that OC dynamics will respond non-linearly. While short periods of hypoxia may decrease OC burial, increasing prevalence and duration of hypoxia over multiannual timescales has the potential to increase OC burial in freshwater sediment, intensifying the role of freshwaters as sinks in the global carbon cycle.

Acknowledgements

We are grateful for ongoing partnerships with the Western Virginia Water Authority that facilitated this research. Additionally, we thank the Virginia Tech Reservoir Group for helping to collect these data, particularly Adrienne Breef-Pilz for organizing the 2021 field season and helping to collect sediment cores in 2021, James Maze and Dexter Howard for helping to collect sediment cores in 2019, Ryan McClure for leading CTD data collection before 2019, and Alex Hounshell for organizing the 2019 field season. We thank Chip Frazier and Jeb Barrett for providing access to laboratory equipment and Jeff Parks in the VT ICP-MS lab for analyzing Fe samples. This work is supported by the Institute for Critical Science and Applied Technology at Virginia Tech and the U.S. National Science Foundation (NSF) foundation grants DGE-1651272, DEB-1753639, SCC-1737424, DBI-1933016, and DBI-1933102.

Author Contributions

ASL conceptualized this study with CCC and MES. ASL performed chemical Fe-OC extractions, analyzed data, developed figures, and wrote this manuscript with MES, MEL, and CCC. BRN led analytical chemistry methods development and performed DOC analyses. NWH and MES oversaw whole-ecosystem Fe sampling, analysis, and data collation. AD helped to design and run the microcosm experiment and process sediment samples. HLW collated and processed DOC and YSI data and reviewed code for this manuscript. CCC oversaw whole-

ecosystem experiments. All authors edited and approved the final manuscript.

Open Research

All data used in this study are available in the Environmental Data Initiative (Carey et al., 2021; Carey, Lewis, Gantzer, et al., 2022; Carey, Lewis, McClure, et al., 2022; Carey, Wander, McClure, et al., 2022; Lewis et al., 2022; Lewis, Schreiber, et al., 2022; Schreiber et al., 2022). Code to reproduce results in this manuscript is available in a Zenodo repository (Lewis, 2022).

References

- Akima, H., Gebhardt, A., Petzold, T., Maechler, M., & code), bilinear. (2022). akima: Interpolation of Irregularly and Regularly Spaced Data (Version 0.6-3.4). Retrieved from <https://CRAN.R-project.org/package=akima>
- American Public Health Association. (2018a). 3125 metals by inductively coupled plasma-mass spectrometry. In *Standard Methods For the Examination of Water and Wastewater*. American Public Health Association. <https://doi.org/10.2105/smww.2882.048>
- American Public Health Association. (2018b). 5310 total organic carbon (toc). In *Standard Methods For the Examination of Water and Wastewater*. American Public Health Association. <https://doi.org/10.2105/SMWW.2882.104>
- Arndt, S., Jørgensen, B. B., LaRowe, D. E., Middelburg, J. J., Pancost, R. D., & Regnier, P. (2013). Quantifying the degradation of organic matter in marine sediments: A review and synthesis. *Earth-Science Reviews*, 123, 53–86. <https://doi.org/10.1016/j.earscirev.2013.02.008>
- Auguie, B. (2019). egg: Extensions for “ggplot2”: Custom Geom, Custom Themes, Plot Alignment, Labelled Panels, Symmetric Scales, and Fixed Panel Size (Version 0.4.5). Retrieved from <https://CRAN.R-project.org/package=egg>
- Bai, J., Luo, M., Yang, Y., Xiao, S., Zhai, Z., & Huang, J. (2021). Iron-bound carbon increases along a freshwater–oligohaline gradient in a subtropical tidal wetland. *Soil Biology and Biochemistry*, 154, 108128. <https://doi.org/10.1016/j.soilbio.2020.108128>
- Ball, J. W., & Nordstrom, D. K. (1991). *User’s manual for WATEQ4F, with revised thermodynamic data base and text cases for calculating speciation of major, trace, and redox elements in natural waters* (USGS Numbered Series No. 91–183). *User’s manual for WATEQ4F, with revised thermodynamic data base and text cases for calculating speciation of major, trace, and redox elements in natural waters* (Vol. 91–183). U.S. Geological Survey. <https://doi.org/10.3133/ofr91183>
- Bartosiewicz, M., Przytulska, A., Lapierre, J.-F., Laurion, I., Lehmann, M. F., & Maranger, R. (2019). Hot tops, cold bottoms: Synergistic climate warming and shielding effects increase carbon burial in lakes. *Limnology and Oceanography Letters*, 4(5), 132–144. <https://doi.org/10.1002/lol2.10117>
- Bastviken, D., Olsson, M., & Tranvik, L. (2003). Simultaneous measurements of organic carbon mineralization and

bacterial production in oxic and anoxic lake sediments. *Microbial Ecology*, 46(1), 73–82. <https://doi.org/10.1007/s00248-002-1061-9>Bastviken, D., Persson, L., Odham, G., & Tranvik, L. (2004). Degradation of dissolved organic matter in oxic and anoxic lake water. *Limnology and Oceanography*, 49(1), 109–116. <https://doi.org/10.4319/lo.2004.49.1.0109>Bastviken, D., Tranvik, L. J., Downing, J. A., Crill, P. M., & Enrich-Prast, A. (2011). Freshwater methane emissions offset the continental carbon sink. *Science*, 331(6013), 50–50. <https://doi.org/10.1126/science.1196808>Battin, T. J., Luyssaert, S., Kaplan, L. A., Aufdenkampe, A. K., Richter, A., & Tranvik, L. J. (2009). The boundless carbon cycle. *Nature Geoscience*, 2(9), 598–600. <https://doi.org/10.1038/ngeo618>Björnerås, C., Weyhenmeyer, G. A., Evans, C. D., Gessner, M. O., Grossart, H.-P., Kangur, K., et al. (2017). Widespread increases in iron concentration in European and North American freshwaters. *Global Biogeochemical Cycles*, 31(10), 1488–1500. <https://doi.org/10.1002/2017GB005749>Brothers, S., Köhler, J., Attermeyer, K., Grossart, H. P., Mehner, T., Meyer, N., et al. (2014). A feedback loop links brownification and anoxia in a temperate, shallow lake. *Limnology and Oceanography*, 59(4), 1388–1398. <https://doi.org/10.4319/lo.2014.59.4.1388>Carey, C. C., Doubek, J. P., McClure, R. P., & Hanson, P. C. (2018). Oxygen dynamics control the burial of organic carbon in a eutrophic reservoir. *Limnology and Oceanography Letters*, 3(3), 293–301. <https://doi.org/10.1002/lol2.10057>Carey, C. C., Wander, H. L., Woelmer, W. M., Lofton, M. E., Breef-Pilz, A., Doubek, J. P., et al. (2021). Water chemistry time series for Beaverdam Reservoir, Carvins Cove Reservoir, Falling Creek Reservoir, Gatewood Reservoir, and Spring Hollow Reservoir in southwestern Virginia, USA 2013–2020 [Data set]. Environmental Data Initiative. <https://doi.org/10.6073/PASTA/6343E979A970E8A2590B4A450E851DD2>Carey, C. C., Hanson, P. C., Thomas, R. Q., Gerling, A. B., Hounshell, A. G., Lewis, A. S. L., et al. (2022). Anoxia decreases the magnitude of the carbon, nitrogen, and phosphorus sink in freshwaters. *Global Change Biology*, 28(16), 4861–4881. <https://doi.org/10.1111/gcb.16228>Carey, C. C., Lewis, A. S. L., Gantzer, P. A., Bierlein, K. A., & WVWA. (2022). Bathymetry for Falling Creek Reservoir and Beaverdam Reservoir, Virginia, USA [Data set]. Environmental Data Initiative. Retrieved from <https://portal-s.edirepository.org/nis/mapbrowse?packageid=edi.939.2>Carey, C. C., Thomas, R. Q., & Hanson, P. C. (2022). General Lake Model-Aquatic EcoDynamics model parameter set for Falling Creek Reservoir, Vinton, Virginia, USA 2013–2019 [Data set]. Environmental Data Initiative. <https://doi.org/10.6073/PASTA/9F7D037D9A133076A0A0D123941C6396>Carey, C. C., Wander, H. L., McClure, R. P., Lofton, M. E., Hamre, K. D., Doubek, J. P., et al. (2022). Secchi depth data and discrete depth profiles of photosynthetically active radiation, temperature, dissolved oxygen, and pH for Beaverdam Reservoir, Carvins Cove Reservoir, Falling Creek Reservoir, Gatewood Reservoir, and Spring Hollow Reservoir in southwestern Virginia, USA 2013–2021 [Data set]. Environmental Data Initiative. <https://doi.org/10.6073/PASTA/887D8AB8C57FB8FDF3582507F3223CD6>Carey,

C. C., Lewis, A. S. L., McClure, R. P., Gerling, A. B., Breef-Pilz, A., & Das, A. (2022). Time series of high-frequency profiles of depth, temperature, dissolved oxygen, conductivity, specific conductance, chlorophyll a, turbidity, pH, oxidation-reduction potential, photosynthetic active radiation, and descent rate for Beaverdam Reservoir, Carvins Cove Reservoir, Falling Creek Reservoir, Gatewood Reservoir, and Spring Hollow Reservoir in Southwestern Virginia, USA 2013-2021 [Data set]. Environmental Data Initiative. <https://doi.org/10.6073/PASTA/C4C45B5B10B4CB4CD4B5E613C3EFFBD0>Carey, C. C., Wander, H. L., Howard, D. W., Niederlehner, B. R., Woelmer, W. M., Lofton, M. E., et al. (2022). Water chemistry time series for Beaverdam Reservoir, Carvins Cove Reservoir, Falling Creek Reservoir, Gatewood Reservoir, and Spring Hollow Reservoir in southwestern Virginia, USA 2013-2021 [Data set]. Environmental Data Initiative. <https://doi.org/10.6073/PASTA/7BD797155CDBB5F1ACDF0547C6BA9023>Carpenter, S. R. (1996). Microcosm experiments have limited relevance for community and ecosystem ecology. *Ecology*, 77(3), 677–680. <https://doi.org/10.2307/2265490>Chapman, M. J., Cravotta III, C. A., Szabo, Z., & Lindsey, B. D. (2013). Naturally occurring contaminants in the Piedmont and Blue Ridge crystalline-rock aquifers and Piedmont Early Mesozoic basin siliciclastic-rock aquifers, eastern United States, 1994–2008. Retrieved June 25, 2022, from <https://pubs.er.usgs.gov/publication/sir20135072>Chen, C., Meile, C., Wilmoth, J., Barcellos, D., & Thompson, A. (2018). Influence of pO₂ on Iron Redox Cycling and Anaerobic Organic Carbon Mineralization in a Humid Tropical Forest Soil. *Environmental Science & Technology*, 52(14), 7709–7719. <https://doi.org/10.1021/acs.est.8b01368>Chen, C., Hall, S. J., Coward, E., & Thompson, A. (2020). Iron-mediated organic matter decomposition in humid soils can counteract protection. *Nature Communications*, 11(1), 2255. <https://doi.org/10.1038/s41467-020-16071-5>Chen, K.-Y., Chen, T.-Y., Chan, Y.-T., Cheng, C.-Y., Tzou, Y.-M., Liu, Y.-T., & Teah, H.-Y. (2016). Stabilization of Natural Organic Matter by Short-Range-Order Iron Hydroxides. *Environmental Science & Technology*, 50(23), 12612–12620. <https://doi.org/10.1021/acs.est.6b02793>Curti, L., Moore, O. W., Babakhani, P., Xiao, K.-Q., Woulds, C., Bray, A. W., et al. (2021). Carboxyl-richness controls organic carbon preservation during coprecipitation with iron (oxyhydr)oxides in the natural environment. *Communications Earth & Environment*, 2(1), 1–13. <https://doi.org/10.1038/s43247-021-00301-9>Dadi, T., Wendt-Potthoff, K., & Koschorreck, M. (2017). Sediment resuspension effects on dissolved organic carbon fluxes and microbial metabolic potentials in reservoirs. *Aquatic Sciences*, 79(3), 749–764. <https://doi.org/10.1007/s00027-017-0533-4>Davison, W., Grime, G. W., Morgan, J. a. W., & Clarke, K. (1991). Distribution of dissolved iron in sediment pore waters at submillimetre resolution. *Nature*, 352(6333), 323–325. <https://doi.org/10.1038/352323a0>Dean, W. E., & Gorham, E. (1998). Magnitude and significance of carbon burial in lakes, reservoirs, and peatlands, 4.Deemer, B. R., Harrison, J. A., Li, S., Beaulieu, J. J., DelSontro, T., Barros, N., et al. (2016). Greenhouse gas emissions from reservoir water surfaces: A new global synthesis. *BioScience*, 66(11), 949–964. <https://doi.org/10.1093/biosci/biw117>DelSontro, T., Beaulieu, J.

J., & Downing, J. A. (2018). Greenhouse gas emissions from lakes and impoundments: Upscaling in the face of global change. *Limnology and Oceanography Letters*, 3(3), 64–75. <https://doi.org/10.1002/lol2.10073>Dokulil, M. T., de Eyto, E., Maberly, S. C., May, L., Weyhenmeyer, G. A., & Woolway, R. I. (2021). Increasing maximum lake surface temperature under climate change. *Climatic Change*, 165(3), 56. <https://doi.org/10.1007/s10584-021-03085-1>Dzialowski, A. R., Rzepecki, M., Kostrzevska-Szlakowska, I., Kalinowska, K., Palash, A., & Lennon, J. T. (2014). Are the abiotic and biotic characteristics of aquatic mesocosms representative of in situ conditions? *Journal of Limnology*, 73(3). <https://doi.org/10.4081/jlimnol.2014.721>Einola, E., Rantakari, M., Kankaala, P., Kortelainen, P., Ojala, A., Pajunen, H., et al. (2011). Carbon pools and fluxes in a chain of five boreal lakes: A dry and wet year comparison. *Journal of Geophysical Research: Biogeosciences*, 116(G3). <https://doi.org/10.1029/2010JG001636>Eusterhues, K., Neidhardt, J., Hädrich, A., Küsel, K., & Totsche, K. U. (2014). Biodegradation of ferrihydrite-associated organic matter. *Biogeochemistry*, 119(1–3), 45–50. <https://doi.org/10.1007/s10533-013-9943-0>Fisher, B. J., Faust, J. C., Moore, O. W., Peacock, C. L., & März, C. (2021). Technical Note: Uncovering the influence of methodological variations on the extractability of iron bound organic carbon, 20.Garmo, Ø. A., Skjelkvåle, B. L., de Wit, H. A., Colombo, L., Curtis, C., Fölster, J., et al. (2014). Trends in surface water chemistry in acidified areas in Europe and North America from 1990 to 2008. *Water, Air, & Soil Pollution*, 225(3), 1880. <https://doi.org/10.1007/s11270-014-1880-6>Gavin, A. L., Nelson, S. J., Klemmer, A. J., Fernandez, I. J., Strock, K. E., & McDowell, W. H. (2018). Acidification and climate linkages to increased dissolved organic carbon in high-elevation lakes. *Water Resources Research*, 54(8), 5376–5393. <https://doi.org/10.1029/2017WR020963>Gerling, A. B., Browne, R. G., Gantzer, P. A., Mobley, M. H., Little, J. C., & Carey, C. C. (2014). First report of the successful operation of a side stream supersaturation hypolimnetic oxygenation system in a eutrophic, shallow reservoir. *Water Research*, 67, 129–143. <https://doi.org/10.1016/j.watres.2014.09.002>Gerling, A. B., Munger, Z. W., Doubek, J. P., Hamre, K. D., Gantzer, P. A., Little, J. C., & Carey, C. C. (2016). Whole-catchment manipulations of internal and external loading reveal the sensitivity of a century-old reservoir to hypoxia. *Ecosystems*, 19(3), 555–571. <https://doi.org/10.1007/s10021-015-9951-0>Gibbs, M. M. (1979). A simple method for the rapid determination of iron in natural waters. *Water Research*, 13(3), 295–297. [https://doi.org/10.1016/0043-1354\(79\)90209-4](https://doi.org/10.1016/0043-1354(79)90209-4)Grolemund, G., & Wickham, H. (2011). Dates and Times Made Easy with lubridate. *Journal of Statistical Software*, 40, 1–25. <https://doi.org/10.18637/jss.v040.i03>Hamre, K. D., Lofton, M. E., McClure, R. P., Munger, Z. W., Doubek, J. P., Gerling, A. B., et al. (2018). In situ fluorometry reveals a persistent, perennial hypolimnetic cyanobacterial bloom in a seasonally anoxic reservoir. *Freshwater Science*, 37(3), 483–495. <https://doi.org/10.1086/699327>Hanson, P. C., Pace, M. L., Carpenter, S. R., Cole, J. J., & Stanley, E. H. (2015). Integrating landscape carbon cycling: research needs for resolving organic carbon budgets of lakes. *Ecosystems*,

18(3), 363–375. <https://doi.org/10.1007/s10021-014-9826-9>Hargrave, B. T. (1969). Similarity of oxygen uptake by benthic communities. *Limnology and Oceanography*, 14(5), 801–805. <https://doi.org/10.4319/lo.1969.14.5.0801>Harris, D., Horwath, W. R., & Kessel, C. van. (2001). Acid fumigation of soils to remove carbonates prior to total organic carbon or CARBON-13 isotopic analysis. *Soil Science Society of America Journal*, 65(6), 1853–1856. <https://doi.org/10.2136/sssaj2001.1853>Hemingway, J. D., Rothman, D. H., Grant, K. E., Rosengard, S. Z., Eglinton, T. I., Derry, L. A., & Galy, V. V. (2019). Mineral protection regulates long-term global preservation of natural organic carbon. *Nature*, 570(7760), 228–231. <https://doi.org/10.1038/s41586-019-1280-6>Hounshell, A. G., McClure, R. P., Lofton, M. E., & Carey, C. C. (2021). Whole-ecosystem oxygenation experiments reveal substantially greater hypolimnetic methane concentrations in reservoirs during anoxia. *Limnology and Oceanography Letters*, 6(1), 33–42.Huang, W., Wang, K., Ye, C., Hockaday, W. C., Wang, G., & Hall, S. J. (2021). High carbon losses from oxygen-limited soils challenge biogeochemical theory and model assumptions. *Global Change Biology*, 27(23), 6166–6180. <https://doi.org/10.1111/gcb.15867>Jane, S., Hansen, G., Kraemer, B., Leavitt, P., Mincer, J., North, R., et al. (2021). Widespread deoxygenation of temperate lakes. *Nature*, 594. <https://doi.org/10.1038/s41586-021-03550-y>Jenny, J.-P., Francus, P., Normandeau, A., Lapointe, F., Perga, M.-E., Ojala, A., et al. (2016). Global spread of hypoxia in freshwater ecosystems during the last three centuries is caused by rising local human pressure. *Global Change Biology*, 22(4), 1481–1489. <https://doi.org/10.1111/gcb.13193>Kaiser, K., & Guggenberger, G. (2003). Mineral surfaces and soil organic matter. *European Journal of Soil Science*, 54(2), 219–236. <https://doi.org/10.1046/j.1365-2389.2003.00544.x>Kaiser, K., Mikutta, R., & Guggenberger, G. (2007). Increased stability of organic matter sorbed to ferrihydrite and goethite on aging. *Soil Science Society of America Journal*, 71(3), 711–719. <https://doi.org/10.2136/sssaj2006.0189>Kalbitz, K., Schwesig, D., Rethemeyer, J., & Matzner, E. (2005). Stabilization of dissolved organic matter by sorption to the mineral soil. *Soil Biology and Biochemistry*, 37(7), 1319–1331. <https://doi.org/10.1016/j.soilbio.2004.11.028>Kappler, A., Bryce, C., Mansor, M., Lueder, U., Byrne, J. M., & Swanner, E. D. (2021). An evolving view on biogeochemical cycling of iron. *Nature Reviews Microbiology*, 1–15. <https://doi.org/10.1038/s41579-020-00502-7>Kassambara, A. (2020). ggpubr: “ggplot2” Based Publication Ready Plots (Version 0.4.0). Retrieved from <https://CRAN.R-project.org/package=ggpubr>Kassambara, A. (2021). rstatix: Pipe-Friendly Framework for Basic Statistical Tests (Version 0.7.0). Retrieved from <https://CRAN.R-project.org/package=rstatix>Keitt, T. (2022). colorRamps: Builds Color Tables (Version 2.3.1). Retrieved from <https://CRAN.R-project.org/package=colorRamps>Kim, J., & Kim, T.-H. (2020). Distribution of Humic Fluorescent Dissolved Organic Matter in Lake Shihwa: the Role of the Redox Condition. *Estuaries and Coasts*, 43(3), 578–588. <https://doi.org/10.1007/s12237-018-00491-0>Kirk, G. (2004). Reduction and Oxidation. In G. Kirk (Ed.), *The Biogeochemistry of Submerged Soils* (pp. 93–134). John Wiley & Sons, Ltd.

<https://doi.org/10.1002/047086303X.ch4>Kleber, M., Mikutta, R., Torn, M. S., & Jahn, R. (2005). Poorly crystalline mineral phases protect organic matter in acid subsoil horizons. *European Journal of Soil Science*, 56(6), 717–725. <https://doi.org/10.1111/j.1365-2389.2005.00706.x>Kleber, M., Eusterhues, K., Keiluweit, M., Mikutta, C., Mikutta, R., & Nico, P. S. (2015). Chapter One - Mineral–Organic Associations: Formation, Properties, and Relevance in Soil Environments. In D. L. Sparks (Ed.), *Advances in Agronomy* (Vol. 130, pp. 1–140). Academic Press. <https://doi.org/10.1016/bs.agron.2014.10.005>Knoll, L. B., Vanni, M. J., Renwick, W. H., Dittman, E. K., & Gephart, J. A. (2013). Temperate reservoirs are large carbon sinks and small CO₂ sources: Results from high-resolution carbon budgets. *Global Biogeochemical Cycles*, 27(1), 52–64. <https://doi.org/10.1002/gbc.20020>Kramer, M. G., & Chadwick, O. A. (2018). Climate-driven thresholds in reactive mineral retention of soil carbon at the global scale. *Nature Climate Change*, 8(12), 1104–1108. <https://doi.org/10.1038/s41558-018-0341-4>Kramer, M. G., Sanderman, J., Chadwick, O. A., Chorover, J., & Vitousek, P. M. (2012). Long-term carbon storage through retention of dissolved aromatic acids by reactive particles in soil. *Global Change Biology*, 18(8), 2594–2605. <https://doi.org/10.1111/j.1365-2486.2012.02681.x>Krueger, K. M., Vavrus, C. E., Lofton, M. E., McClure, R. P., Gantzer, P., Carey, C. C., & Schreiber, M. E. (2020). Iron and manganese fluxes across the sediment-water interface in a drinking water reservoir. *Water Research*, 182, 116003. <https://doi.org/10.1016/j.watres.2020.116003>Lalonde, K., Mucci, A., Ouellet, A., & Gélinas, Y. (2012). Preservation of organic matter in sediments promoted by iron. *Nature*, 483(7388), 198–200. <https://doi.org/10.1038/nature10855>LaRowe, D. E., & Van Cappellen, P. (2011). Degradation of natural organic matter: A thermodynamic analysis. *Geochimica et Cosmochimica Acta*, 75(8), 2030–2042. <https://doi.org/10.1016/j.gca.2011.01.020>Lau, M. P., & del Giorgio, P. (2020). Reactivity, fate and functional roles of dissolved organic matter in anoxic inland waters. *Biology Letters*, 16(2), 20190694. <https://doi.org/10.1098/rsbl.2019.0694>Le Quéré, C., Moriarty, R., Andrew, R. M., Peters, G. P., Ciais, P., Friedlingstein, P., et al. (2015). Global carbon budget 2014. *Earth System Science Data*, 7(1), 47–85. <https://doi.org/10.5194/essd-7-47-2015>Lewis, A. S. L. (2022). Effects of hypoxia on coupled carbon and iron cycling in two freshwater reservoirs v1.0.0. Zenodo. Retrieved from <https://doi.org/10.5281/zenodo.6845416>Lewis, A. S. L., Niederlehner, B. R., Das, A., Wander, H. L., Schreiber, M. E., & Carey, C. C. (2022). Experimental microcosm incubations assessing the effect of hypoxia on aqueous iron and organic carbon, pH, sediment organic carbon, and sediment iron-bound organic carbon. Environmental Data Initiative. Retrieved from <https://portal-s.edirepository.org/nis/mapbrowse?packageid=edi.880.3>Lewis, A. S. L., Schreiber, M. E., Niederlehner, B. R., Das, A., & Carey, C. C. (2022). Total organic carbon, total nitrogen, and iron-bound organic carbon in surficial sediment and settling particulate material from Falling Creek and Beaverdam Reservoirs in 2019 and 2021. Environmental Data Initiative. Retrieved from <https://portal-s.edirepository.org/nis/mapbrowse?packageid=edi.881.4>Marking,

L. L., & Dawson, V. K. (1973). *Toxicity of quinaldine sulfate to fish* (Report No. 48) (pp. 0–8). La Crosse, WI. Retrieved from <http://pubs.er.usgs.gov/publication/2001015>

McClure, R. P., Schreiber, M. E., Lofton, M. E., Chen, S., Krueger, K. M., & Carey, C. C. (2021). Ecosystem-Scale Oxygen Manipulations Alter Terminal Electron Acceptor Pathways in a Eutrophic Reservoir. *Ecosystems*, 24(6), 1281–1298. <https://doi.org/10.1007/s10021-020-00582-9>

Mendonça, R., Müller, R. A., Clow, D., Verpoorter, C., Raymond, P., Tranvik, L. J., & Sobek, S. (2017). Organic carbon burial in global lakes and reservoirs. *Nature Communications*, 8(1), 1694. <https://doi.org/10.1038/s41467-017-01789-6>

Mikutta, R., & Kaiser, K. (2011). Organic matter bound to mineral surfaces: Resistance to chemical and biological oxidation. *Soil Biology and Biochemistry*, 43(8), 1738–1741. <https://doi.org/10.1016/j.soilbio.2011.04.012>

Munger, Z. W., Carey, C. C., Gerling, A. B., Doubek, J. P., Hamre, K. D., McClure, R. P., & Schreiber, M. E. (2019). Oxygenation and hydrologic controls on iron and manganese mass budgets in a drinking-water reservoir. *Lake and Reservoir Management*, 35(3), 277–291. <https://doi.org/10.1080/10402381.2018.1545811>

Nierop, K. G. J., Jansen, B., & Verstraten, J. M. (2002). Dissolved organic matter, aluminium and iron interactions: precipitation induced by metal/carbon ratio, pH and competition. *The Science of the Total Environment*, 300(1–3), 201–211. [https://doi.org/10.1016/s0048-9697\(02\)00254-1](https://doi.org/10.1016/s0048-9697(02)00254-1)

O'Reilly, C. M., Sharma, S., Gray, D. K., Hampton, S. E., Read, J. S., Rowley, R. J., et al. (2015). Rapid and highly variable warming of lake surface waters around the globe. *Geophysical Research Letters*, 42(24), 10,773–10,781. <https://doi.org/10.1002/2015GL066235>

Oyewumi, O., & Schreiber, M. E. (2017). Using column experiments to examine transport of As and other trace elements released from poultry litter: Implications for trace element mobility in agricultural watersheds. *Environmental Pollution*, 227, 223–233. <https://doi.org/10.1016/j.envpol.2017.04.063>

Pacheco, F. S., Roland, F., & Downing, J. A. (2014). Eutrophication reverses whole-lake carbon budgets. *Inland Waters*, 4(1), 41–48. <https://doi.org/10.5268/IW-4.1.614>

Pan, W., Kan, J., Inamdar, S., Chen, C., & Sparks, D. (2016). Dissimilatory microbial iron reduction release DOC (dissolved organic carbon) from carbon-ferrihydrite association. *Soil Biology and Biochemistry*, 103, 232–240. <https://doi.org/10.1016/j.soilbio.2016.08.026>

Patzner, M. S., Mueller, C. W., Malusova, M., Baur, M., Nikeleit, V., Scholten, T., et al. (2020). Iron mineral dissolution releases iron and associated organic carbon during permafrost thaw. *Nature Communications*, 11(1), 6329. <https://doi.org/10.1038/s41467-020-20102-6>

Peter, S., & Sobek, S. (2018). High variability in iron-bound organic carbon among five boreal lake sediments. *Biogeochemistry*, 139(1), 19–29. <https://doi.org/10.1007/s10533-018-0456-8>

Peter, S., Isidorova, A., & Sobek, S. (2016). Enhanced carbon loss from anoxic lake sediment through diffusion of dissolved organic carbon. *Journal of Geophysical Research: Biogeosciences*, 121(7), 1959–1977. <https://doi.org/10.1002/2016JG003425>

Peter, S., Agstam, O., & Sobek, S. (2017). Widespread release of dissolved organic carbon from anoxic boreal lake sediments. *Inland Waters*, 7(2), 151–163.

<https://doi.org/10.1080/20442041.2017.1300226>Raymond, P. A., Hartmann, J., Lauerwald, R., Sobek, S., McDonald, C., Hoover, M., et al. (2013). Global carbon dioxide emissions from inland waters. *Nature*, *503*(7476), 355–359. <https://doi.org/10.1038/nature12760>Riedel, T., Zak, D., Biester, H., & Dittmar, T. (2013). Iron traps terrestrially derived dissolved organic matter at redox interfaces. *Proceedings of the National Academy of Sciences*, *110*(25), 10101–10105. <https://doi.org/10.1073/pnas.1221487110>Rumpel, C., & Kögel-Knabner, I. (2011). Deep soil organic matter—a key but poorly understood component of terrestrial C cycle. *Plant and Soil*, *338*(1), 143–158. <https://doi.org/10.1007/s11104-010-0391-5>Schindler, D. W. (1998). Whole-ecosystem experiments: replication versus realism: the need for ecosystem-scale experiments. *Ecosystems*, *1*(4), 323–334. <https://doi.org/10.1007/s100219900026>Schreiber, M. E., Hammond, N. W., Krueger, K. M., Munger, Z. W., Ming, C. L., Breef-Pilz, A., & Carey, C. C. (2022). Time series of total and soluble iron and manganese concentrations from Falling Creek Reservoir and Beaverdam Reservoir in southwestern Virginia, USA from 2014 through 2021 [Data set]. Environmental Data Initiative. <https://doi.org/10.6073/PASTA/7CDF3D7A234963B265F09B7D6D08F357>Shields, M. R., Bianchi, T. S., G  linas, Y., Allison, M. A., & Twilley, R. R. (2016). Enhanced terrestrial carbon preservation promoted by reactive iron in deltaic sediments. *Geophysical Research Letters*, *43*(3), 1149–1157. <https://doi.org/10.1002/2015GL067388>Skoog, A. C., & Arias-Esquivel, V. A. (2009). The effect of induced anoxia and reoxygenation on benthic fluxes of organic carbon, phosphate, iron, and manganese. *Science of The Total Environment*, *407*(23), 6085–6092. <https://doi.org/10.1016/j.scitotenv.2009.08.030>Sobek, S., Durisch-Kaiser, E., Zurbr  gg, R., Wongfun, N., Wessels, M., Pasche, N., & Wehrli, B. (2009). Organic carbon burial efficiency in lake sediments controlled by oxygen exposure time and sediment source. *Limnology and Oceanography*, *54*(6), 2243–2254. <https://doi.org/10.4319/lo.2009.54.6.2243>Stoddard, J. L., Jeffries, D. S., L  kewille, A., Clair, T. A., Dillon, P. J., Driscoll, C. T., et al. (1999). Regional trends in aquatic recovery from acidification in North America and Europe. *Nature*, *401*(6753), 575–578. <https://doi.org/10.1038/44114>Tavakkoli, E., Rengasamy, P., Smith, E., & McDonald, G. K. (2015). The effect of cation–anion interactions on soil pH and solubility of organic carbon. *European Journal of Soil Science*, *66*(6), 1054–1062. <https://doi.org/10.1111/ejss.12294>Thompson, A., Chadwick, O. A., Rancourt, D. G., & Chorover, J. (2006). Iron-oxide crystallinity increases during soil redox oscillations. *Geochimica et Cosmochimica Acta*, *70*(7), 1710–1727. <https://doi.org/10.1016/j.gca.2005.12.005>Tranvik, L. J., Cole, J. J., & Prairie, Y. T. (2018). The study of carbon in inland waters—from isolated ecosystems to players in the global carbon cycle. *Limnology and Oceanography Letters*, *3*(3), 41–48. <https://doi.org/10.1002/lol2.10068>Trapletti, A., Hornik, K., & code), B. L. (BDS test. (2022). tseries: Time Series Analysis and Computational Finance (Version 0.10-51). Retrieved from <https://CRAN.R-project.org/package=tseries>Virginia Division of Mineral Resources. (2003). Digital representation of the 1993 geologic map of Virginia.von

Wachenfeldt, E., Sobek, S., Bastviken, D., & Tranvik, L. J. (2008). Linking allochthonous dissolved organic matter and boreal lake sediment carbon sequestration: The role of light-mediated flocculation. *Limnology and Oceanography*, 53(6), 2416–2426. <https://doi.org/10.4319/lo.2008.53.6.2416>

Walker, R. R., & Snodgrass, W. J. (1986). Model for sediment oxygen demand in lakes. *Journal of Environmental Engineering*, 112(1), 25–43. [https://doi.org/10.1061/\(ASCE\)0733-9372\(1986\)112:1\(25\)](https://doi.org/10.1061/(ASCE)0733-9372(1986)112:1(25))

Weyhenmeyer, G. A., Prairie, Y. T., & Tranvik, L. J. (2014). Browning of boreal freshwaters coupled to carbon-iron interactions along the aquatic continuum. *PloS One*, 9(2), e88104. <https://doi.org/10.1371/journal.pone.0088104>

Wickham, H., Averick, M., Bryan, J., Chang, W., McGowan, L. D., François, R., et al. (2019). Welcome to the Tidyverse. *Journal of Open Source Software*, 4(43), 1686. <https://doi.org/10.21105/joss.01686>

Williamson, C. E., Overholt, E. P., Pilla, R. M., Leach, T. H., Brentrup, J. A., Knoll, L. B., et al. (2015). Ecological consequences of long-term browning in lakes. *Scientific Reports*, 5(1), 1–10. <https://doi.org/10.1038/srep18666>

Winslow, L., Read, J., Woolway, R., Brentrup, J., Leach, T., Zwart, J., et al. (2019). rLakeAnalyzer: Lake Physics Tools (Version 1.11.4.1). Retrieved from <https://CRAN.R-project.org/package=rLakeAnalyzer>

Woodward, H. P. (1932). *Geology and Mineral Resources of the Roanoke Area, Virginia*.